AD NUMBER

AD827922

NEW LIMITATION CHANGE

TO

Approved for public release, distribution unlimited

FROM

Distribution authorized to U.S. Gov't. agencies and their contractors; Critical Technology; OCT 1967. Other requests shall be referred to Air Force Rocket Propulsion Lab., Attn: RPPR-STINFO, Research and Technology Div., Edwards AFB, CA 93523.

AUTHORITY

AFRPL ltr dtd 27 Oct 1971

AFRPL-TR-67-284

AD 827927

DEVELOPMENT OF A TEMPERATURE-INDICATING SENSOR FOR USE IN ABLATIVE ROCKET NOZZLES

FIRST PHASE REPORT

J. DeAcetis and D. C. Rousar

Aerojet-General Corporation

Period Covered: 1 August 1967 through 6 October 1967

TECHNICAL REPORT AFRPL-TR-67-284

October 1967

Air Force Rocket Propulsion Laboratory
Research and Technology Division
Air Force Systems Command
Edwards Air Force Base, California

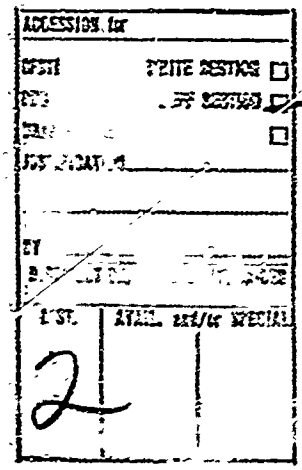

Report AFRPL-TR-67-284

This document is subject to special export controls and each transmittal to foreign governments or foreign nationals may be made only with prior approval of AFRPL (RPPR-STINFO), Edwards, California, 93523.

When U.S. Government drawings, specifications, or other data are used for any purpose other than a definitely related Government procurement operation, the Government thereby incurs no responsibility nor any obligation whatsoever, and the fact that the Government may have formulated, furnished, or in any way supplied the said drawings, specifications, or other data, is not to be regarded by implication or otherwise, or in any manner licensing the holder or any other person or corporation, or conveying any rights or permission to manufacture, use, or sell any patented invention that may in any way be related thereto.

AFRPL-TR-67-284
October 1967

DEVELOPMENT OF A TEMPERATURE-INDICATING SENSOR FOR USE IN ABLATIVE ROCKET NOZZLES

Phase I Report

J. DeAcetis and D. C. Rousar

10163T

FOREWORD

This first-phase technical report covers all work performed under Contract F04611-67-C-0118 from 1 August 1967 to 6 October 1967. The manuscript was released by the author on 12 October 1967 for publication as an RTD Technical Report.

The work on this contract, by the Research and Technology Operations of the Aerojet-General Corporation, Sacramento, California, is being administered under the direction of the Air Force Rocket Propulsion Laboratory, Edwards Air Force Base, California, with Mr. H. Binder as the project officer and Mr. D. Thrasher as project technical coordinator.

This program is under the technical management of Dr. J. DeAcetis. Heat transfer analyses were conducted by Mr. D. C. Rousar and Mr. R. W. Michel, and the literature survey was conducted by Johanna C. Ross.

This report contains no classified information extracted from other classified documents.

This technical report has been reviewed and is approved.

Harold I. Binder
AFRPL Project Engineer

ABSTRACT

The primary purpose of this program is to develop a high temperature (3500 to 6000°F) indicating system to obtain internal temperature measurements in ablative type materials during rocket motor firings.

During the first phase of work a state-of-the-art survey was conducted to determine those necessary factors which would permit the accurate measurement of in-depth temperatures. A high temperature indicating system was designed on the basis of the phase equilibrium of refractory materials in the 3500 to 6000°F range.

TABLE OF CONTENTS

APPENDIXES

TABLE LIST

FIGURE LIST

FIGURE LIST (cont.)

SECTION I

INTRODUCTION

A. GENERAL

This program was initiated under the sponsorship of the Air Force Rocket Propulsion Laboratory. The objectives were: (1) to develop a high temperature sensor capable of detecting temperatures in the 3500 to 6000°F temperature range, and (2) to determine the char temperature profiles for several ablative reinforced plastics during rocket motor firings.

The program was divided into the following three phases of work:

Phase I, Study and System Design
Phase II, Test and Evaluation
Phase III, Field Utilization of the Systems

The purpose of Phase I, Study and System Design, is to (1) conduct a state-of-the-art survey on high-temperature-sensing devices for the temperature range of 3500 to 6000°F; and (2) develop and design temperature-indicating sensors for this temperature range.

The purpose of Phase II, Test and Evaluation, is to fabricate and experimentally test models of the developed techniques and evaluate the test results.

The purpose of Phase III, Field Utilization of the Systems, is to fabricate and deliver several temperature-sensor systems to the Air Force Rocket Propulsion Laboratory for use in evaluating the temperatures of ablative plastics in a series of motor test firings.

I, A, General (cont.)

This report covers Phase I, conducted during the period 1 August 1967 to 6 October 1967. It contains a detailed lay-out of the developed high-temperature-sensing technique and an organized plan to test the technique.

Past research to develop instrumentation for ablating material has concentrated on thermocouples so that temperatures might be determined as a function of firing duration. Though great strides have been made in accomplishing accurate thermocouple measurement, such instrumentation is plagued by thermocouple breakage, questionable calibration, heat conduction away from the junction by the thermocouple wires, and poor response times. Also, the highest temperature thermocouple, W-3% Re/W-25% Re, is limited to 4200°F which is almost 2000°F below the operating temperature of the char surface.

The successful development of accurate temperature sensors will extend the temperature measurement range above 4200°F and enable the char surface temperature to be determined. These data are needed to better predict surface regression rates and thermal insulation capability.

B. PROGRAM OBJECTIVES

The objectives of this program are: (1) design and fabricate temperature-indicating sensors which cover the temperature range from 3500 to 6000°F for installation in ablating materials for rocket nozzles, (2) calibrate and verify the accuracy of temperature measurement, and (3) using these developed temperature sensors, establish the temperature profiles of NOMAD nozzle components during motor firings.

SECTION II

SUMMARY

A. LITERATURE SURVEY AND SYSTEM DESIGN

A state-of-the-art survey was made to determine the present capabilities of obtaining temperature measurements in the range of 3500 to 6000°F. On the basis of this survey and analyses of the data found, a system was developed and designed to be compatible with several ablative reinforced plastic materials. It was found that the 3500 to 6000°F temperatures could be obtained by utilizing high temperature refractory metal-carbon eutectic and peritectic compositions. Encapsulating precalibrated mixtures of these compositions into a graphite container of such a size that a minimum temperature disturbance is caused in the region of measurement provides a system that is chemically compatible; the sensor material with the container and the container with the ablative material.

B. PROGRAM FOR EVALUATION AND FIELD UTILIZATION OF SYSTEM

A program was planned to evaluate and field test the developed technique. The evaluation of the designed system is planned to consist of two major categories; fabrication of containers to encapsulate mixtures of eutectic powders, and implantation of the fabricated sensors into several ablative plastic materials for laboratory testing in a plasma arc stream. The ablative materials will consist of carbon- and graphite-reinforced phenolics, asbestos-reinforced phenolics, kraft paper-reinforced phenolic, and five pyrolyzed-reinforced phenolics. Field utilization of the design system was planned to consist of sensor and thermocouple instrumentation of nozzle components made of the above materials followed by a series of three motor firings at the Air Force Rocket Propulsion Laboratory.

SECTION III

TECHNICAL DISCUSSION

A. LITERATURE SURVEY

A literature survey was made on all open literature sources using the Aerojet-General Corporation Machine Retrieval System and Card Catalog. All subject matter pertaining to high temperature sensing devices, high temperature measurements, and techniques to obtain high temperatures (above 3500°F in each case) in solid materials was sought and reviewed. In addition to the open literature sources, requests were made to the NASA and DDC agencies for any additional references. A bibliography of the references found is shown in Appendix I. All articles found were primarily concerned with either pyrometric measurements or metallic thermocouple measurements. The references dealing with pyrometric techniques were neither considered nor included in Appendix I.

Kasanof and Kimmel (App I) discussed a different approach to obtaining temperature measurements in solids. They discuss the use of fusible indicators manufactured in miniature pellets for use in the temperature range of 100 to 3000°F. The fusible indicators consist essentially of a group of compounds which liquefy at precalibrated temperatures. No mention was made of the specific compounds used to obtain temperatures to 3000°F. It was mentioned, however, that the compounds used were chemically stable for long-term storage and at elevated temperatures up to their melting points. Also, the same compounds have a low order of toxicity and are relatively inert to most materials of construction in order to avoid reaction with surfaces being examined. The pellets are available in commercial form (1/8 x 1/8 in.) and are intended for use in oxidizing or inert atmospheres when extended heating periods are involved. For the anticipated application here, their approach appears to be limited only by size and the maximum temperature obtained.

III, A, Literature Survey (cont.)

Thermocouples have been the most widely used temperature sensors because of their relative simplicity of construction and availability. Because of an increasing need to obtain reliable high temperatures above 3500°F in both inert and oxidizing environments, some progress has been made in developing thermocouple systems to accurately measure temperatures to 4500°F $\pm$ 50°F.

Tungsten-rhenium alloy thermocouples are the most widely used thermocouples for temperature measurements above 3500°F because of their excellent heat transfer characteristics and high melting point. The temperature-millivolt relationships for these thermocouples have been established by several investigators to 4200°F for tungsten vs tungsten-26% rhenium and tungsten-5% rhenium vs tungsten-26% rhenium, and to 4350°F for the tungsten-3% rhenium vs tungsten-25% rhenium.

To make reliable temperature measurements at 4000°F, consideration must be given to the insulator used in the thermocouple to electrically and thermally separate the thermoelements. Beryllium oxide has been the most widely used thermocouple insulator for high temperature work, but its melting point ($\approx$ 4590°F) limits its usefulness at higher temperatures. Thoria oxide has received some attention as an insulator (m.p. $\approx$ 5500°F), but its uncertainties in electrical properties and compatibility with the refractory metals makes its use questionable.

B. TEMPERATURE MEASUREMENT IN ABLATIVE PLASTICS

To effectively use a sensor system to provide temperature measurements within ablative plastic chars in the upper temperature range of 3500 to 6000°F, a knowledge is required of how ablative plastics perform; how much surface regression and charred material can occur; and what general region

III, B, Temperature Measurement in Ablative Plastics (cont.)

of the char can be expected to reach the subject temperature range. Without this knowledge, many temperature sensors would be wasted in improper locations as the area in question extends inward from the flame surface, seldom exceeds 0.060 in. in depth, and is constantly receding from the original position of the flame surface.

Aerojet has currently instrumented 13 NOMAD nozzles applying over 50 thermocouple plugs each of which contains four thermocouples. This instrumentation has provided considerable insight into the temperature gradient through ablative components.

Figures 1 through 6 are plots of thermocouple data from various NOMAD motor nozzle firings, plotted to show the temperature-time history in depth through the ablative plastics. The postfire surface regression data are also included in the plots. These data have been cross-plotted on the same figure to show the temperature gradient through the char and virgin material at 60 sec. From the measured total surface regression, peak surface temperatures of approximately 6000°F appear to be possible for carbon phenolic, MX4926 (Figure 1), and kraft paper phenolic, FM5272 (Figure 5) at nozzle locations indicated on each figure. Peak surface temperature of 3400°F seems to characterize both asbestos and silica phenolics as shown, respectively, in Figures 4 and 6. Graphite phenolic (Figure 2) and carbon felt phenolic (Figure 3) appear to exhibit surface temperatures up to about 4700°F. Also, it can be noted from the above figures that carbon phenolic (Figure 1) has the largest char thickness (0.190 in.) over the 3000 to 6000°F range, while, of course, silica and asbestos phenolic (Figures 4 and 6) have the least or no char thickness corresponding to this same temperature range.

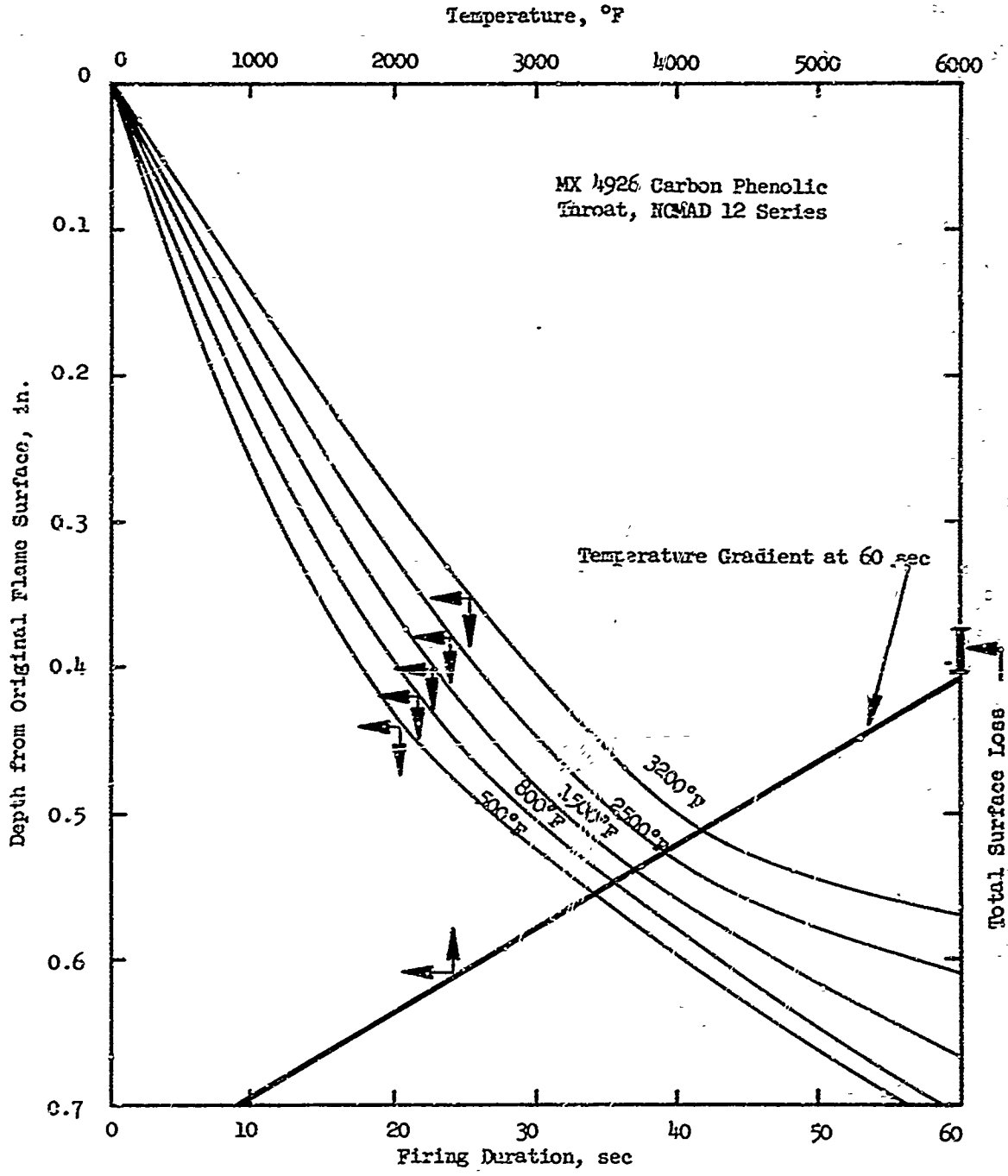

Figure 1. Distance vs Time for Various Isotherms in Carbon-Reinforced Phenolic Material

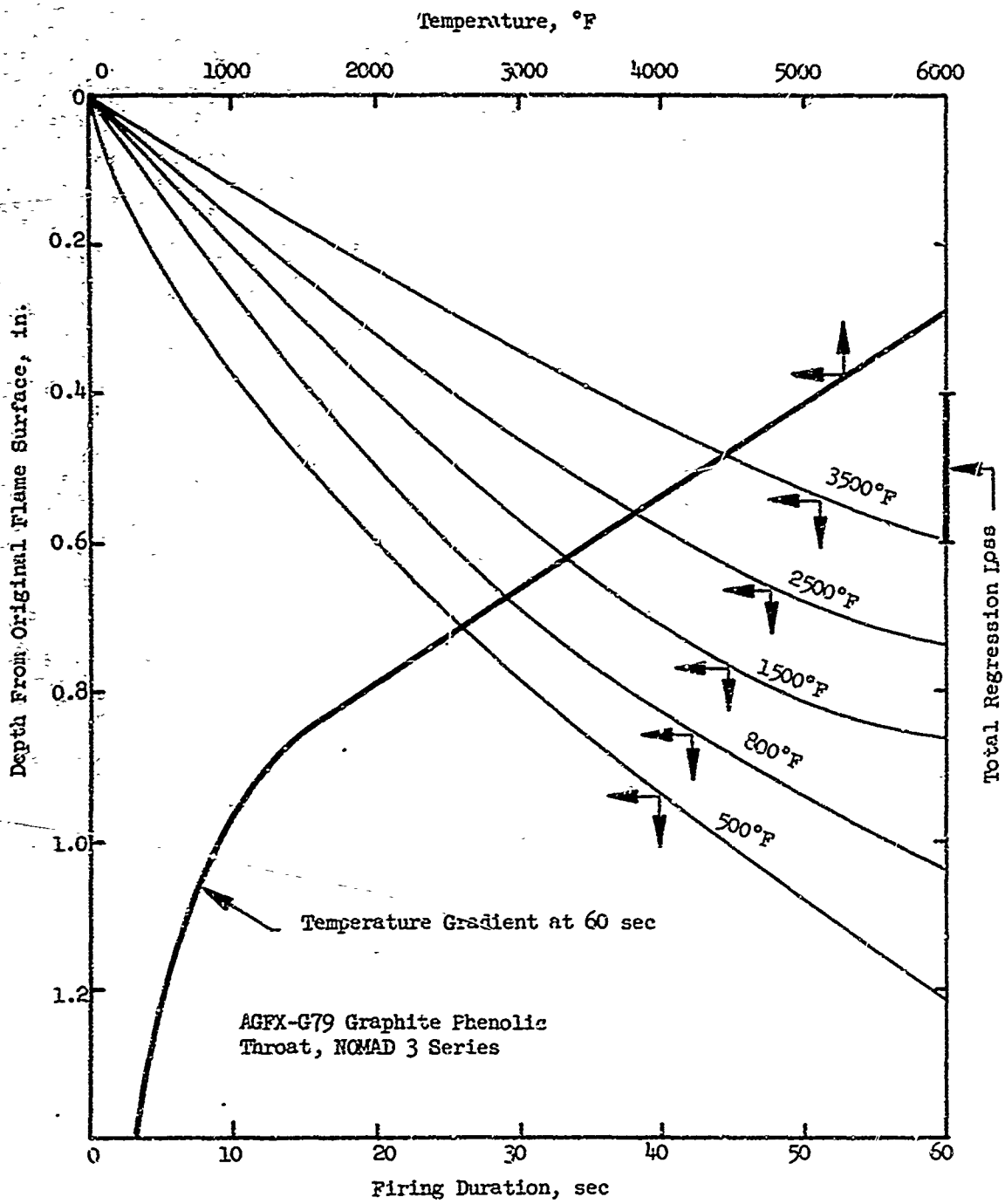

Figure 2. Distance vs Time for Various Isotherms in Graphite-Reinforced Phenolic Material

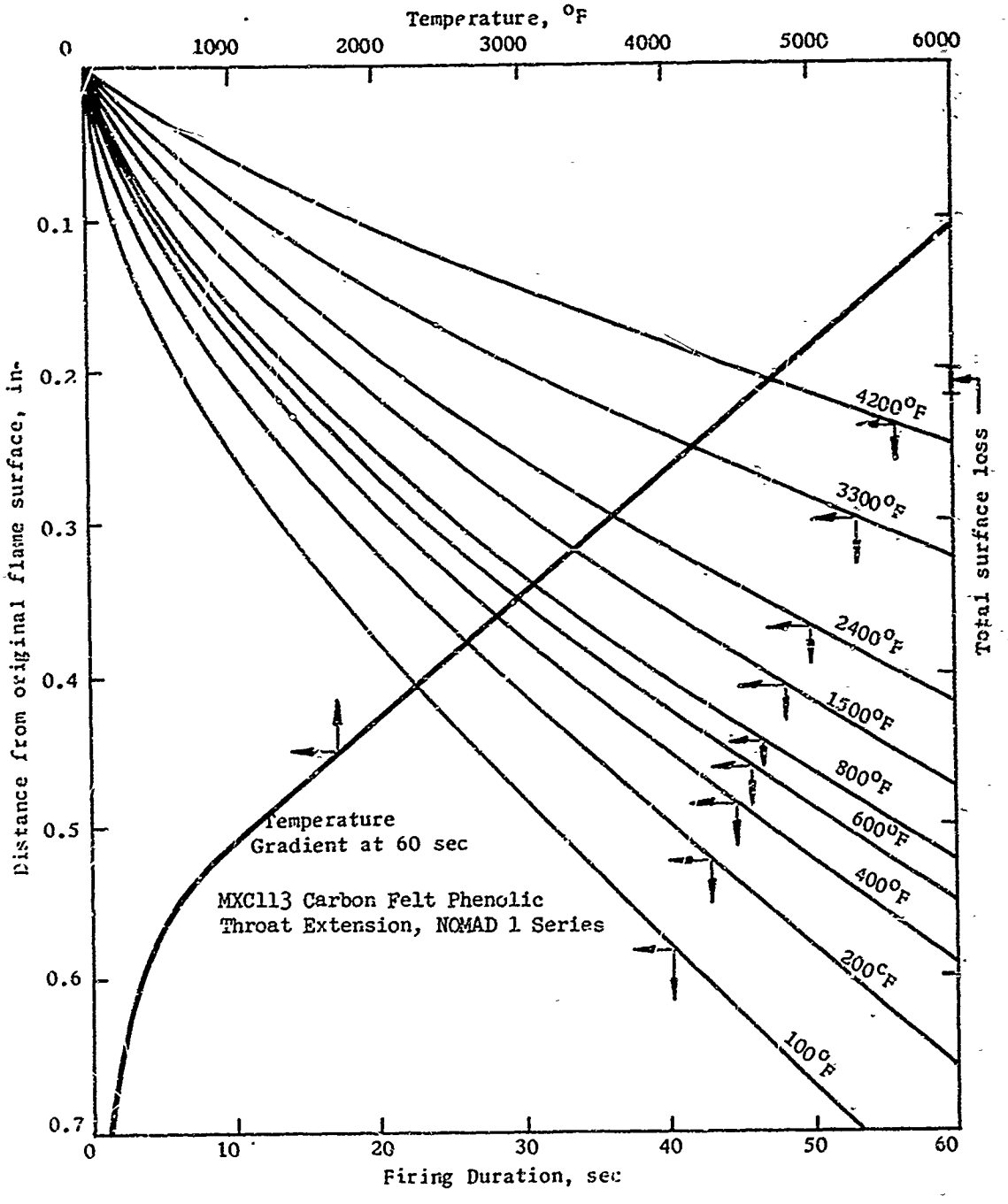

Figure 3. Distance vs Time for Various Isotherms in Carbon Felt Reinforced-Phenolic Material

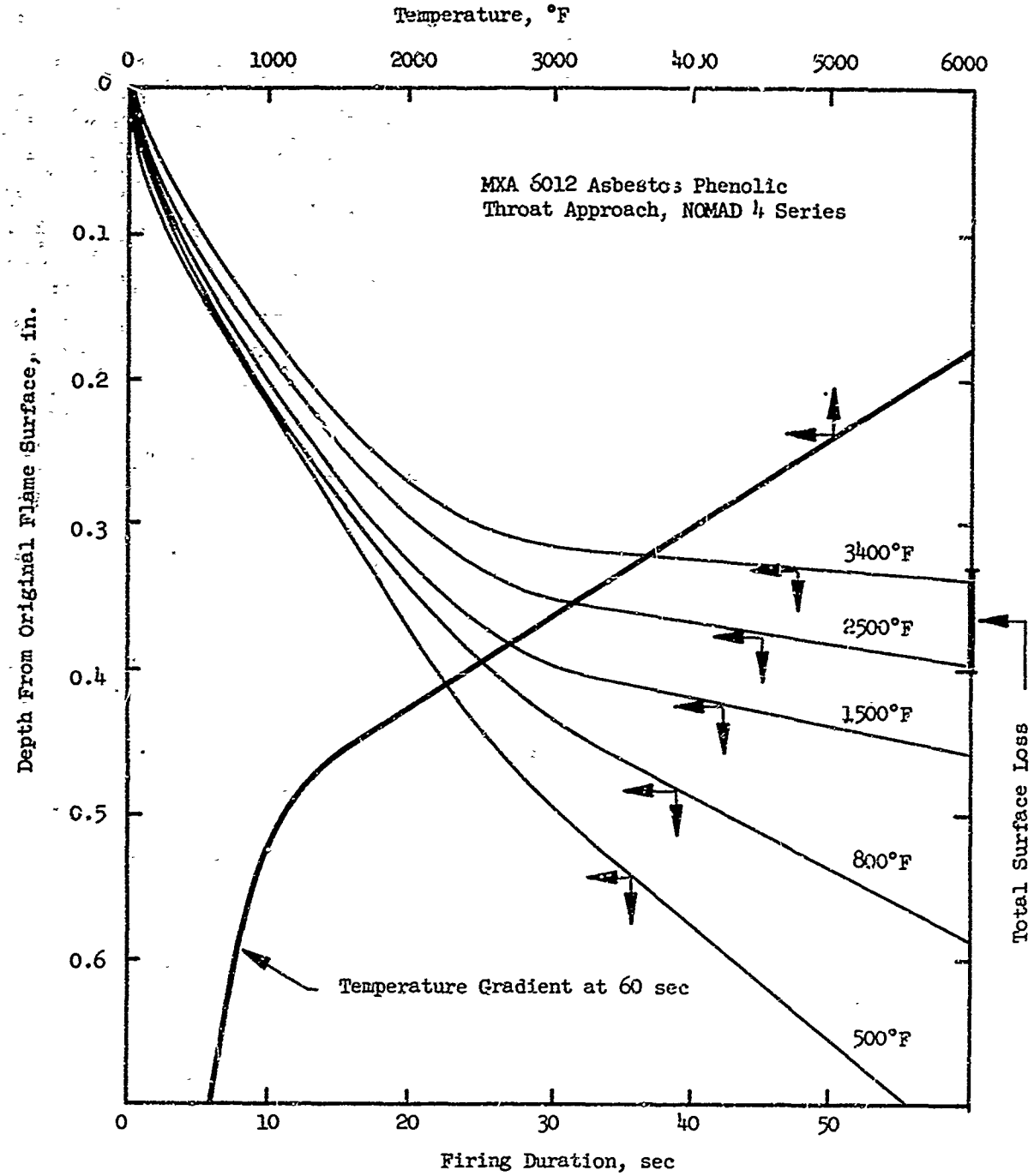

Figure 4. Distance vs Time for Various Isotherms in Asbestos-Reinforced Phenolic Material

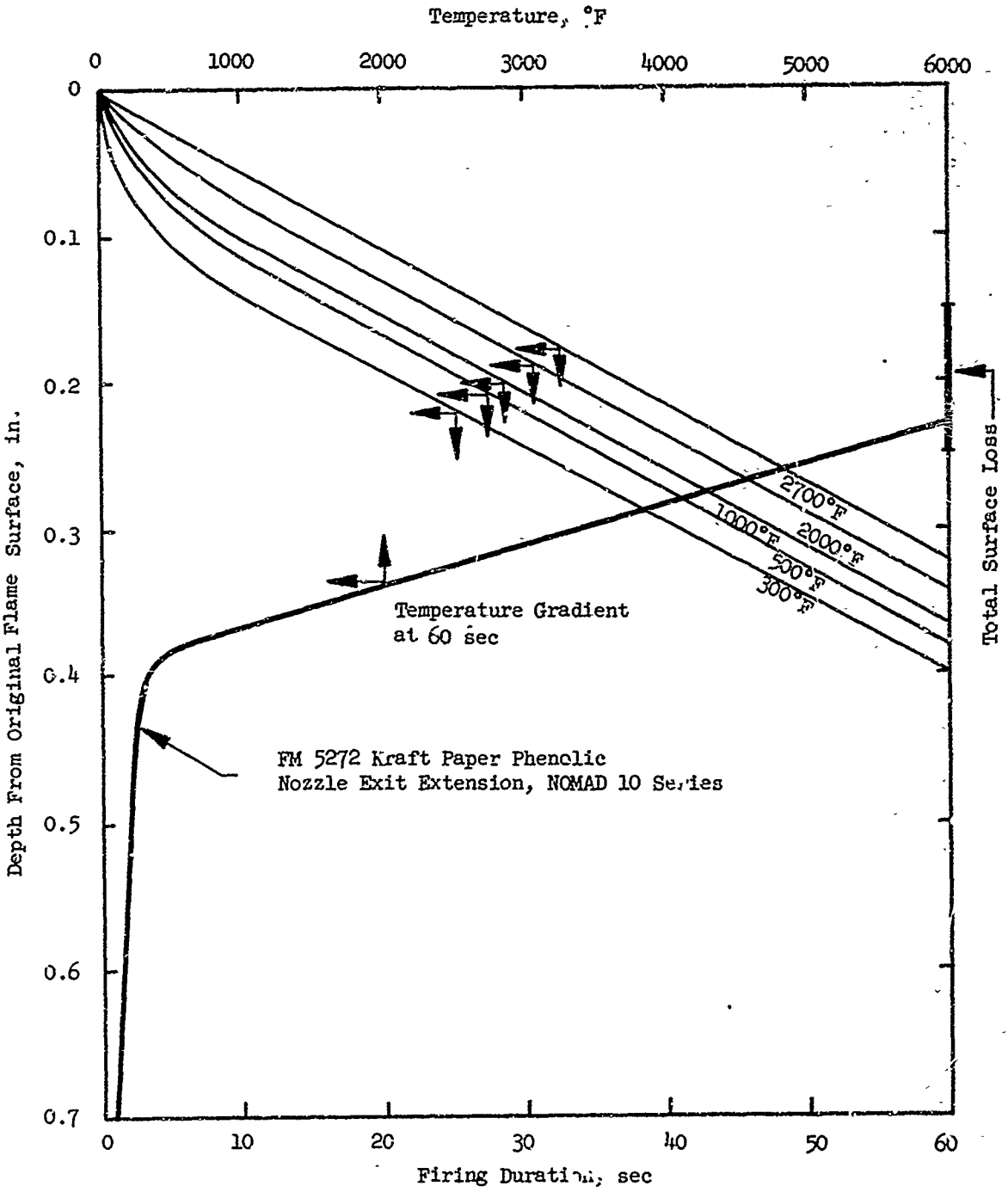

Figure 5. Distance vs Time for Various Isotherms in Kraft Paper Reinforced-Phenolic Material

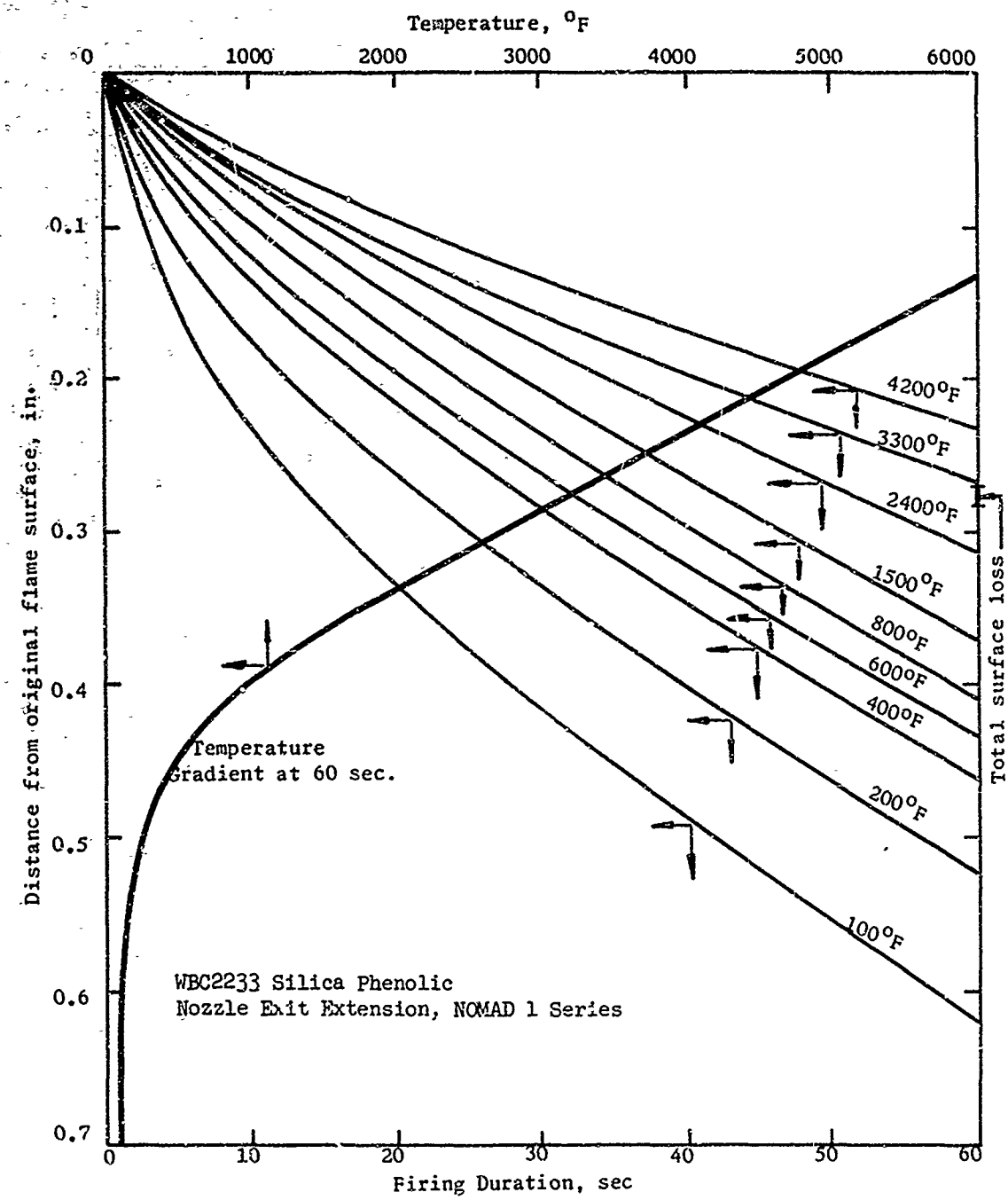

Figure 6. Distance vs Time for Various Isotherms in Silica-Reinforced Phenolic Material

III, B, Temperature Measurement in Ablative Plastics (cont.)

Although the accuracy of the measurements has not been established, it appears that few measurements can be made above 3000°F in the silica and asbestos phenolics. A probable error in this analysis, in addition to that of thermocouple inaccuracy, is char shrinkage.

C. SENSOR MATERIALS SELECTION

The primary criteria for the selection of sensor material systems are:

(1) An irreversible temperature indication that occurs between 3500 and 6000°F,

(2) Chemical compatibility with charred ablative material,

(3) Ease of fabricability into small sensors that will not affect normal heat flow, and

(4) Ease of detection of the irreversible indication.

The governing criterion in the selection of the sensor system is chemical compatibility. First, the container material must be compatible with the charred ablative material in which the temperature sensor is placed and, secondly, the sensor material must be compatible with the container material. The nozzle materials, in which the sensors will be placed, are composite structures which can be considered as being 100% carbon. The only ingredients that are not 100% carbon are the asbestos-reinforced material and the phenolic resins. However, the asbestos melts at <3500°F and the phenolic resin decomposes at approximately 1000°F, leaving behind a carbon residue. Therefore, the sensor container material must be chemically compatible with carbon. Graphite (or carbon) is the only material which can be unequivocally selected as compatible. Ceramic oxides are reduced by carbon and metals are carburized forming low melting eutectics. Chromium, for example, with a melting temperature of 3430°F (ideal for indicating the bottom of the temperature range) will form a eutectic with carbon that melts at 2690°F.

III, C, Sensor Materials Selection (cont.)

By taking advantage of the formation of metal eutectics with carbon, ideal sensor indicators can be made that are compatible with graphite as a container material. The melting of premixed powders of the eutectic will provide an irreversible indication of temperature. A thorough understanding of the phase relationships existing in refractory metals with carbon has been obtained by Aerojet in Contract AF 33(615)-1249. Dr. E. Rudy, et al., has written over 33 reports which are listed in Appendix II documenting the melting temperatures and phase changes that occur in these systems.

In the temperature range of 3500 to 6000°F, Dr. Rudy has found that eutectic reaction rates are extremely fast and occur at precise temperatures. The melting temperatures of 15 selected binary eutectic compositions that melt between 3000°F and 6000°F are listed in Table I. In preparing this list, consideration has been given to all refractory metal carbon eutectics and peritectics that melt between the above temperatures. Where two systems had approximately the same melting temperature, preference was given first to the carbon rich eutectic, then the metal rich eutectic and last the intermediate eutectics and peritectics. Ternary systems were not selected because intermediate reactions make it difficult to select a composition that will give a discrete melt temperature. In the following paragraphs, specific examples of selection considerations are given.

Figure 7 is the phase diagram of the Molybdenum-Carbon system, selected for discussion because four of the selected sensor materials are based on this phase diagram. The mixture of 17 atomic % C and Mo powders will melt upon reaching 2200 $\pm$ 5°C (3992 $\pm$ 14°F). Such a system is relatively insensitive to composition. Ninety percent or more of the powders will melt between 15.3 and 17.9 atomic % carbon. As the temperature is increased above 3992°F, carbon will be picked up from the graphite container and the composition of the melt will change, but will not alter the fact that melting has occurred. It is apparent, however, that care must be taken so that sensors containing molybdenum of different compositions not be mixed.

TABLE I

TEMPERATURE-SENSING MATERIALS

Eutectic Phases	Composition of Eutectic	Melting Temperature °C	Melting Temperature °F
Pt + C	3 At.% C	1732 ± 15	3150 ± 27
Zr + ZrC	5 At.% C	1835 ± 15	3335 ± 27
Mo + β-Mo_2C	17 At.% C	2200 ± 5	3992 ± 9
Nb + βNb_2C	10.5 ± 0.5 At.% C	2353 ± 10	4267 ± 18
ZrB_2 + C	33 ± 2 At.% C	2390 ± 15	4334 ± 27
HfB_2 + C	38 ± 2 At.% C	2515 ± 10	4559 ± 18
α MoC_{1-x} + C	45 At.% C	2534 ± 5	4683 ± 9
VC + C	49.5 ± 0.5 At.% C	2625 ± 12	4757 ± 22
WC_{1-x} + WC	41.0 At.% C	2720 ± 10	4928 ± 18
TiC + C	63 ± 1 At.% C	2776 ± 6	5029 ± 11
Ta + βTa_2C	12 ± 0.5 At.% C	2843 ± 15	5149 ± 27
ZrC + C	64.5 ± 1 At.% C	2911 ± 12	5272 ± 22
HfC + C	65 ± 1 At.% C	3180 ± 20	5756 ± 36
NbC + C	60 ± 1 At.% C	3305 ± 20	5981 ± 36
TaC + C	61 ± 0.5 At.% C	3445 ± 26	6233 ± 47

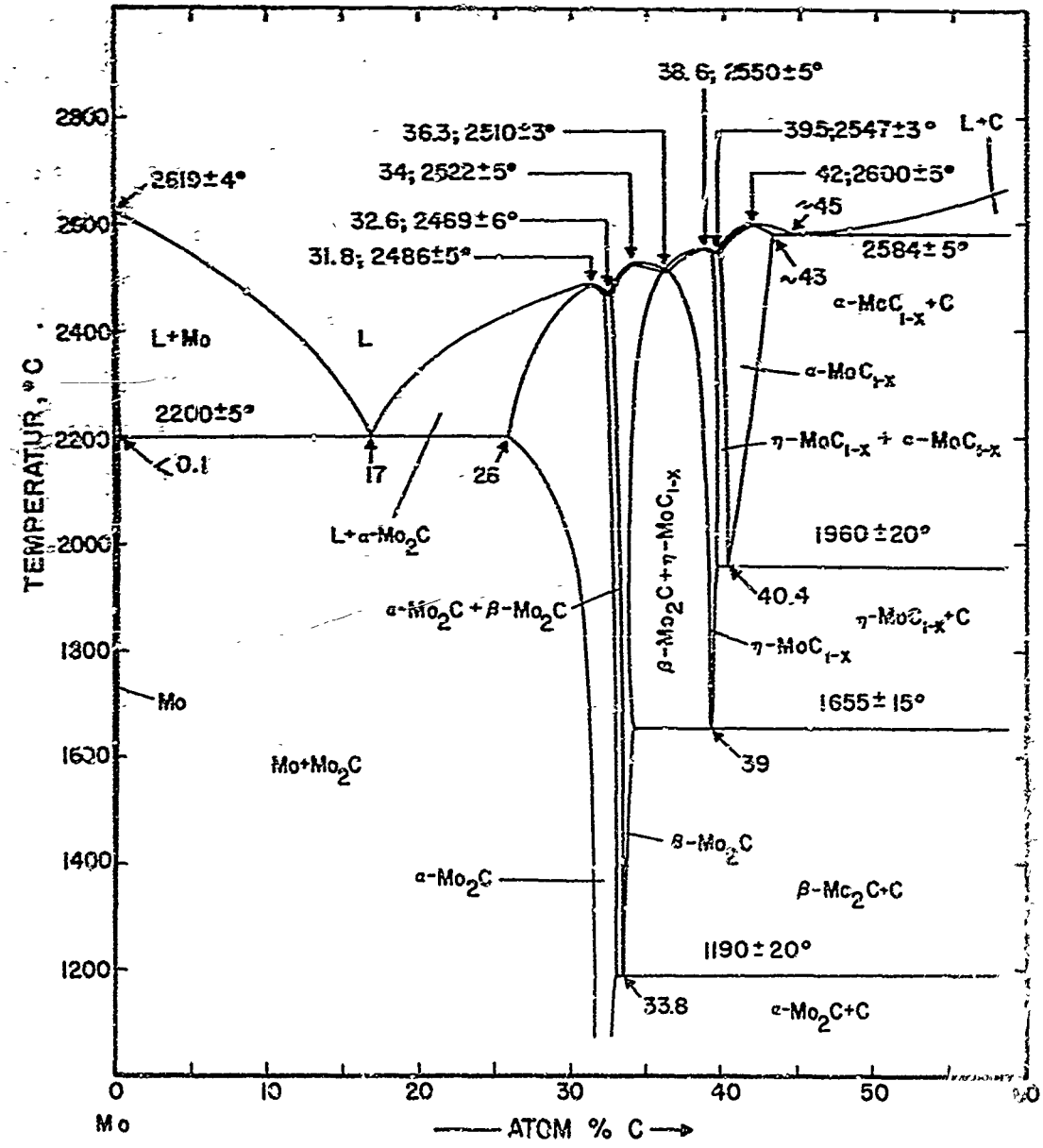

Figure 7. The Phase Diagram of the System Molybdenum Carbon

III, C, Sensor Materials Selection (cont.)

The initial composition of MoC_{1-x} + C will provide the 2584 ± 5°C (4683 ± 19°F) eutectic melt. Like the Mo-rich eutectic, the C-rich eutectic is relatively insensitive to composition. Ninety percent or more of the powders will melt between 44.9 and 50.5 atomic percent carbon. As the temperature increases above 4683°F, the melt will absorb carbon from the graphite container. This absorption of carbon does not alter the fact that melting occurred at 4683°F. The microstructure of the sample would provide a qualitative indication of temperature, but with such limited accuracy as to make the metallographic evaluation not economically feasible.

Composition-control must be maintained more accurately with the intermediate eutectics than with the metal or carbon-rich eutectics. This can be readily achieved by mixtures of the various molybdenum carbide powders. One of these intermediate eutectics was not selected because an intermediate temperature between the 4559°F for HfB_2 + C, and 4683°F for α MoC + C, was not considered necessary.

By comparison of the Mo + Mo_2C and the α MoC + C eutectics, it is apparent that there is a greater permissible composition range with the carbon-rich eutectic than with the metal-rich eutectic. Also, the shifting composition upon superheating the melt makes it easier for subsequent identification of the sensor for the carbon-rich eutectic should a mixup occur. Therefore, in all instances where a carbon-rich eutectic provided the same temperature as a metal-rich eutectic, the carbon-rich composition was selected. In other instances, the simpler system providing a similar temperature was selected.

An example of a temperature range containing a large number of eutectics from which to select is 4910 to 5029°F. These temperatures are provided by the following material mixtures: W+W_2C (4910°F), WC_{1-x}+WC (4928°F),

III, C, Sensor Materials Selection (cont.)

Cs+C (4950°F), β W_2C + WC_{1-x} (4955°F), WC+C (5020°F) and TaC+C (5029°F). Selection of the WC_{1-x}+WC instead of W+W_2C was made because it is the carbon-rich eutectic. TiC+C was selected instead of WC+C because the latter being a peritectic could be easily confused with the WC_{1-x} + WC if a mixup occurred.

Another system, Ir+C (4144°F), is possible but was not selected because minor contamination in the composition markedly decreases the melt temperature. The contaminants present in graphite as minor impurities are such that it would be difficult to control this composition.

The only other system to be given serious consideration as sensor materials are the ternary eutectics. However, melting of the compositions is not as straightforward as it would appear to be from the phase diagrams. A eutectic trough exists between the ZrC + C and HfC + C eutectics in the ternary system so that all temperatures between 5272 and 5756°F appear feasible. Since no binary eutectic exists in this range, utilization of this system would be desirable. However, it has been reported that crystallization, instead of discrete melting, occurs. Should the investigation of sensor response in subsequent tests indicate that it is necessary to develop this type system, more consideration will be given to its evaluation.

III, Technical Discussion (cont.)

D. HEAT TRANSFER ANALYSIS

Heat transfer analyses were performed to determine the influence on the temperature field within ablative materials during a transient heating period after implantation of small temperature sensing devices. The two types of sensing devices considered were encapsulated sensor materials and sheathed and bare-wire thermocouples. The materials considered were a carbon-reinforced phenolic, an asbestos-reinforced phenolic, and a paper-reinforced phenolic. The thermal properties of materials used in this analysis are presented in Table II and in Figure 8.

1. Sensor Element Analysis

The first step of the analysis was to investigate the effect of the parameters listed below on the temperature measurement error encountered with sensor elements.

1. Sensor size
2. Sensor distribution
3. Ablative material properties
4. Contact resistance
5. Gas-side conditions
6. Heat of fusion

The analysis was performed assuming two-dimensional conduction in an axisymmetric coordinate system. Conduction in the region of the sensor was evaluated using the node network shown in Figure 9. This system consists of a 0.55-in. radius cylinder of charred ablative material about 1.5 in. long which is subdivided into 28 cylindrical elements. An adiabatic boundary condition was assumed at the outer radius of the cylinder and at one end,

TABLE II

THERMAL PROPERTIES OF ABLATIVE AND SENSOR MATERIALS

Material	Temp. °F	k, Btu/sec in. °F	C_p, Btu/lb-°F
MX 4926 (Carbon Phenolic)	RT	(See Figure 8)	0.18
Sp.Gr. = 1.23	1000		0.38
	2000		0.48
	3000		0.53
	4000		0.55
	5000		0.56
MXA 6012 (Asbestos Phenolic)		(See Figure 8)	0.28 (assumed constant)
Sp.Gr. = 1.40			
FM 5272 (Paper Phenolic)	4000	2.31×10^{-5} (assumed constant)	Same as MX 4926 (all temp)
Sp.Gr. = 0.40			
G-90 Graphite	3000 to 6000	4.0×10^{-4} (with grain)	-
	3000 to 6000	2.9×10^{-4} (against grain)	-
	RT to 5000		Same as MX 4926
Mo + Mo_2C (17 At.%C)	-	8.4×10^{-4} (Constant values assumed)	ρC_p = 0.027 Btu/in.^{3}-°F

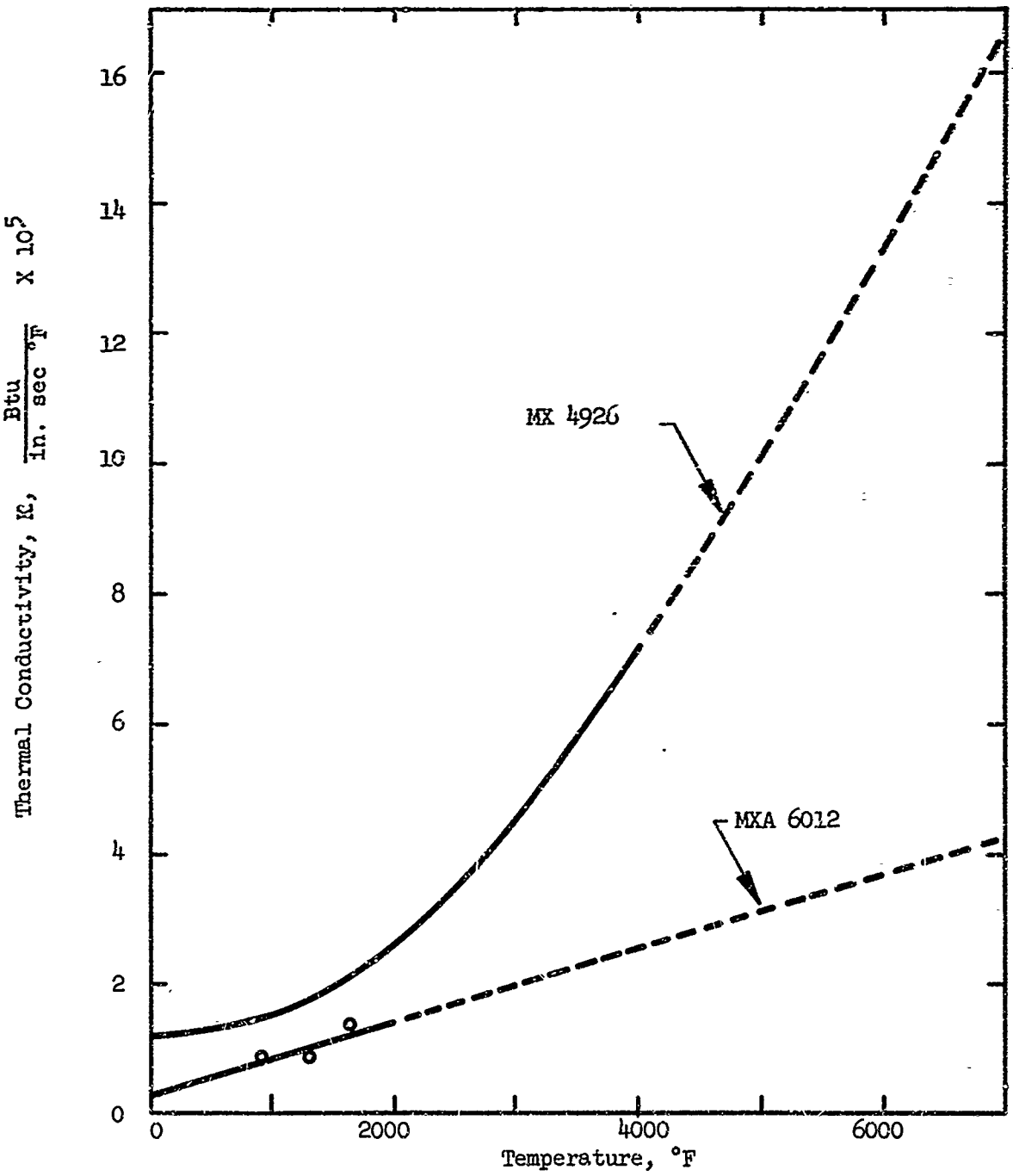

Figure 8. Thermal Conductivity of MX4926 and MXA6012

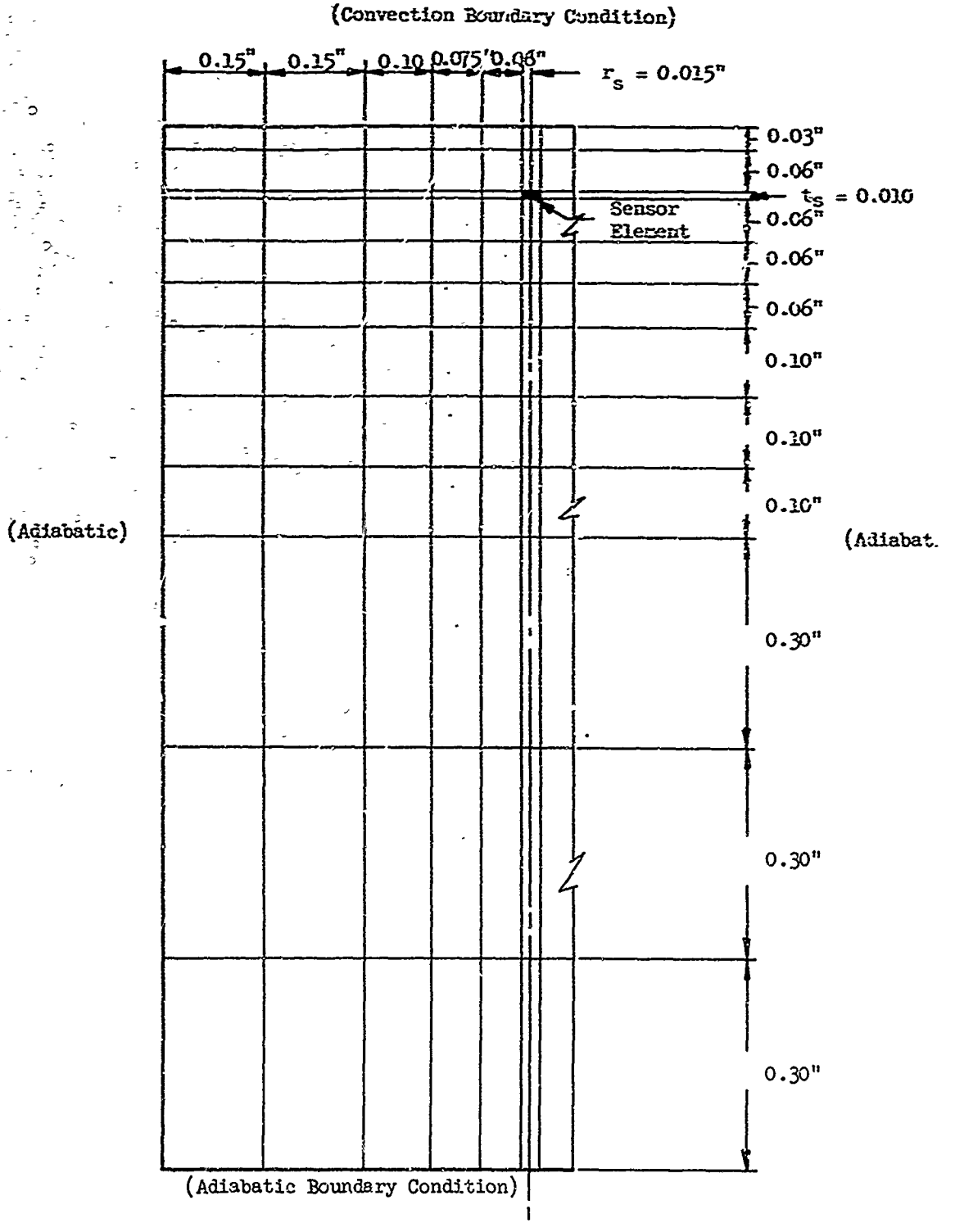

Figure 9. Node Network

III, D, Heat Transfer Analysis (cont.)

and a convective boundary condition was employed at the other end of the cylinder. The sensor was assumed to be embedded 0.09 in. from the heated surface at the center line of the cylinder. The sensor temperature was considered to be uniform and conduction into and out of the sensor was evaluated using the resistance network shown in Figure 10.

Temperature measurement errors were determined by comparing the temperature responses obtained for the sensor and a reference point on the outer cylinder edge when the heated end of the cylinder was suddenly subjected to convective heating. The reference point at the edge of the cylinder was at the same distance from the heated surface as the sensor midpoint, and was sufficiently removed from the sensor so that the temperature response at this point was one-dimensional.

The process of charring was not considered because results from the one-dimensional conduction analyses showed that the temperature distribution in the region of a char layer where the temperature is 3500°F or more (the range of interest for these sensor elements) depends almost completely on the char layer properties and is relatively independent of the virgin material properties and the heat of char. All calculations were performed for the Mo + Mo_2C sensor element material. This mixture appears to have a higher thermal conductivity than the other sensor materials which are planned for use, and the analysis using this material should, therefore, represent the maximum error condition.

The theoretical combustion temperature for propellant ARC-APG114D of 6540°F was assumed as the driving force temperature in the convective boundary condition. A heat-transfer coefficient of 0.00407 Btu/in.^{2} sec °F was also assumed in the majority of the calculations. This value was obtained from the simplified Bartz equation for a gas-side wall

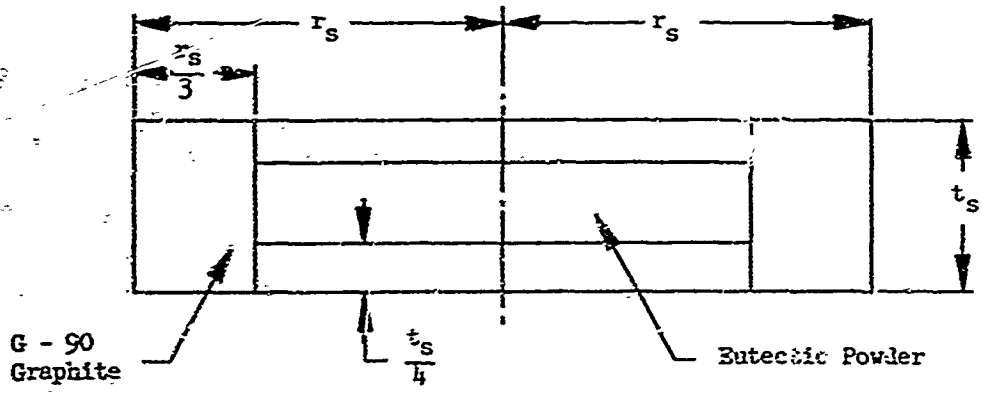

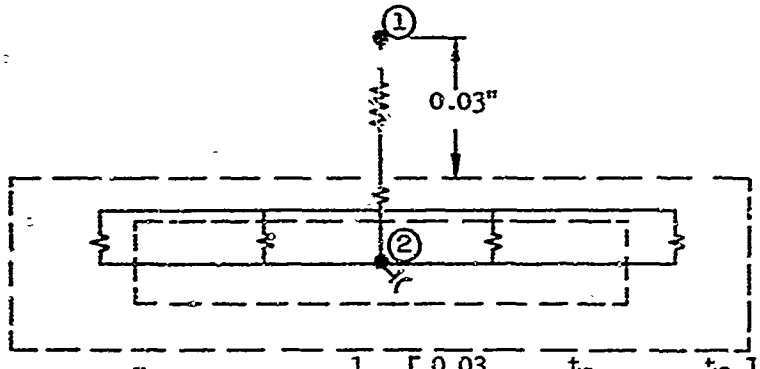

Axial Conduction Network

$$R_{1-2} = \frac{1}{\pi r_s^2}\left[\frac{0.03}{k_{char}} + \frac{t_s}{4k_{graph}} + \frac{t_s}{4\bar{k}}\right]$$

$$\bar{k} = \frac{5}{9}\,k_{graph} + \frac{4}{9}\,k_{powder}$$

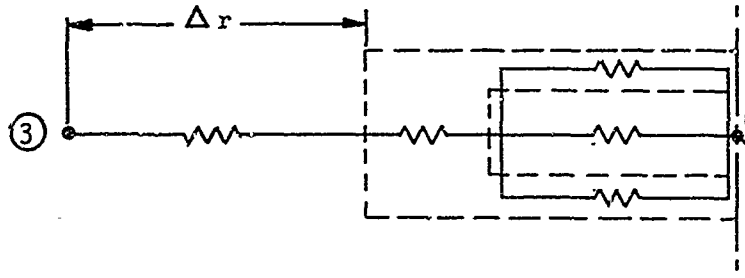

Radial Conduction Network

$$R_{3-2} = \frac{1}{\pi t_s}\left[\frac{1}{k_{mean}} + \frac{1}{5k_{graph}} + \frac{1}{k_{char}}\left(\frac{1}{1 + \frac{2r_s}{\Delta r}}\right)\right]$$

$$k_{mean} = \frac{1}{2}\,(k_{graph} + k_{powder})$$

Figure 10. Sensor Element Configuration

III, D, Heat Transfer Analysis (cont.)

temperature of 4500°F. Solution of the temperature responses was obtained by the use of the Thermal Network Analyzer, Computer Program E12901, on the IBM 360 computer.

a. Effect of Sensor Size

The effect of sensor diameter and thickness on the measurement error for a single sensor embedded in ablative material was investigated for diameters ranging from 0.03 to 0.10 in. and thicknesses ranging from 0.01 to 0.03 in. The results, as shown in Figure 11, indicate that the diameter has a significant effect on the measurement error and that small diameters are desirable. At the 3500°F temperature level for a 0.01-in.-thick sensor, an error of 10 to 40°F was indicated for a 0.03-in.-dia sensor and an error of 25 to 130°F was indicated for a 0.10-in.-dia sensor. The larger errors were obtained for the material (FM5272) with lowest thermal conductivity at high temperatures. The error does not appear to increase with thickness appreciably for the range covered; however, a thickness as small as practical considerations will allow, seems appropriate from the standpoint of minimizing the uncertainty involved in relating the sensor reading to a particular point in the char layer.

A general trend toward decreased error at the higher temperatures is indicated in Figure 11. This is apparently due to the decreased temperature gradient in the region of the sensor at the higher wall temperatures.

b. Effect of Sensor Distribution

The feasibility of stacking sensor elements, i.e., placing one above the other and separating them with a disk of ablative material, has also been investigated (a node network similar to that shown in Figure 9 was used). Figure 12 shows the results obtained for two stacked sensors 0.03-in. dia

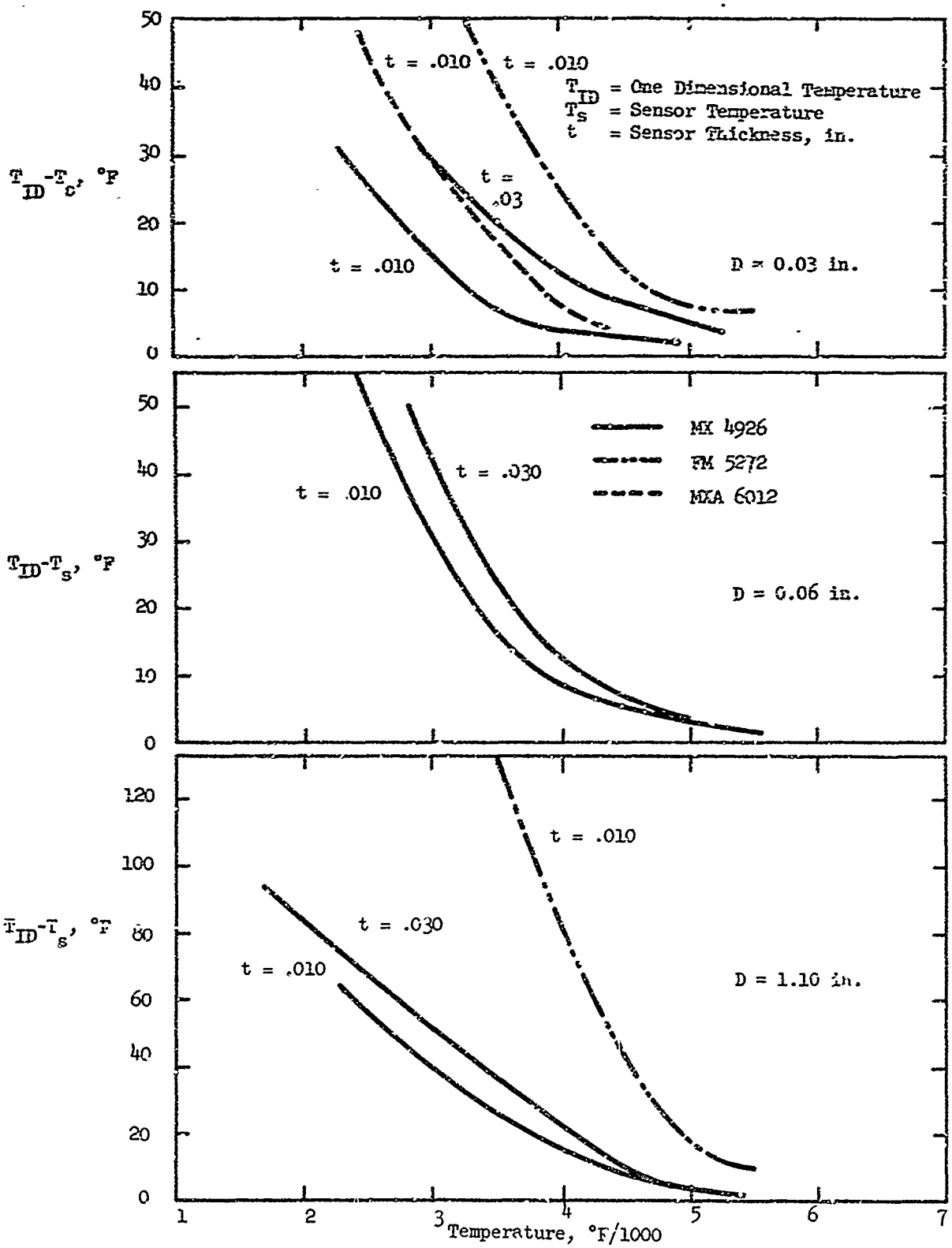

Figure 11. Effect of Diameter, Thickness, and Ablative Material on Sensor Error

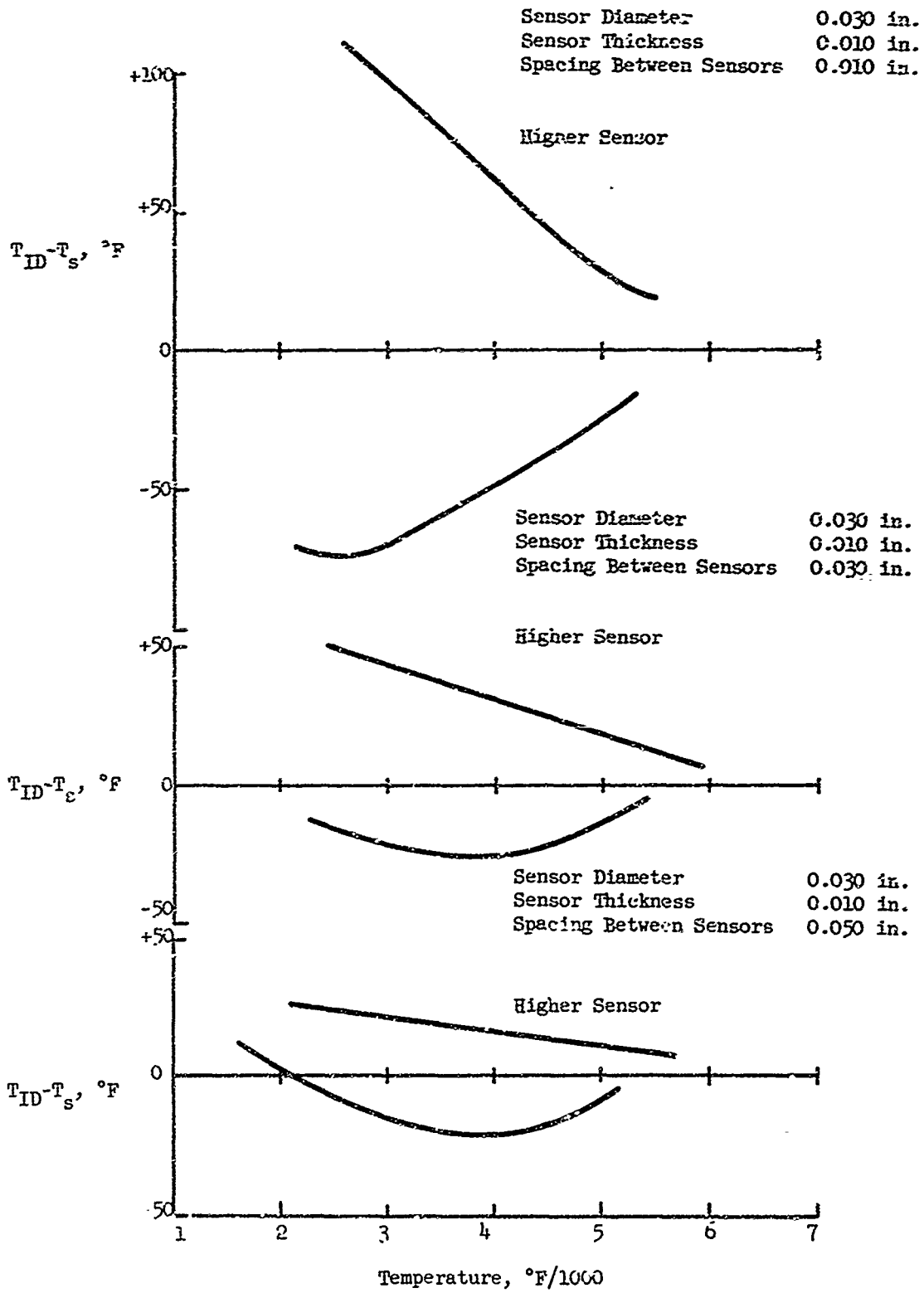

Figure 12. Errors for Two Stacked Sensors in MX4926

III,D, Heat Transfer Analysis (cont.)

by 0.01-in. thick, embedded in MX4926 material and separated by 0.01-, 0.03-, and 0.05-in.-thick ablative disks. It is apparent that the error decreases with increasing separation thickness and that an allowable error of ±50°F is obtained for separation distances of 0.03 in. or greater. The general trend of the results shown in Figure 12 is that the upper sensor (nearest the heated surface) tends to read low while the lower sensor tends to read high. These upper sensor results are similar to those obtained for a single sensor (Figure 11). The relatively high temperature of the lower sensor is due to the relatively low thermal resistance of the upper sensor.

An analysis of three stacked sensors has also been conducted. Sensor diameters of 0.03 and 0.10 in. by 0.01 in. in thickness were evaluated in MX4926 and FM5272 char material at separation distances of 0.03 in. The results as shown in Figure 13 indicate that, as in the single sensor case, large errors are encountered with a larger sensor diameter and in the lower thermal conductivity materials. The maximum error for the 0.03-in.-dia sensor ranges from 40 to 75°F at 3500°F while errors from 100 to 300°F are indicated at this temperature for the 0.10-in.-dia case.

The minimum radial spacing of sensor elements is also of interest from a design standpoint so that a relatively large number of sensors can be installed in a reasonably small area. Radial temperature distributions obtained from the midpoint plane of the sensor elements in the single sensor analysis indicate that the perturbation produced by the sensor is approximately 10°F or less if a minimum radial spacing of one diameter is maintained.

c. Effect of Contact Resistance

The effect of contact resistance at the graphite/ablative material interface (outer surface) and the eutectic powder/graphite interface (inner surface) has also been investigated. A precise prediction of the contact

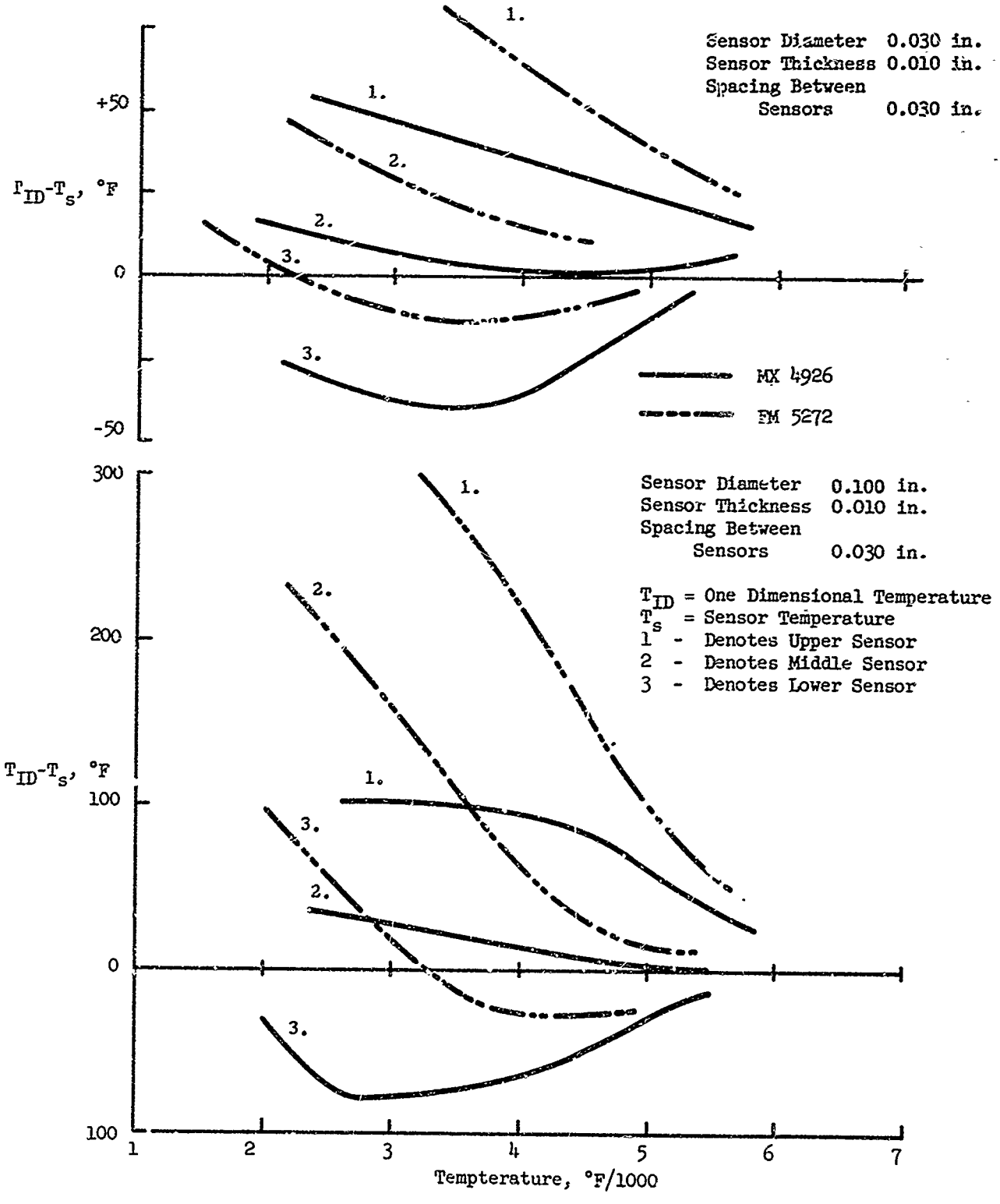

Figure 13. Errors for Three Stacked Sensors in MX4926 and in FM5272

III, D, Heat Transfer Analysis (cont.)

resistance is difficult; however, previous studies (Ref 1) on bonded surfaces and metal to graphite joints indicate that contact conductance values ranging from 0.002 to 0.020 Btu/in.^{2}sec°F can be expected.

The results obtained from a single 0.03-in.-dia by 0.01-in.-thick sensor show that incorporation of the higher contact conductance value (lowest contact resistance) into the analysis does not yield an error appreciably higher than was obtained assuming no contact resistance. As shown in Figure 14, a 25°F error is indicated at 3500°F for this case while a 10°F error was obtained previously. However, the 0.002 Btu/in.^{2}sec°F contact conductance value (highest contact resistance) produces a significantly larger error; a 135°F error is indicated at 3500°F temperature. Similarly, a 100°F error at 3500°F is indicated for the case where contact resistance is neglected on the inner surface and where the lower contact conductance value is assumed on the outer surface.

d. Effect of Gas-Side Conditions

The effect of the gas-side heat transfer coefficient on the temperature response of a sensor was investigated by obtaining temperature-sensor errors for a 0.03-in.-dia by 0.01-in.-thick sensor with heat-transfer coefficients ranging ±50% of the nominal value (0.00407 Btu/in.^{2} sec °F). The results of this analysis, shown in Figure 14, indicate that essentially identical temperature errors were obtained for the range of values chosen for the heat transfer coefficient. Therefore, the results appear applicable for both planned nozzle instrumentation locations since the heat transfer coefficient at these two locations is not expected to differ from the nominal value by more than 50%.

Ref (1) Experimental Interface Heat Transfer Contact Coefficients in the Minuteman Solid Rocket Nozzle by E. J. Gilchrist, Contract No. AF 04(694)-258, July 1964.

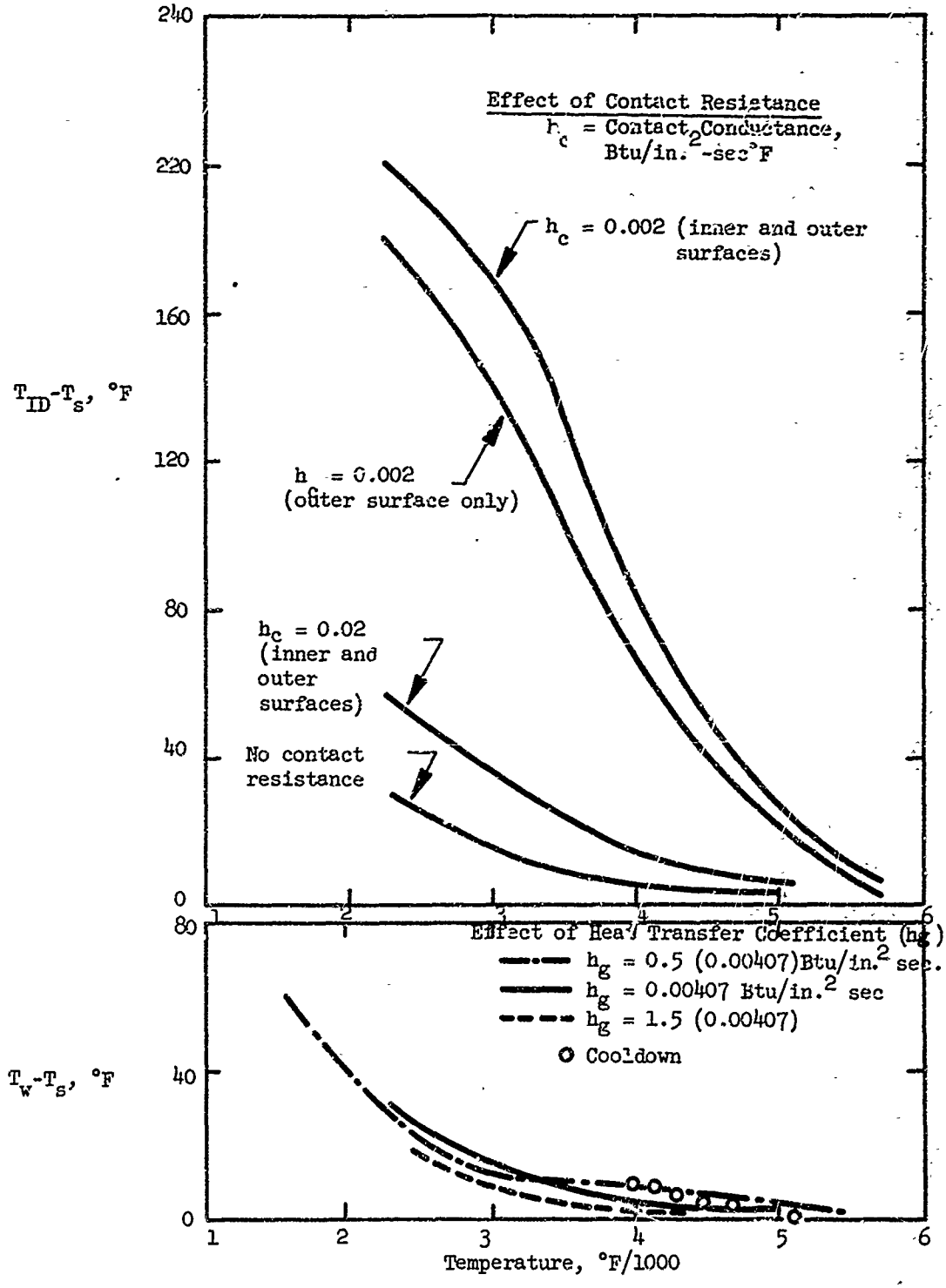

Figure 14. Effect of Contact Resistance and Heat Transfer Coefficient on Sensor Error in MX4926

III, D, Heat Transfer Analysis (cont.)

In addition, the temperature history of the sensor during cooldown of the ablative wall was investigated. The results indicate that at shutdown the sensor temperature will begin to decrease immediately at a slightly faster rate than the ablative material at the same distance from the heated wall as the sensor midpoint (see Figure 14). No unusual increases in sensor temperature were indicated and, therefore, no erroneous temperature indications as a result of postfire phenomena are expected.

e. Effect of Heat of Fusion

The perturbation in temperature distribution produced by fusion of the sensor powder has been found to be small. This is demonstrated in Figure 15 which shows the results obtained in an analysis of three stacked sensors embedded in MX4926. Each sensor in this analysis is 0.03-in. dia, 0.010-in. thickness, and contains Mo + α Mo_2C as sensor material. Arbitrary fusion temperatures of 3500 and 4500°F were assumed for the upper and middle sensors and the sensor thermal properties were assumed to be unaffected by the fusion process. A heat of fusion of 15 Kcal/mole was also assumed as a representative value for all sensor materials.

These results indicate that a period of 0.25 to 0.5 sec is required to completely fuse the sensor depending on the magnitude of the local heat flux. It is apparent that at the higher heat fluxes, the sensor temperature can be as much as 200°F lower than the surrounding ablative material. This temperature difference decreases rapidly, however, as soon as the fusion process is completed since the lower sensor temperature produces relatively high transfer rates from the surroundings to the sensor. Sensor temperatures identical to those obtained without considering fusion effects are achieved within about 1 second after fusion begins.

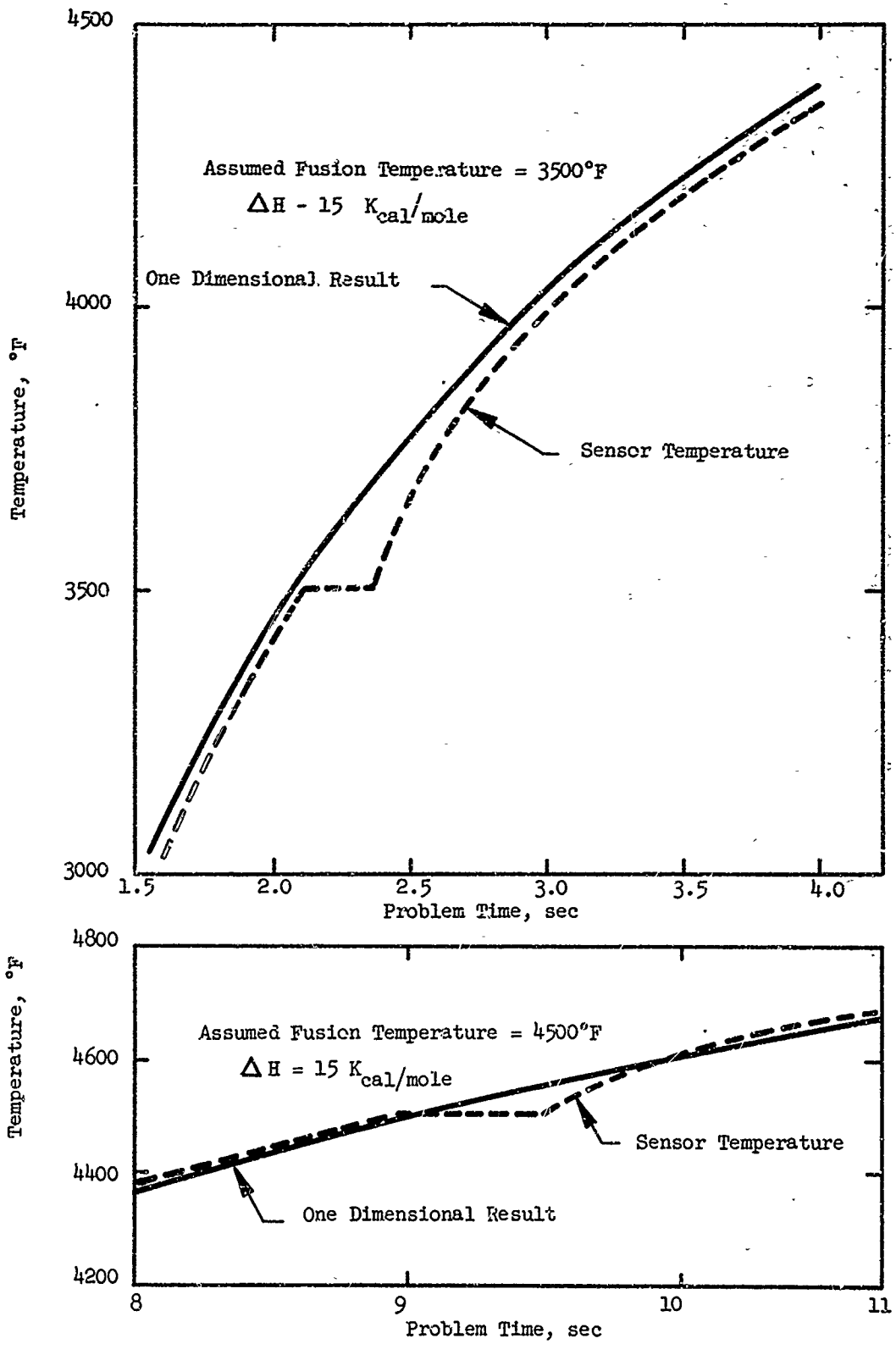

Figure 15. Effect of Heat of Fusion on Sensor Errors

III, D, Heat Transfer Analysis (cont.)

f. Effect of a Moving Boundary

The effect of a moving gas-side surface on sensor response has been evaluated for an 0.030-in.-dia 0.010-in.-thick sensor. MX 4926 and FM 5272 char materials were considered. This effect was investigated using a node network similar to that shown in Figure 9, except that regression of the gas-side surface was simulated by assuming that the layer of char material adjacent to the gas-side surface shrinks at a constant rate. The shrinkage was accounted for by varying the thermal resistance and capacitance of this layer with time. Previous experience in the NOMAD firings indicated that surface regression rates of 0.003 in./sec and 0.012 in./sec were appropriate for MX 4926 and FM 5272 char layers, respectively, and these values were employed in the analysis. A fixed surface temperature of 4000°F and constant thermal properties for the char material and sensor material were also assumed (4000°F thermal properties were used).

The results of the moving boundary analysis along with those obtained for a fixed boundary (also at a 4000°F constant temperature) are shown in Figure 16. They indicate that the effect of a moving boundary on sensor error is relatively small. An additional error of about 20°F is indicated for a sensor in FM 5272 char material, while the effect is essentially negligible for a sensor embedded in MX 4926 char. The higher additional error for FM 5272 char is probably due to the higher regression rate assumed for this material.

Figure 16 results are comparable to the results obtained in the single sensor analysis (Figure 11) in which a fixed boundary and a convective boundary condition were employed. Somewhat lower sensor temperatures are indicated in Figure 16; however, this is inherent in the assumption of a 4000°F wall temperature. Wall temperatures on the order of 6000°F were calculated in the single sensor analysis with a convective boundary condition.

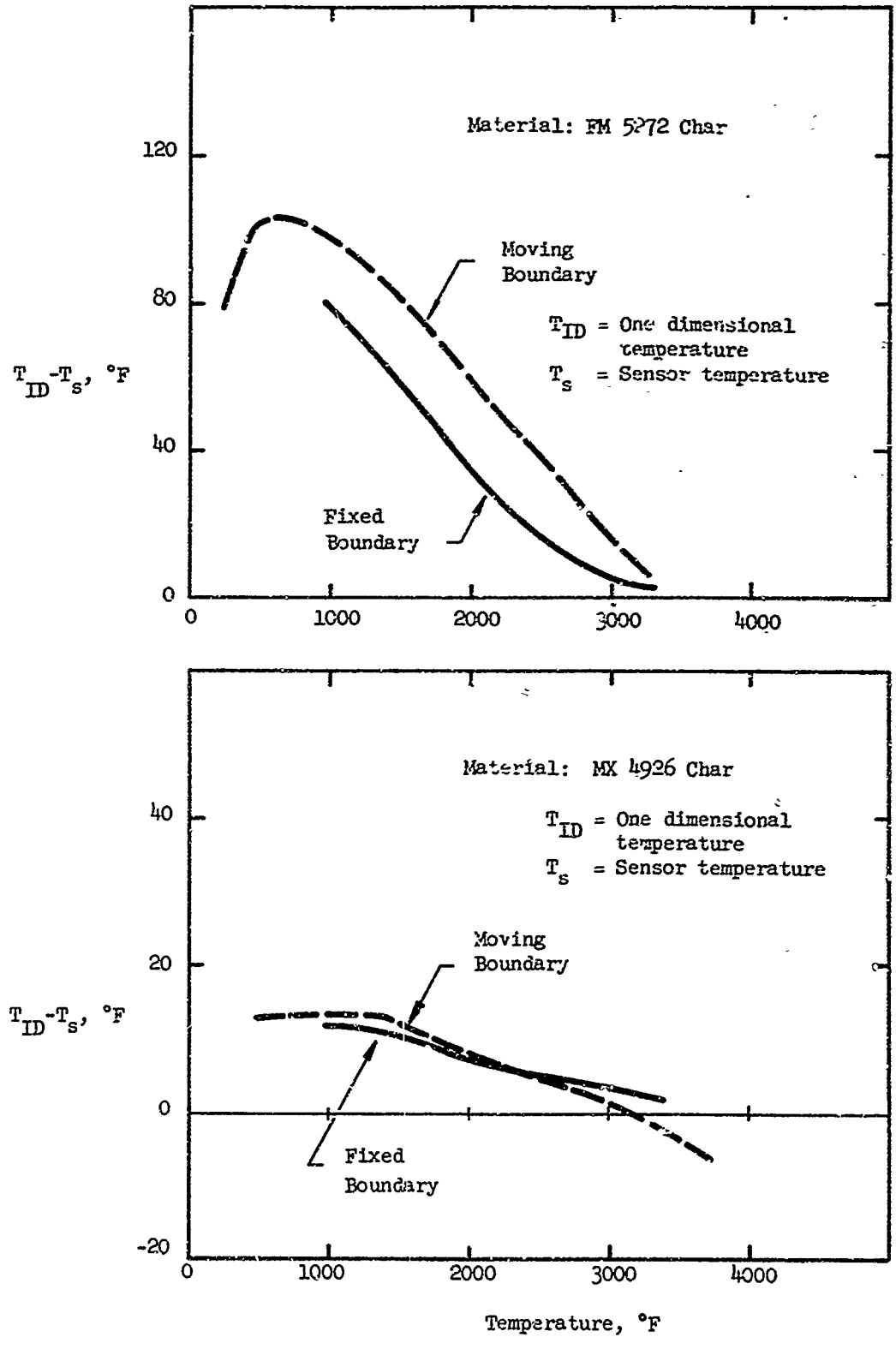

Figure 16. Effect of Moving Boundary on Sensor Response

III, D, Heat Transfer Analysis (cont.)

2. Sheath and Bare Wire-Type Thermocouple Analysis

This section considers the errors that can be associated with sheath-type and bare wire-type thermocouples. These errors arise first because the thermocouple influences the local wall temperature by removing heat from it, and second, because the thermocouple junction temperature differs from the adjacent wall temperature due to less-than-perfect contact between the two. Both types of errors are magnified when the difference between the thermocouple and wall conductivity is large, as in the case with low conductivity ablative materials. The problem, moreover, is a transient one -- the size of the error depends on the transient nature of the heat flux, rather than solely on temperature level -- since ablative materials are characteristically used in a transient mode of operation.

The following cases were analyzed:

1. single sheath-type thermocouple in MX4926;
2. single bare wire-type thermocouple in MX4926;
3. two sheath-type thermocouples in MX4926;
4. single sheath-type thermocouple in MX4926 with different gas-side boundary conditions
5. single sheath-type thermocouple in MX4926 with contact resistance between couple and wall considered;
6. single sheath-type thermocouple in MXA6012.

Cases 1 and 2 (single sheath and single bare wire) serve as base cases. The error associated with the single bare wire was found to be negligible and consequently no variations (multiple couples, different materials or boundary conditions) were investigated. The error possible with a single sheath-type thermocouple is not negligible and hence this type is considered further; specifically, the effect of multiple couples, less severe gas-side boundary conditions, different materials, and the inclusion of an assumed

III, D, Heat Transfer Analysis (cont.)

contact resistance between the thermocouple and the wall. The other material treated, MXA6012, has the lowest conductivity of the three materials of interest, while the HX4926 has the highest; thus, the selection brackets the range of errors that can be expected. Figure 17 shows the two types of thermocouples.

The heat-transfer studies are based on standard finite difference techniques for representing the physical system in terms of a lumped parameter nodal network. Mass is represented as discrete points of thermal capacitance, and heat transfer between points is defined in terms of thermal resistance. Solution of the transient temperature response of the nodal points is by a Thermal Network Analyzer program on the IBM 360 computer.

Figure 18 shows a portion of the nodal point network used in analyzing the sheath-type thermocouple. It is a three-dimensional representation, whose overall dimensions are 1.5 in. thick, 0.5 in. wide, and 1.5 in. deep. The thermocouple junction is located 0.3 in. from the gas-side. The figure is not drawn to scale: except for the gas-side (top), the boundaries are treated as adiabatic; this ignores any heat losses from the back-side (bottom), and assumes that the thermocouple is isolated sufficiently not to influence the far-wall temperatures, and further, that the thermocouple lead normal to the gas-side defines two planes of symmetry that quadrisect the lead. While symmetry in fact prevails only in one plane, the discrepancy is slight.

The relative coarseness of the nodal network is justified by the inherent limitation in fixing the gas-side boundary condition as well as the material thermal properties. Even so, the thermal model involves some hundred capacitances and three hundred resistances. Temperature dependence of material properties is accounted for in this analysis.

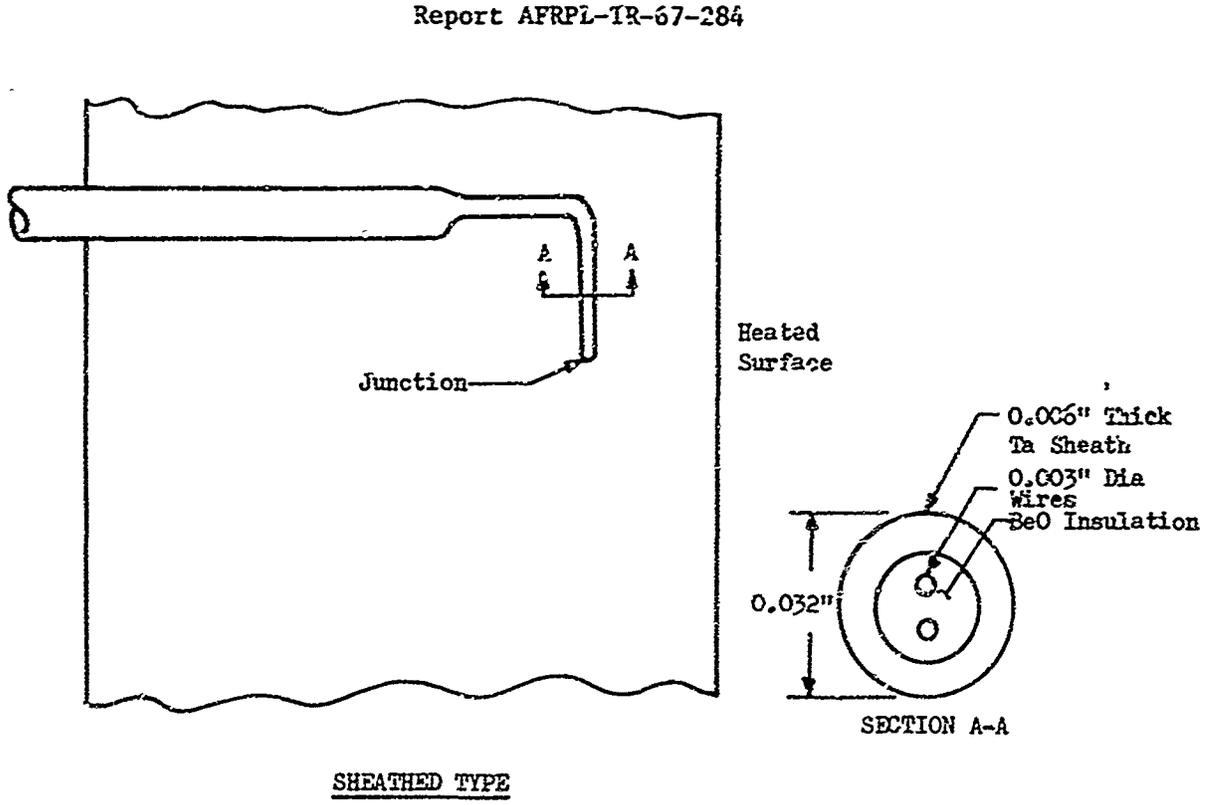

SHEATHED TYPE

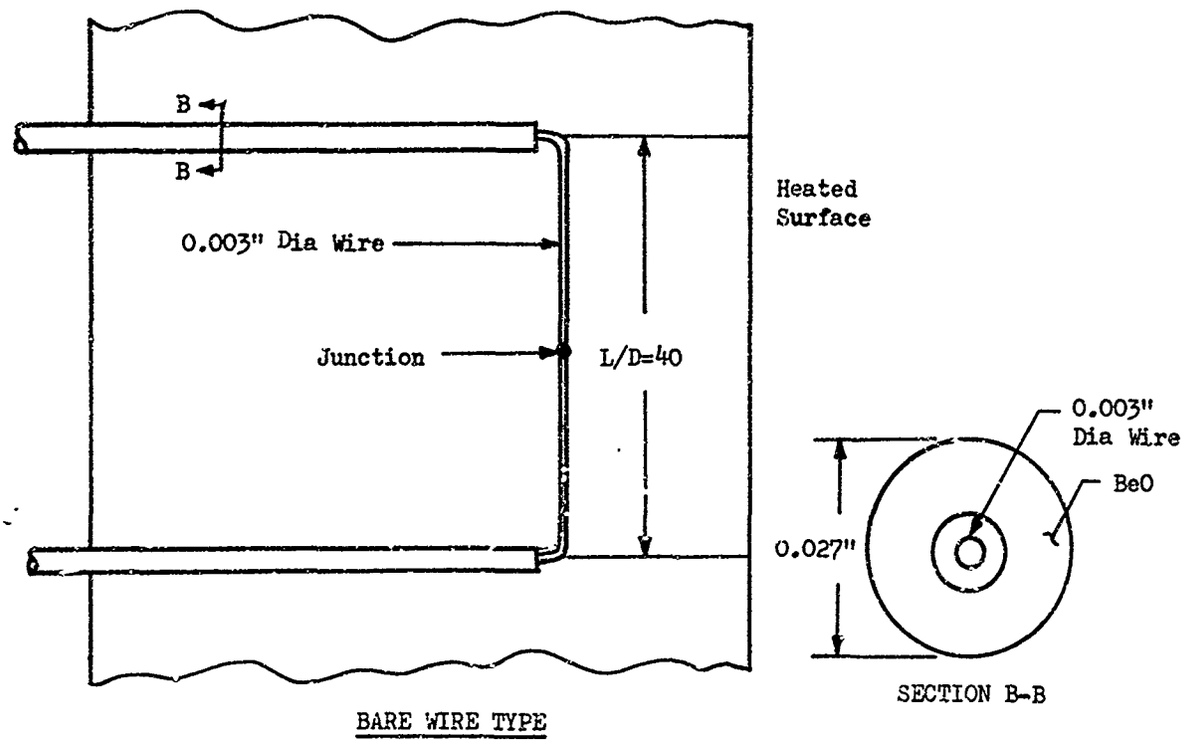

BARE WIRE TYPE

Figure 17. Sheathed and Bare-Wire Type Thermocouples

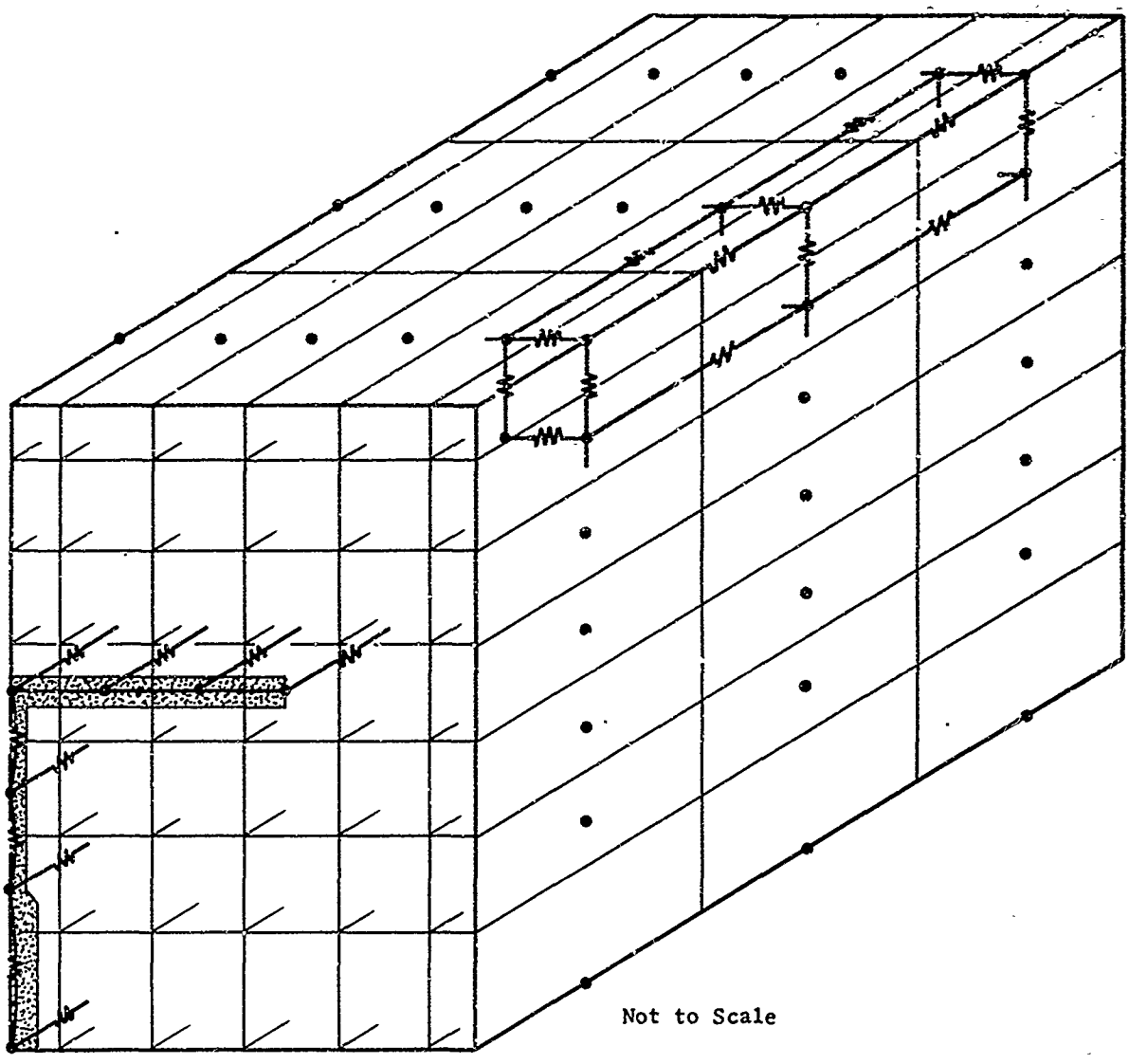

Figure 18. Nodal Network Used for Analysis of Single Sheathed-Type Thermocouple

III, D, Heat Transfer Analysis (cont.)

The capacitance of the thermocouple itself could not be included. When very small capacitances are treated exactly, stability requirements in an explicit time differencing scheme such as that used in the Thermal Network Analyzer necessitate correspondingly small time steps in the calculational procedure. This causes excessive computer run time. The error involved in ignoring the capacitance is not great, and in fact is "conservative", in that it overstates the difference between the thermocouple junction and the adjacent wall temperature. Without capacitance, the predicted wire temperature is less than it would be with capacitance because axial heat flow in the wire can be more readily accommodated. Since the junction temperature lags the adjacent wall material temperature in any event (i.e. is less than), the difference between the two temperatures is predicted to be greater when the wire capacitance is excluded.

Material properties used for the ablative materials are given in Table II. Properties of thermocouple materials are given in Table III. For the sheath-type thermocouple the tantalum and beryllium oxide conductivities are lumped into an effective conductivity; the temperature variations of the two compensate to yield an almost-constant value of 0.00075 Btu/in.-sec°F. The lead wire conductivity is not included in the effective conductivity (which is based on the heat flow area) because the heat flow area is relatively small. For the bare wire-type thermocouple, the lead wire conductivity is considered to be a constant value of 0.0014 Btu/in.-sec°F, and the beryllium oxide conductivity is again in accordance with Table III. The effect of the gap between the lead wire and the beryllium oxide is not treated. In effect, the lumping of conductivities and exclusion of gap resistance presumes that heat flow is strictly axial, or, equivalently, that there is no radial temperature gradient.

TABLE III

THERMAL PROPERTIES OF THERMOCOUPLE MATERIALS

Temperature, °F	k_{Ta}, Btu/in.-sec °F	k_{BeO}, Btu/in.-sec °F
0	0.0008	0.0030
500	0.0008	0.0017
1000	0.0009	0.0008
2000	0.0010	0.0003
4000	0.0011	0.00018

The gas-side film coefficient has a value of 0.00407 Btu/in.^{2}sec°F, as based on the simplified method of Bartz. Recovery temperature is 6540°F.

a. Single Sheath-Type Thermocouple in MX4926

Figure 19 shows the predicted temperature response of the sheath-type thermocouple junction and a point far removed from it, but at the same distance from the gas-side surface. The difference between the two is the error that can be ascribed to this type of thermocouple in this particular material (MX4926), for these particular gas-side heating conditions, on the basis of the assumption that perfect thermal contact exists between the couple and the wall.

Figure 20 shows the error as a function of time. The spike to 100°F and subsequent reduction in error to roughly 30°F is due to the change in wall properties as the material chars; the char conductivity is higher than the virgin material conductivity and hence the heat loss via the thermocouple is relatively less. This is seen on Figure 21, where thermocouple error versus wall temperature for the single sheath-type is plotted. This plot applies only to these particular conditions and not necessarily to any others, although the trend is typical.

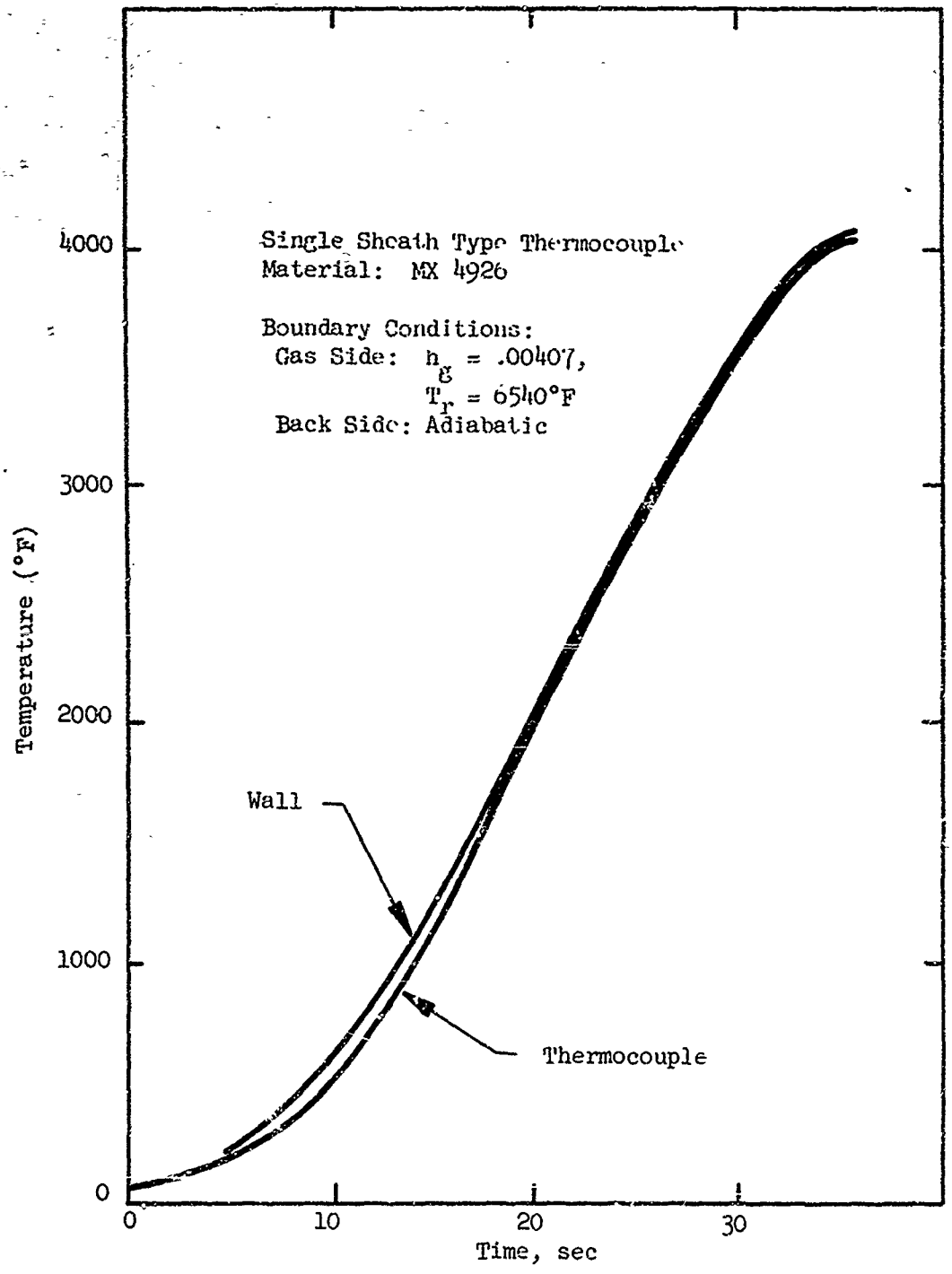

Figure 19. Predicted Temperature Responses Thermocouple Junction and Unaffected Wall at a Depth of 0.3 in.

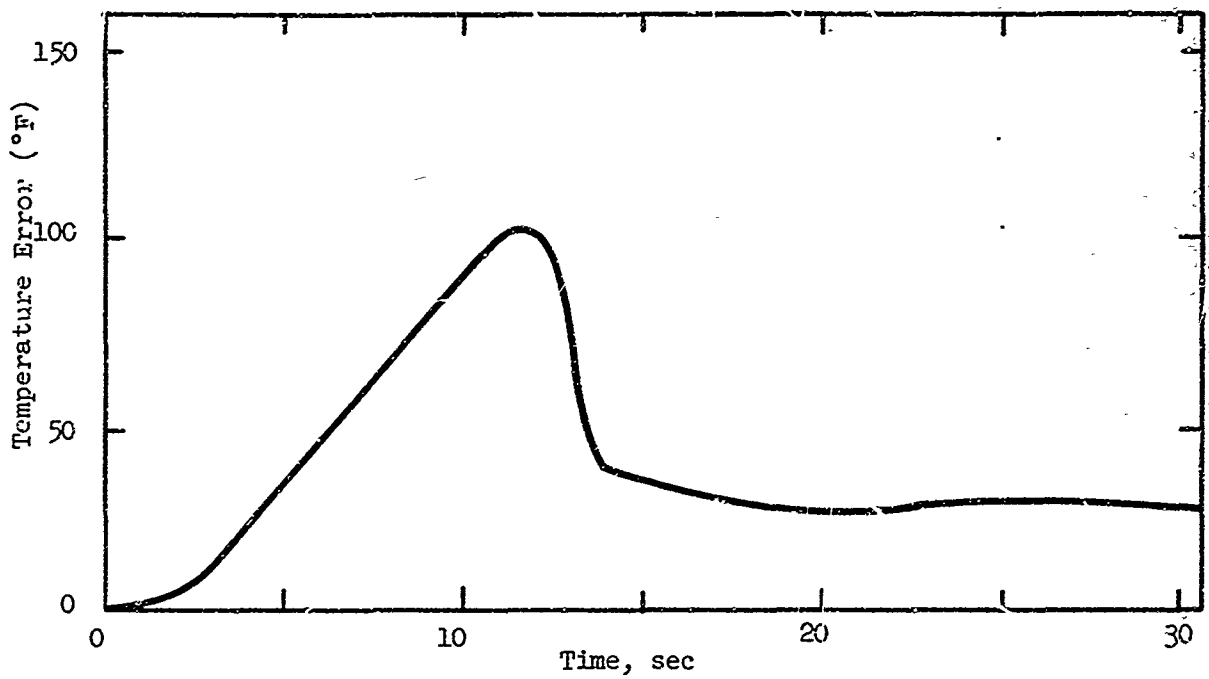

Figure 20. Error in Single Sheath-Type Thermocouple Response vs Time

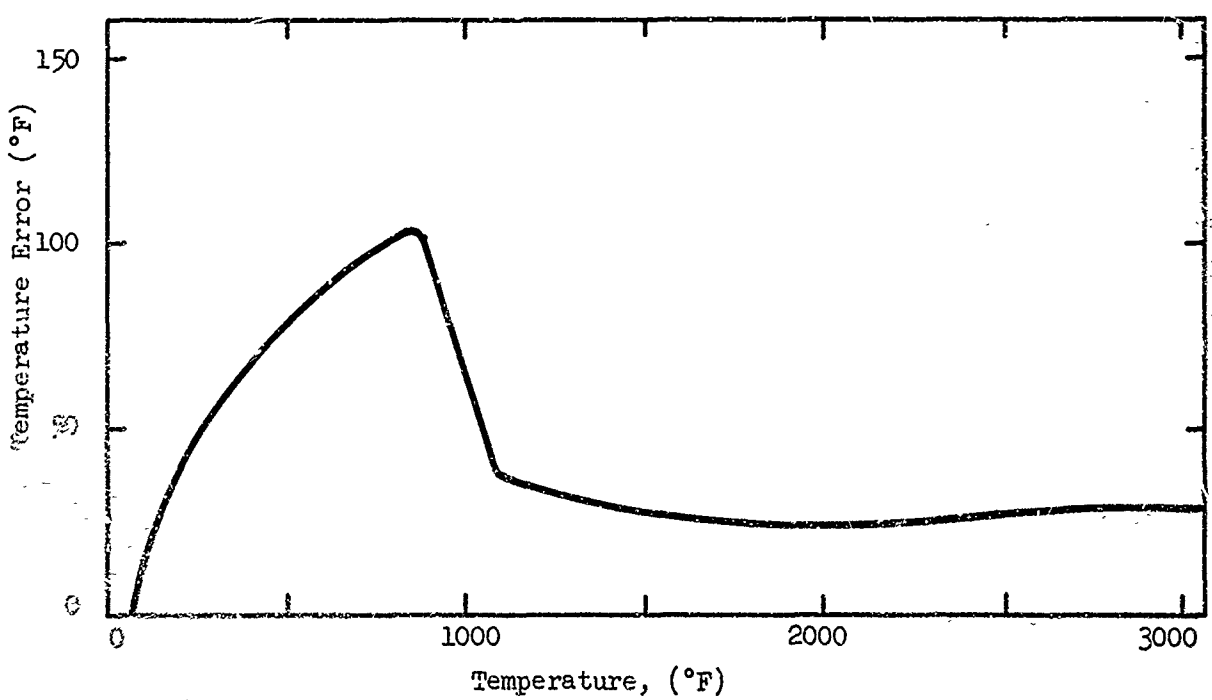

Figure 21. Error in Single Sheath-Type Thermocouple Response vs Temperature

III, D, Heat Transfer Analysis (cont.)

b. Double Sheath-Type Thermocouples in MX4926

Figure 22 compares the errors of the single sheath, double sheath and single bare wire types, as a function of temperature. The single and double sheath errors are nearly identical, indicating that the addition of the second thermocouple at a distance of 0.4 in. from the gas-side had no effect on the first, when displaced 0.1 in. or more from it. The bare wire thermocouple has almost no error, the maximum value being less than 10°F in the temperature range 2000 to 3000°F.

Figure 23 shows the error associated with the sheath-type thermocouples at different distances from the gas-side (0.3 and 0.4 in.) as a function of wall temperature. The dependence of error on temperature is comparable for the two cases, for these particular gas-side conditions.

c. Single Sheath-Type Thermocouples in MX4926 with Different Gas-Side Boundary Conditions

Less severe gas-side conditions (one-half the former convection coefficient) result in a somewhat different relationship between the thermocouple error and the wall temperature, as seen in Figure 24, which relates to a single sheath-type thermocouple at a distance of 0.3 in. from the gas-side. The reduced heat flux results in a greater error in the char temperature range.

d. Single Sheath-Type Thermocouple in MXA6012

Figure 25 compares the error for a sheath-type couple in MXA6012 to that for one in MX4926. Thermal conductivity of MXA6012 is the lowest of the materials of interest; hence the internal heatup is the slowest and the thermocouple error is the greatest. During the 40-sec duration

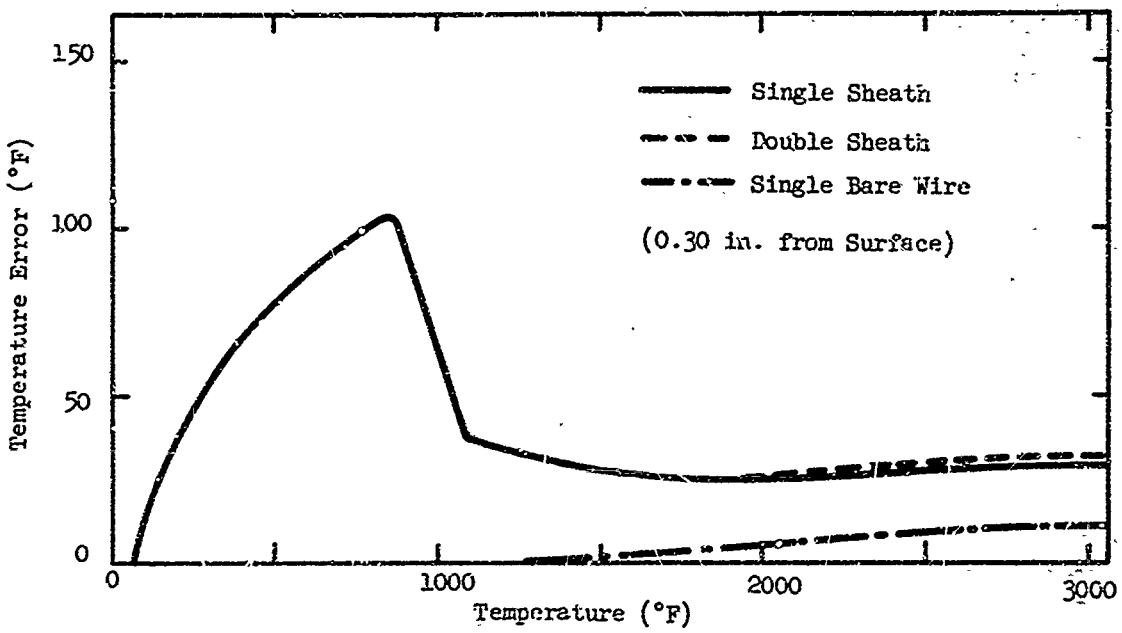

Figure 22. Error in Thermocouple Response vs Temperature

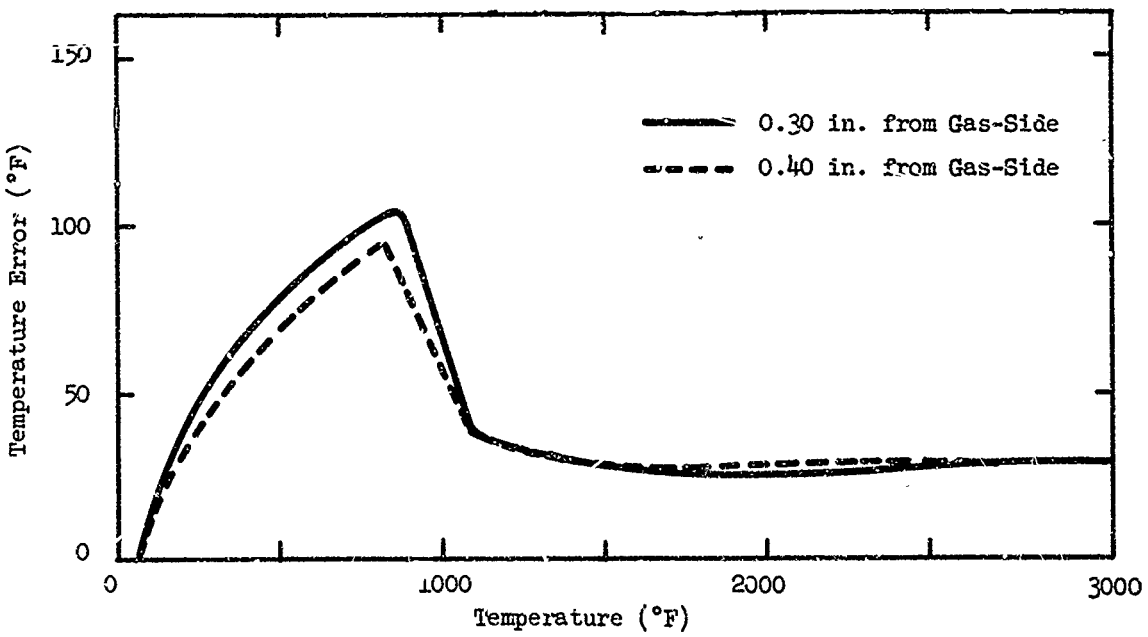

Figure 23. Error in Thermocouple Response vs Temperature (Double Sheath Type)

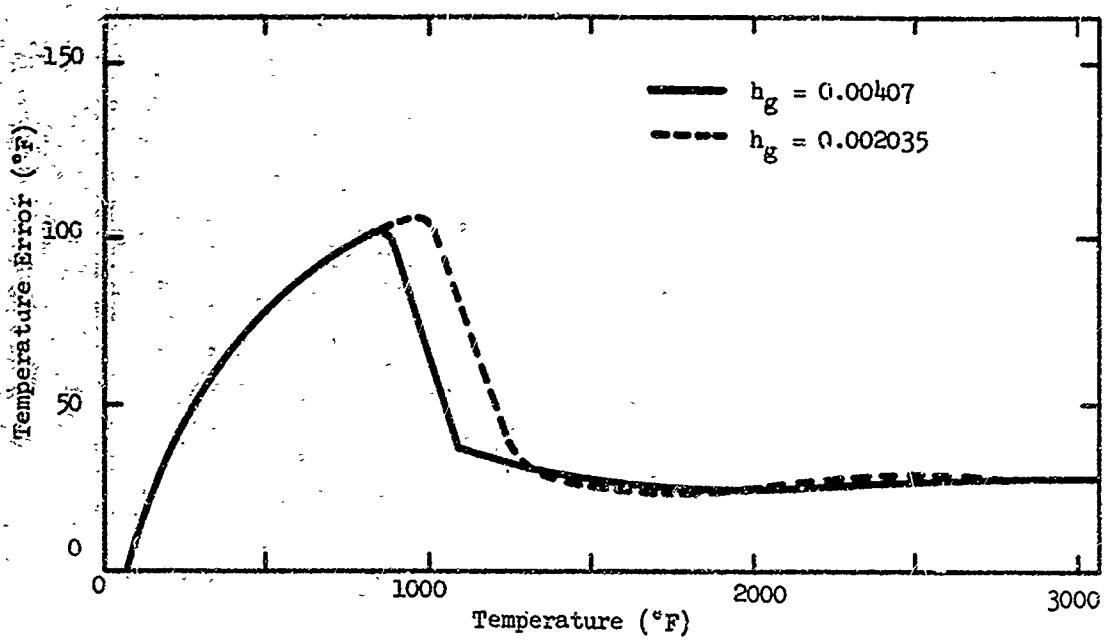

Figure 24. Error in Thermocouple Response vs Temperature

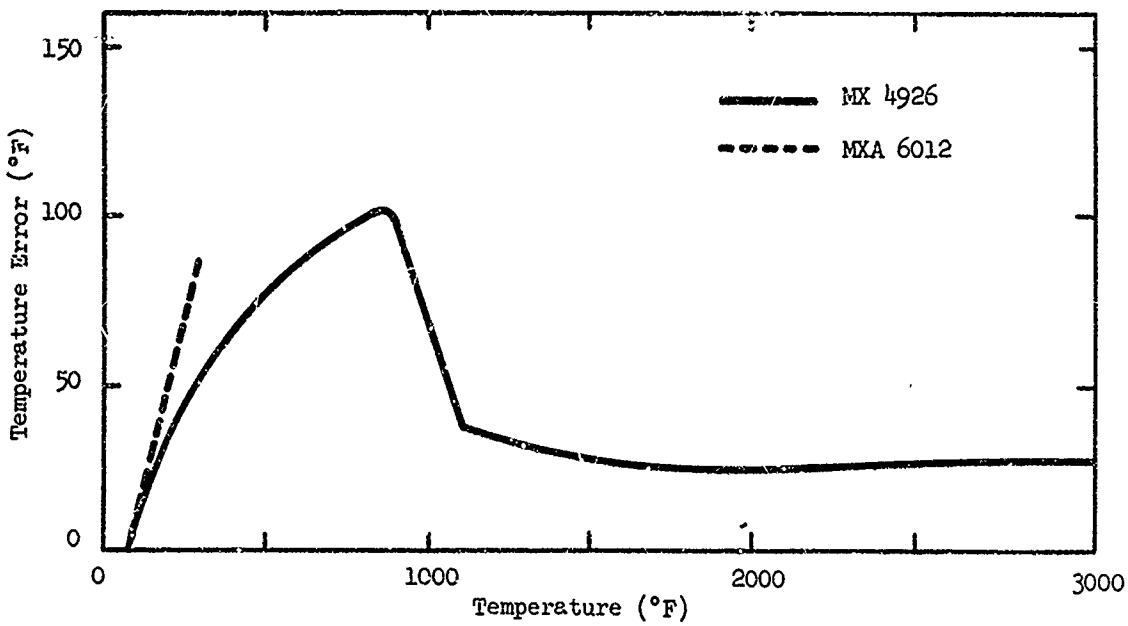

Figure 25. Error in Thermocouple Response vs Temperature

III, D, Heat Transfer Analysis (cont.)

considered in the analysis, the wall temperature at the thermocouple location rises only to some 300°F; the thermocouple junction, however, lags by nearly 100°F. Contact resistance is not accounted for here, and would tend to increase the error.

e. Effect of Contract Resistance

Figure 26 shows the kind of error that could be expected when contact resistance is considered, for a sheath-type couple in MX4926. The arbitrarily chosen value of contact conductance (1000 Btu/hr-ft^2°F) typifies that parameter for epoxied joints between metals and non-metals. The increased thermocouple error manifests itself only in the higher temperature range corresponding to the char material properties, where the error approaches 50°F. The error involved with virgin material is largely unaffected by the inclusion of contact resistance.

3. Thermal Network Analyzer

The Thermal Network Analyzer is a computer program written for the IBM 360 that serves for heat transfer analyses involving conduction, convection, or radiation; it may be used for charring as well.

Input involves a finite difference, or lumped parameter, representation of the physical system being analyzed: nodal points, initial temperatures, thermal capacitances, thermal resistances and their nodal connections. For the case of variable thermal properties; conductivity, specific heat, convection coefficients, etc., they may be entered as functions of temperature or other independent variables.

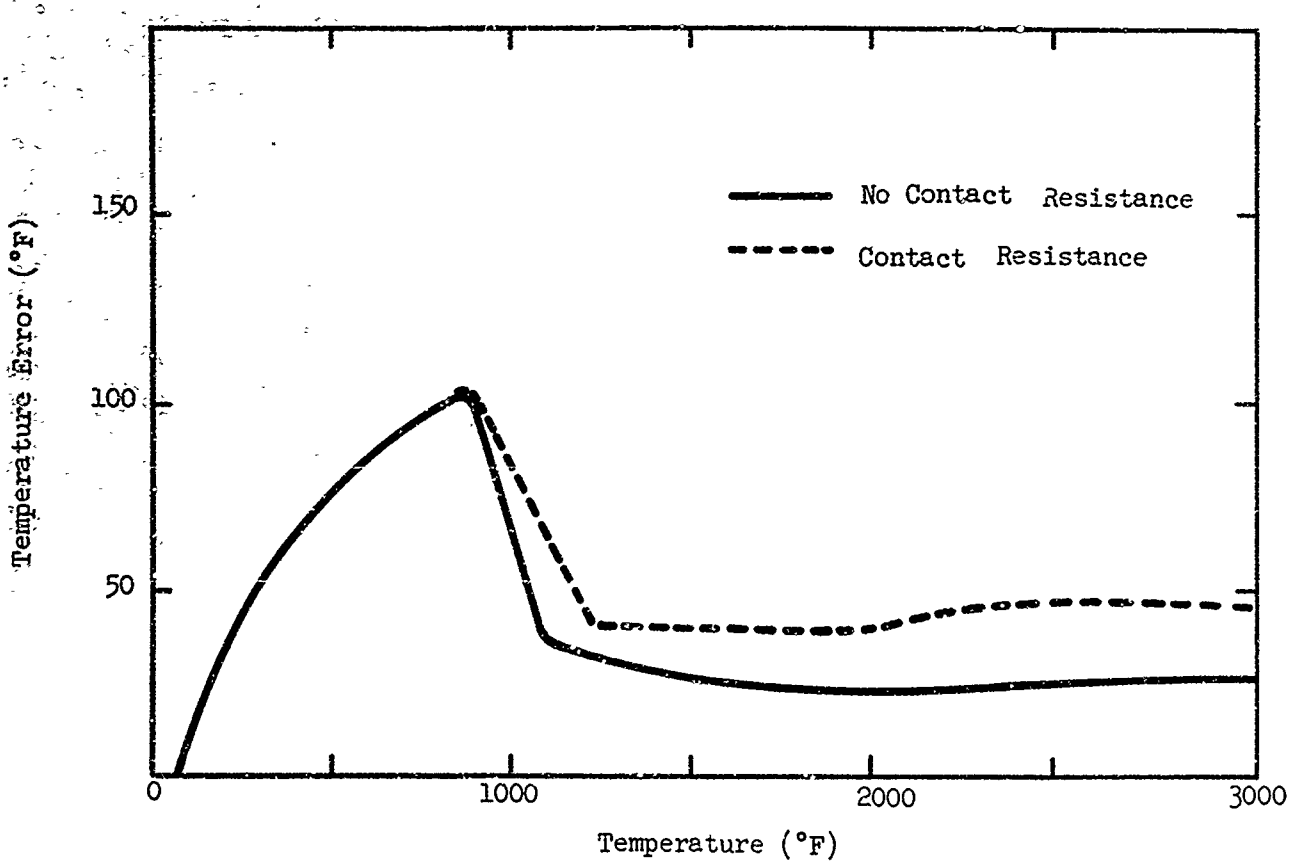

Figure 26. Error in Single Sheath-Type Thermocouple Response vs Temperature

III, D, Heat Transfer Analysis (cont.)

The program solves the heat conduction equation expressed in finite difference form. For the transient condition:

$$T_i\ (t + \Delta t) = \frac{\Delta t}{C_i} \left[\Sigma_j \frac{T_j}{R_{ij}} - T_i \Sigma_j \frac{1}{R_{ij}} \right] + T_i\ (t)$$

where T_i is the temperature of node i, T_j's are the adjacent node temperatures which are connected to T_i by resistances R_{ij}. C_i is the capacitance of node i; t is the time and Δt is the time increment. For the steady-state case:

$$T_i = \Sigma_j \frac{T_i}{R_{ij}} \Big/ \Sigma_j \frac{1}{R_{ij}}$$

III, Technical Discussion (cont.)

E. TEMPERATURE-SENSOR DEVELOPMENT

1. Fabrication

The eutectic composition used as the temperature-sensing device will be contained as very fine mixed powders (approximately 325 mesh) in a graphite microcapsule. The microcapsule will be fabricated from POCO graphite, a very dense (Sp. Gr. = 1.88) non-porous graphite, to the dimensions shown in Figure 27. This material replaces the G-90 graphite considered during the thermal analysis because of its low total impurities (<6 ppm) and fine grain structure. Powders from the eutectic compositions will be hand packed into the capsules and sealed in by a "slip-fit" graphite plug.

2. Calibration

To calibrate the sensors each will be inserted in melting point specimens for testing in the Pirani Melting Point Furnace.

Duplicate pairs of melting point specimens will be fabricated. One specimen of each pair will be heated to a temperature 50°F below eutectic temperature and the other 50°F above. This technique has already been demonstrated using sensor elements slightly larger than those shown in Figure 27. Figure 28 shows the photomicrograph of the ZrC + C system (64.5 At.% C) which was heated to 2862°C and held there for 20 sec. Figure 29 shows the photomicrograph of the same ZrC + C system fused at 2950°C. It can be clearly seen from the photomicrographs that when the melting point has been exceeded, a definite change in microstructure is obtained. Figure 30 shows the standard melting point specimen, which is held between the grips of the melting point furnace. Two such specimens of graphite were drilled to accept sensor capsules. Both contained finely divided powders of ZrC and C. Temperature was recorded at the midpoint by sighting the optical pyrometer in a blackbody hole. Figure 31 shows a radiograph of the two identical samples of the ZrC + C system that were heated to two different temperatures. Sample A of Figure 31

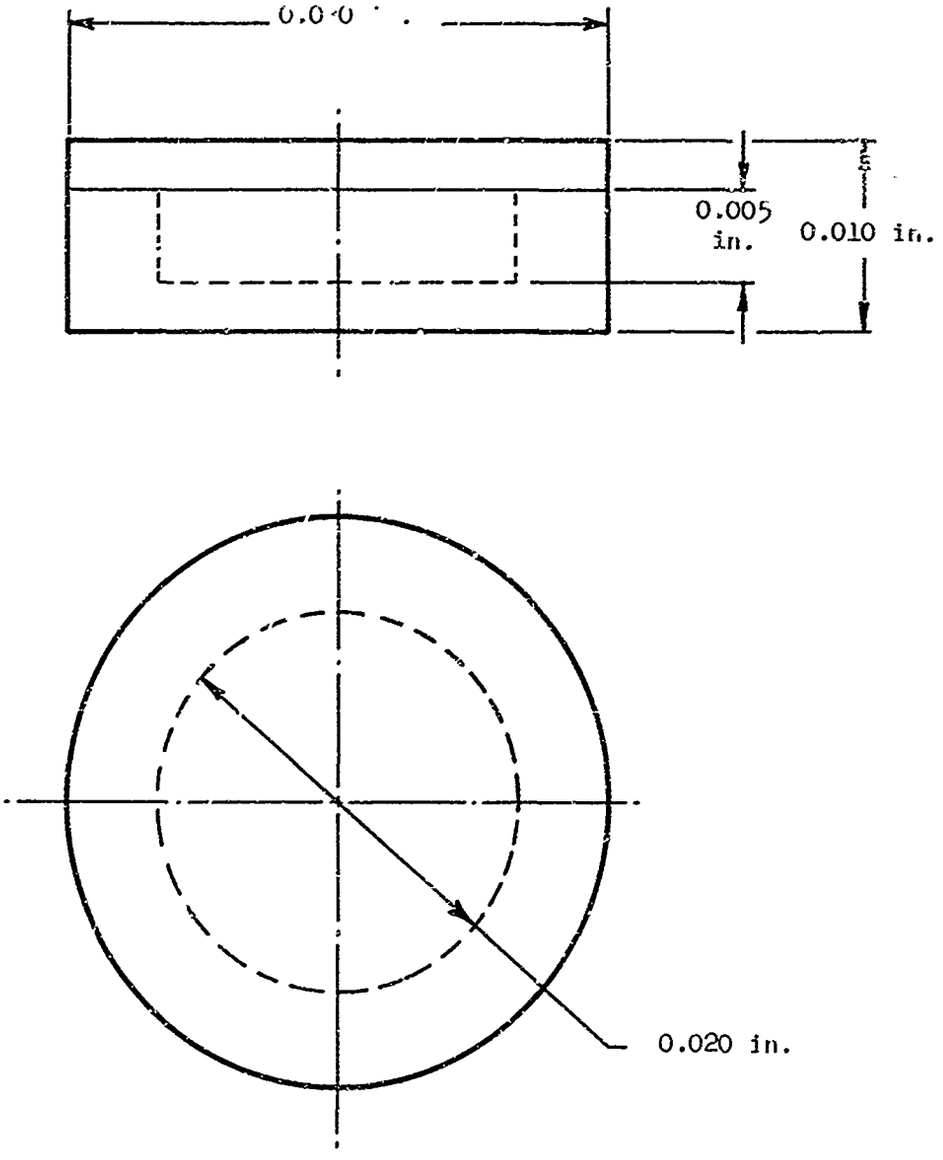

Figure 27. Sketch of the Graphite Microcapsule

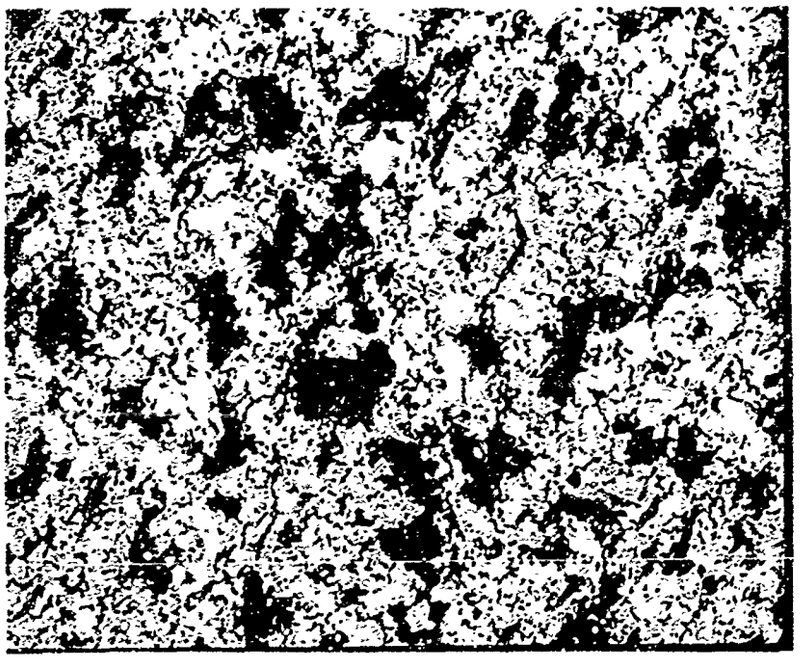

Magnification: 880X, as polished

Heated slowly to 2862°C, held for 20 seconds and cooled slowly. Carbon is the black phase and ZrC is the white phase.

Figure 28. As Sintered ZrC + C

Magnification: 500X, as polished

ZrC + C powders heated slowly to 2950°C and held for 10 seconds. A slight excess of graphite was present. The eutectic lamellae are plainly visible.

Figure 29. Fused ZrC + C

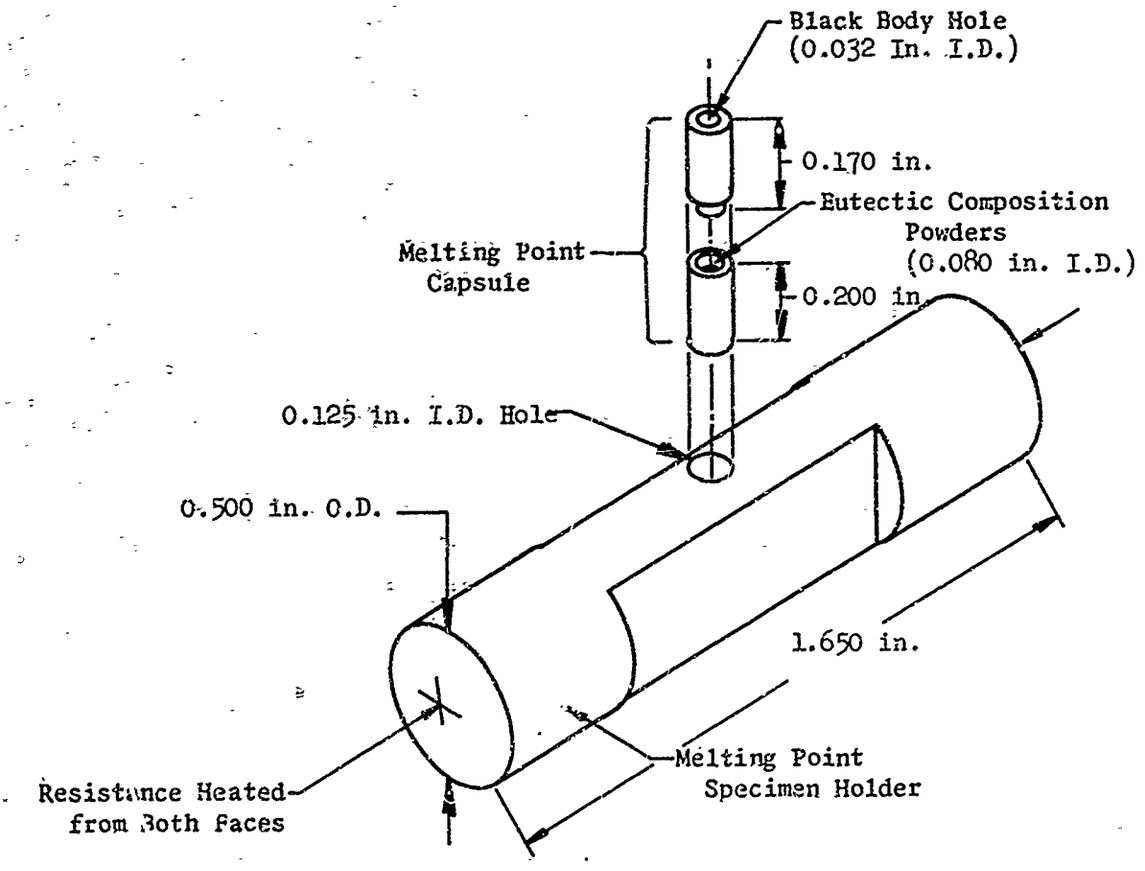

Figure 30. Melting Point Specimen with Holder

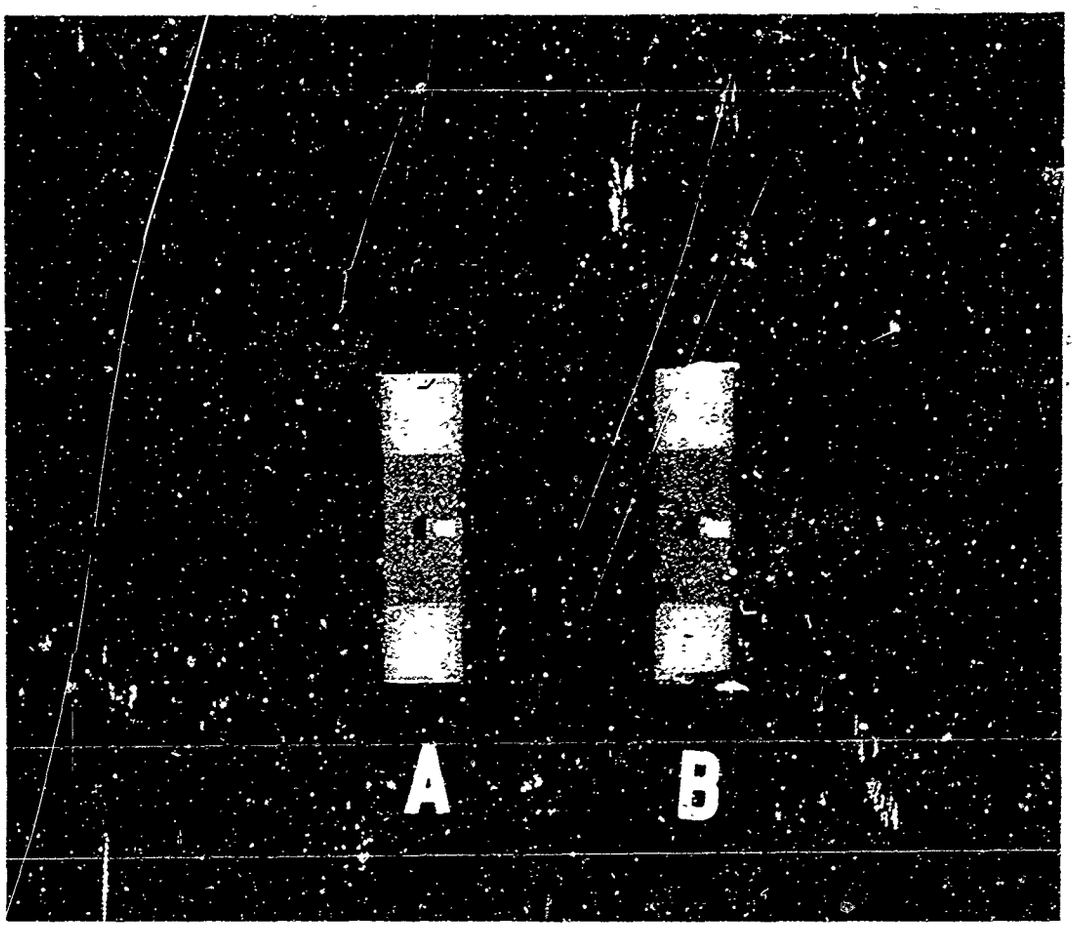

A - Sintered ZrC-C System

B - Fused ZrC-C System

Figure 31. Radiograph of Specimen in Graphite Melting Point Test Holder

III, E, Temperature-Sensor Development (cont.)

shows the result of heating the eutectic mixture below the eutectic temperature and sample B shows the result of heating the eutectic mixture above the eutectic temperature. It is readily observed on the radiograph that melting occurred in sample B, as evidenced by areas of material flow and the formation of voids due to shrinkage. Although it is realized that the above sample is larger than the contemplated sample, the same phenomenon is expected to occur.

In these calibration tests, the optical pyrometers that will be used are microoptical pyrometers manufactured by the Pyrometer Instrument Co., Inc., Bergenfield, New Jersey. These pyrometers have three overlapping blackbody scales on direct reading milliammeters; the ranges on the standard model are 700 to 1400°C, 1300 to 1900°C, and 1800 to 3200-(4500)°C, and the temperatures are measured at an effective wave length of 0.65 microns.

Two separate procedures are involved in the calibration of the pyrometers: calibration of the pyrometer proper, and calibration and adjustment of the meter readout for the filament current.

The objective of the calibration of the pyrometer is to establish a precise relationship between filament current and temperature, using calibrated radiation sources or pyrometers as standards. For temperatures up to 2300°C, the pyrometer is either compared with standard pyrometers certified by the National Bureau of Standards, or against a tungsten ribbon-filament lamp with precisely known current-temperature relationship.

For calibration points at higher temperatures, the carbon-arc technique using an arc-furnace manufactured by the Mole-Richardson Company, Hollywood, California, is employed. On the basis of data from the National Bureau of Standards, a temperature of 3808 $\pm$ 20°K is asserted to the crater of the anode, when operated in the region of the quiet arc. Lower temperature fixed points are obtained in the well-known manner using absorbing glasses of accurately known transmission.

III, E, Temperature-Sensor Development (cont.)

In the calibration runs, at least five readings are taken at each point. The current through the pyrometer filament is determined by the voltage drop across a 10 ohm precision (5 ppm) resistor, and recorded to the nearest one or ten microamps. A temperature-filament current relationship is then established by a least square fit of the data. The same meter and resistor are employed to calibrate the temperature scale of the milliammeter provided with the pyrometer. The calibration is usually started at the low temperature end and at least five readings are taken at each of the selected cardinal points; after averaging, the meter reading is then adjusted to comply with the established pyrometer-filament current relationship.

The total temperature error is composed of several parts: the uncertainties in the calibration equipment and the errors introduced by the individual calibration steps.

Considering the first error sources first, the data given in Table IV represent the uncertainty levels assigned to the certified pyrometers. Although the data probably correspond more to estimates rather than to exact values, the data are claimed to have a confidence level of more than 95%.

Typical uncertainties introduced by the visual matching of test and calibration pyrometers are $\pm$ 1.7°C, and hysteresis effects in the microoptical pyrometers in use amount to approximately 1.8°C; a further uncertainty of approximately $\pm$ 3°C maximum at the high temperature end is introduced by the limit resolution of the ten-turn pot used in the pyrometer. A least square fit of the calibration data, and incorporating the uncertainties of the temperature standards, yielded the error limits listed in Table V.

III, E, Temperature-Sensor Development (cont.)

Table IV

TEMPERATURE UNCERTAINTIES IN THE NBS CERTIFIED STANDARD PYROMETERS AND TUNGSTEN RIBBON-FILAMENT LAMPS (95% Confidence Level)

	Temperature, °C	Uncertainty, °C
Certified Pyrometer	800	± 4
	1063	± 3
	2800	± 8
	4000	± 40 max
Tungsten Ribbon Lamp	800	± 5
	1100	± 3
	2300	± 7

TABLE V

OVERALL TEMPERATURE UNCERTAINTIES FOR THE MICROOPTICAL PYROMETERS

Temperature, °C	Uncertainty, °C
1100	± 4
2000	± 7
2300	± 8
3000	±10
3600	±25

III, E, Temperature-Sensor Development (cont.)

3. Sensor Size and Location in Ablative Plugs

The sensor size was established by considering the results of the heat-transfer analysis, the temperature profiles obtained from the NOMAD motor firings, and the feasibility of economically producing a small capsule. The heat-transfer analysis indicated that various size graphite capsules containing eutectic compositions would not produce or cause temperature perturbations in an amount greater than the calibration accuracy of the eutectic melting points. A capsule size of 0.100 in. in diameter and 0.030 in. in thickness was found to be an upper limit and still not cause a temperature disturbance greater than eutectic melting point accuracies at the higher temperatures. As seen from Figure 1, however, 0.030 in. in thickness corresponds to approximately a 450°F temperature difference within the ablative material. Such a temperature difference would produce an average temperature difference of 225°F across a particular capsule assuming in each case a linear temperature distribution within the material. Since the eutectic compositions are capable of detecting temperature ranges well below 225°F, it appears that the 0.030-in. thickness is too large. Similarly, by considering a thickness of 0.010 in. in capsule thickness for the same material, an average temperature difference of approximately 75°F across a particular capsule is obtained. This latter average temperature difference is within the eutectic sensing accuracy for all practical purposes. The feasibility of economically fabricating a capsule smaller than 0.010 in. in thickness to obtain an average temperature difference of approximately 25°F was considered prohibitive.

Several methods of installation of the individual sensor capsules in the ablative plastic plugs have been considered. The primary emphasis must be placed upon location because, as shown in Figures 1 through 6, the depth of the char in which the temperature range of interest (3500 to 6000°F) occurs may be very small. Also, the region will progress as recession occurs,

III, E, Temperature-Sensor Development (cont.)

from a finite position at the initial surface upon initiation of firing to a location approximately 1/2 in. below the original surface at the throat of a carbon or graphite phenolic material in a typical 60-sec firing. Obviously, all sensors located in the regressed region will be lost during firing. It is also apparent that multiple, identical sensors in depth will be required so that adjacent sensors will indicate a temperature by one melting and the next one not melting. The proposed method of installation is shown in Figure 32. Installation of 4000°F indicating thermocouples in the plug at the depths of the 4000°F sensors using the bare wire technique employed on Contract AF 04(611)-11646 is also shown in the plug configuration.

It was indicated by the heat-transfer design calculations that stacking of the graphite sensors was a possible approach to ascertain a particular isotherm during a motor firing. It is clearly understood that only one sensor is needed to locate any one temperature level at a specific depth in the material. However, with the present state-of-the-art techniques for predicting these locations, this approach is still not possible. Using the stacking approach, the minimum distance allowable between sensors was found to be 0.030 in. for the 0.010-in.-thick sensors. Therefore, any number of sensors can be stacked to meet these criteria and each sensor will respond independently of its nearest neighbor sensor. The question then becomes one of how many sensors are necessary to adequately establish a temperature level and yet be within practical limits. A rigorous answer to this question is hardly possible, but by considering the results of the heat-transfer calculations, motor firing data available on the ablative materials, and the reliability of present methods to predict material regression behavior, it is possible to estimate the number of sensors needed. Data obtained from the NOMAD firings have indicated that the maximum range of thickness of the 3500 to 6000°F temperature interval for the ablative materials being considered was 0.190 in. for a carbon phenolic material (MX 4926), and the minimum range of thickness over this same temperature interval was 0.000 in. for several other materials. An average thickness

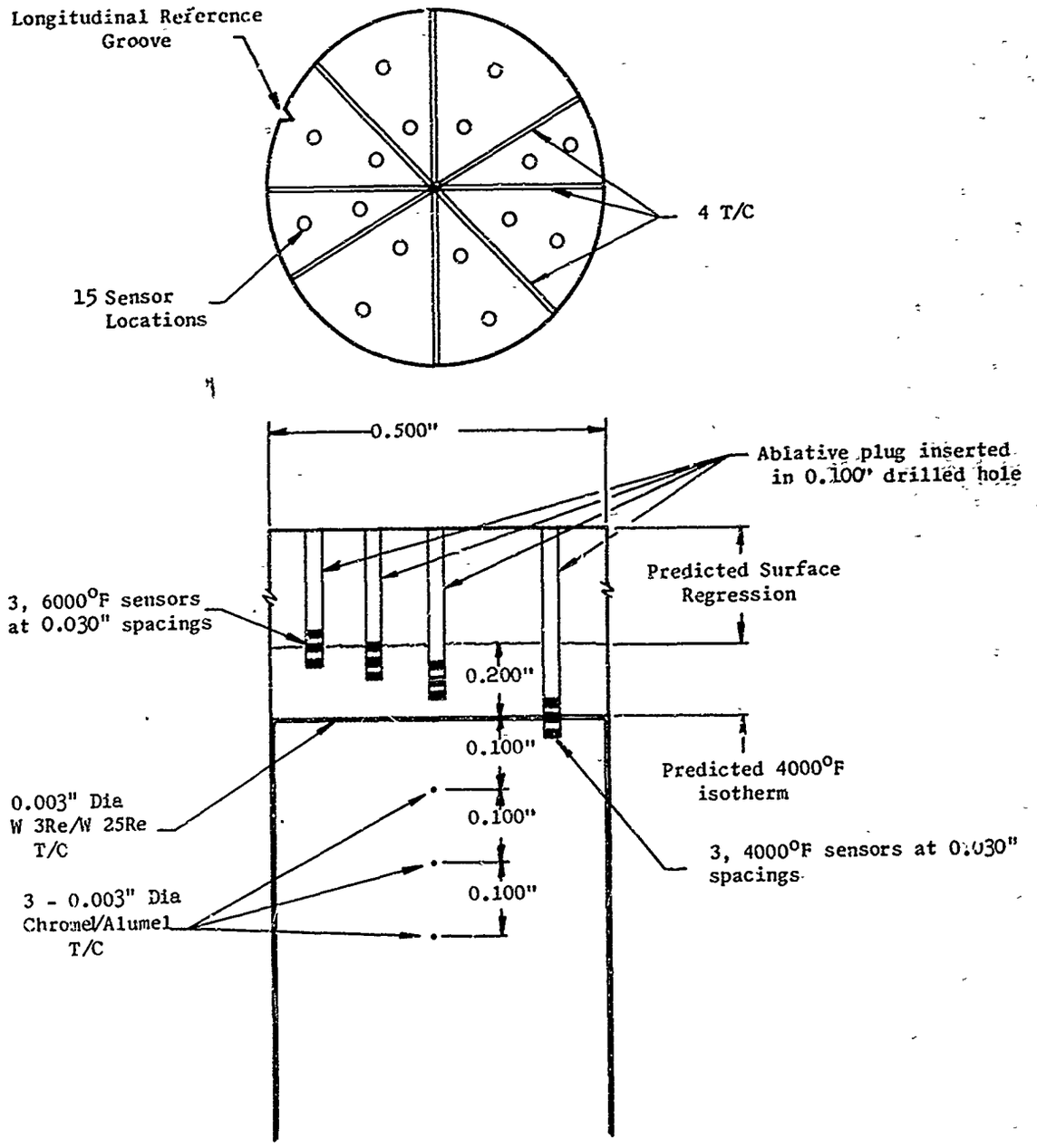

Figure 32. Ablative Plug Configuration with Installed Sensors and Thermocouples

III, E, Temperature-Sensor Development (cont.)

for this interval then is about 0.095 in. with all other materials, except MX 4926, amounting to this value or less. Due to a lack of information, pyrolyzed phenolics will be considered to exhibit similar characteristics as the carbon and graphite phenolics, and, therefore, it will be assumed that their average thickness is also about 0.095 in. Thus, in order to cover this range, three sensors, each 0.010 in. in thickness, and each spaced 0.030 in. from one to the other, will cover the entire temperature interval from 3500 to 6000°F, while each sensor covers a thickness of material which corresponds to a temperature interval at approximately 150°F. In the case of MX 4926, the stacked sensors will be staggered, as shown in Figure 32, to cover the entire temperature range. For most of the materials where the 3500 to 6000°F range is seen to be of the order of 0.095 in. in thickness or less, all sensors will essentially cover the same char increment over this temperature range. This region covered by the stacking of the three sensors is considered to be sufficient in order to allow a margin of safety in predicting the location of this temperature region.

The plug configuration shown in Figure 32, with the sensor and thermocouple orientations, is an initial configuration to be tested in the experimental phase of the program. Should this sensor orientation prove to be insensitive to the resulting temperature distribution through the material, an alternative sensor orientation will be used. Such an alternative orientation may be one in which all sensor materials are placed at equal depths and extend over the same increment of material thickness. In this case, and similar to the one shown in the above figure, several identical sensors would cover the increment of thickness by placing one sensor immediately below another identical one, and so on. As shown in this same figure, it appears that a predetermined temperature profile will result according to the positions occupied by the sensors and their characteristic temperatures. However, as seen in Figure 32, there will be 15 different sensor wells at different levels extending over a maximum of 0.190 in. of material depth, and thus, there will be much overlapping in temperature sensing capability.

III, E, Temperature-Sensor Development (cont.)

Each capsule will be bonded into place by hand using a minimum amount of epoxy resin to provide good contact with the ablative material. A spacer, which is a disc of the ablative material, will be bonded between sensors in a similar fashion. An ablative plug will then be bonded into place above the sensors.

Utilizing the concept shown in Figure 32, the capability of the sensor elements to provide reliable temperature data will be tested and evaluated. Plugs will be prepared of six materials supplied by AFRPL, currently identified as follows:

a. Carbon phenolic, MX 4926
b. Asbestos phenolic, MXA 6012
c. Three different pyrolyzed (precharred) carbon and graphite-reinforced phenolics
d. Carbon felt phenolic, MXC 113 (supplied by AGC)
e. Paper phenolic, FM 5272

Identifications, spacial locations, and depths of all placed sensor eutectics will be maintained by suitably marking the base of each plug assembly and comparing each assembly to an identifying template. The exact depth of each sensing eutectic from the flame surface will be determined by taking radiographs before and after exposure to the flame front. It will be possible to visually observe all sensors placed in a plug assembly on one radiograph by properly spacing each "sensor-well" so that the resulting X-ray appears as shown in Figure 32. A direct reference and comparison can then be made between the original plug assembly and the post-test plug assembly. By controlling the orientation of thermocouple wires and relative positions of the sensor materials, identification of the different types of eutectic mixes should not be difficult. However, should a mixup appear to have occurred, the eutectic compositions readily lend themselves to identification by X-ray diffraction.

III, E, Temperature-Sensor Development (cont.)

The location of the sensors in the ablative material prior to test firing can be determined by two ways: (1) by physical measurement during assembly of the sensors and spacers into drilled holes of known depths, and (2) by X-ray photographs after complete assembly of the ablative plug with sensors and thermocouples. The latter approach will be used because of its ease, accuracy, and availability. From the initial X-ray photographs, location of the sensors can be very accurately measured, and can then be used later as a reference for the fired ablative plugs. Identification of each sensor after assembly will be accomplished by a reference template, as shown in the top view of Figure 32. Each identical set of three sensors per drilled location will have a particular radial position from a reference groove, and this radial position for each set of identical sensors will be maintained for all ablative plug materials. In this manner, location and identification of the sensors after test firing will be possible by using the template and X-ray photographs in conjunction with each other.

Prior to test firing of the ablative plugs, no problems are anticipated in either locating or identifying the sensors after complete assembly. However, after test firing, complications could arise in relocating the sensors because of material delamination, spallation of the material, physical distortion, or thermal expansion of either the ablative material or of the graphite capsule material. Any of these complications could obscure initial X-ray photographs that are taken in the same fashion as the unfired plugs, but by taking several photographs at various circumferential locations, all of the sensors can be found and then located with respect to the back side of the ablative plug. Positive identification of any sensor is always possible by sectioning the part and examining by metallographic techniques regardless of the complication.

X-ray photographs of the assembled ablative plugs will be taken with a Picker Portable X-Ray unit using Type M-2 X-ray film. This

III, E, Temperature-Sensor Development (cont.)

technique generally involves a 15-sec exposure time at a power setting of 70 KV and 0.003 amp at a distance of 14 in. An aluminum filter is used to ensure as much contrast as possible. The film is then developed under standard X-ray dark room procedures.

Identification of the sensors by metallographic techniques first involves specimen preparation by grinding mounted specimens on silicon carbide papers using grit sizes down to 600. Polishing will then be performed on microcloth, for example, using Linde "B" alumina (0.05μ) in Murakami's solution. The etchant to be used will depend primarily on the sensor material system, as determined in the work indicated in Appendix II, but of the various possible etchants, such as, electroetch in 2% NaOH or a solution of 4 gm of $KMnO_4$ and 4 gm of NaOH in 100 ml. of water, the etchant will produce a characteristic microstructure that can then be compared to systems of known microstructures. The specimens are generally etched at room temperature; the times required to produce sufficient development of the microstructure varies up to 10 sec. The micrographs will be examined and photographed on a Zeiss Ultraphot II metallograph.

The plugs will be installed in billets of the same ablative material. These billets will serve to simulate a section of an ablative component and will also shield the plug assembly from side heating during tests which will be performed with the plasma arc. Because the temperature profiles throughout the specimen is the criterion used for evaluation, an inert plasma gas will be utilized so that surface material loss during the tests is minimal. Each plug containing 15 different sensor materials with melting temperature spanning the 3500 to 6000°F range, installed in a series of three each, will be employed. Each plug will also contain the four thermocouples (as determined in the NOMAD program) shown in Figure 32 to accurately establish the in-depth temperature profiles and verify thermocouple accuracies. During testing, the temperature reading of the W-W Re thermocouple will be monitored and the heat

III, E, Temperature-Sensor Development (cont.)

source will be removed when it reaches 4000°F. After testing, each plug containing its sensors will be removed from the billet in which it was installed and will be radiographed. The molten eutectic will be identifiable by change in shape as previously discussed and shown in Figure 31. After X-ray, each plug will be disassembled, and the capsules removed and examined to verify the radiographic analysis. A thorough correlation analysis of sensor temperature indications and thermocouple temperature indications will be made to determine the temperature profiles at times of maximum temperature. Based upon the results of these analyses, the necessary modifications to the system will be made and a duplicate test with each ablative plastic material will be performed.

Upon completion of the above testing and evaluation, 12 plugs containing sensing elements and thermocouples will be fabricated and provided to AFRPL for installation in rocket nozzle components.

The success of experimentally determining the 3500 to 6000°F temperature range during firing will depend upon the ability to place the combined plug assembly with sensors at the proper depth location within the ablative material, so that, at the end of the motor firing, the regression depth equals the depth to which the uppermost sensor(s) were placed. To ensure the proper depth location of the sensor materials and obtain maximum information from the sensor plug, the total surface regression of the particular material must be known to within about $\pm$ 0.050 in.

Current techniques of directly predicting the regression rate are not reliable enough for this purpose. However, data recently generated on the NOMAD programs for the materials listed above provide a reliable source of regression behavior to guide the location of the sensor plugs. Further, temperature-time histories, as determined for these materials in the NOMAD program will also be an invaluable guide in locating the sensors within the

III, E, Temperature-Sensor Development (cont.)

ablative plugs. Finally, from the physical and chemical properties determined for these materials in the NOMAD program and in conjunction with the nozzle design (Figure 33) and the propellant to be used for the test motor firings, a conduction analysis program will be used to predict and verify the regression of the materials used at the various nozzle locations. In addition, the program will be used to place the sensors at their respective temperature locations within the ablative plug. Data obtained from the plasma-arc tests will also be used as a guide in this latter prediction.

The conduction analysis program which will be used represents a solution to the ablation-corrosion problems. This program, "Charring-Ablation Program" (CAP), describes the transient thermal response of a composite material which reacts or decomposes in the heat affected area. It includes the effect of gaseous reaction products and heterogeneous reactions between the decomposition gases and the char. The boundary conditions include surface regression due to surface reaction with propellant combustion product and regression due to shear failure at the surface as a function of local shearing forces and wall temperature. In addition, internal gas pressure drop and resulting material failure due to spallation are included in the calculations.

The particular method of solution is numerical, wherein the given configuration is again divided into a large number of individual small elements. Each element is small enough that accuracy and convergence of the numerical solution is achieved. Temperature variation of thermal properties can be incorporated. Output format allows each of the following parameters to be printed at any desired time intervals; a. Erosion Depth, b. Char Depth, c. Pyrolysis Gas Formation Rate, d. Temperature Distribution, and e. Density Distribution in Decomposition Zone.

To facilitate performing ablation-corrosion analyses, one additional program is used, namely; "The Thermo-Chemical Equilibrium Program" (TEP). This routine computes the equilibrium composition of the gas adjacent

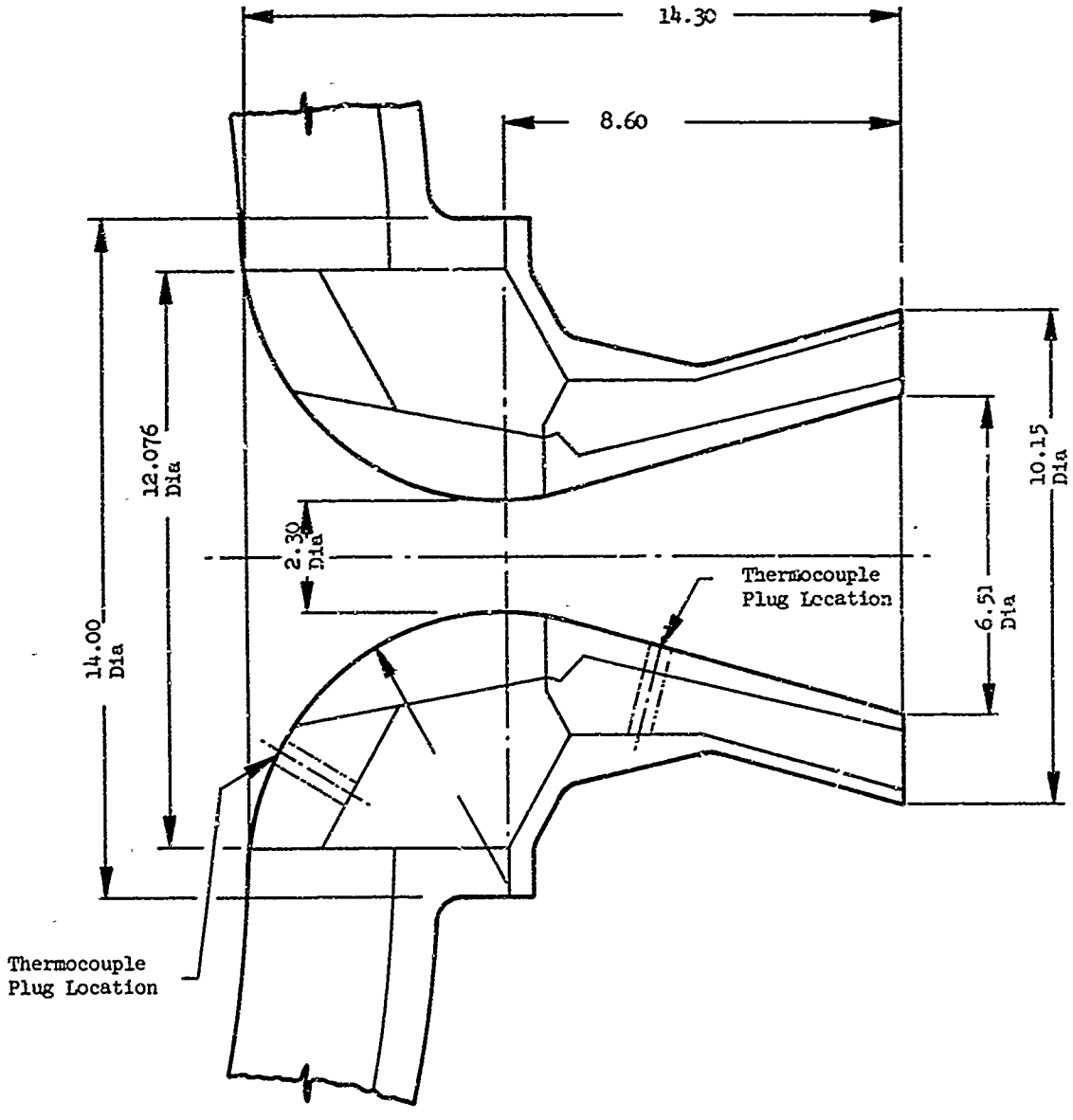

Figure 33. Char Motor Nozzle Design

III, E, Temperature-Sensor Development (cont.)

to the wall considering either (1) no reaction with the wall material, (2) pyrolysis gas flowing with non-reacting wall material, or (3) pyrolysis gas blowing with a reacting wall material. Output from this program is compatible with input surface equilibrium data requirements of the (CAP) program and includes surface temperature and total enthalpy (chemical and sensible) of the gas mixture as a function of pyrolysis gas rates and char removal rates.

Additional input requirements include: (1) thermal conductivity and specific heat of both charred and virgin materials, (2) pyrolysis gas enthalpy, (3) rate constants for the kinetically controlled decomposition reactions, and (4) heat of formation of the virgin and fully charred materials.

It is anticipated that the successful application of this program will require that existing analytical techniques be supplemented with empirically derived correlation coefficients (for some materials). For this reason, the existing computer program that is based on the analytical model described herein will be used in conjunction with experimental data that has been accumulated in existing programs, and data that will be generated during this program to obtain experimental-analytical correlation parameters for use with each material. These correlation factors will then be incorporated as an optional part of the computer program input for prediction of specific materials performance in the various nozzle locations.

The conduction analysis as discussed above pertains to both the heat-up as well as the subsequent cool-down. The only changes required are boundary conditions appropriate to each mode of heat transfer (i.e., convection during heating and radiation and convection during cool-down).

Should one attempt to offer more reliability in plug performance and location, it would be possible to install several instrumented sensor plugs circumferentially at various overlapping depths and at the same

III, E, Temperature-Sensor Development (cont.)

axial location. Such a task, however, is believed to become prohibitive in the amount of additional fabrication and analyses required. It is anticipated that the different temperature-sensing elements can be reduced from the 15 evaluated in the plasma-arc tests because of a more accurate establishment of the temperature range existing between the upper limit of the W-Re thermocouple and the surface temperature (the surface temperature of the graphite phenolic is probably approximately 5000°F instead of 6000°F). The reduction in the number of sensors will be partially offset by the possible requirement for a greater test coverage of each sensor material to decrease uncertainty of results. It is anticipated that 35 sensor elements per plug will be sufficient instead of the 45 sensor elements per plug used in the plasma-arc tests.

After static testing of each nozzle by AFRPL, disassembly of the thermocouple plugs from the nozzle components, and their return to Aerojet, the post-test analysis will be performed on each plug taking into account the thermocouple measurements provided by AFRPL and the temperature indications from the sensors.

The thermocouple data will be analyzed by plotting the thermocouple locations as a function of firing time for various temperatures, as shown in Figures 1 through 6. This will generate a family of isotherms which can be used to determine the temperature profile through the ablative material at any time. The thermocouple distance versus firing time data may be further extrapolated to temperatures beyond the thermocouple capabilities from the relationships produced by the higher temperature isotherms. Temperature indications obtained from the lower temperature sensors will be directly compared to the thermocouple temperature versus distance data. At the lower temperatures (3000 to 4500°F), any discrepancies between the two temperature indicators will be noted and explained. Temperature indications obtained from the higher temperature sensors will be plotted as a function of distance along

III, E, Temperature-Sensor Development (cont.)

with the thermocouple data. If the sensors and thermocouple each indicate a true temperature, then they will bear the same relationship to each other. If there is in fact a difference in temperatures measured by the two indicators, then, extrapolation of the thermocouple data or extrapolation of the sensor data to the thermocouple data will show a different functional dependence with distance and, thus, their relationship with temperature and distance will not coincide. Any deviations shown in this latter case will also be described and explained.

F. ALTERNATIVE METHOD TO DISTRIBUTE TEMPERATURE SENSORS AND THERMOCOUPLES WITHIN THE ABLATIVE LINER

As indicated from the discussion on the ablative plug configuration, several machining operations are necessary to place the small sensors into the plug assembly. These operations include the machining of the plug itself, bottoming each sensor well, replugging each sensor well, and the machining operations involved with the instrumentation of the thermocouples. To eliminate or minimize the time-consuming machining operations, an alternative approach is suggested to place both the temperature sensors and thermocouples in the ablative material. The technique shown to place the temperature sensors into the material is depicted in Figure 34. In this technique, precured ply plates are made and then drilled to locate the sensors, as shown in Figure 35. Each ply plate is then coated with resin and allowed to air-dry so that all plies can be assembled and cured into a laminate containing the sensors. Exact location of the sensors is made by X-raying the complete laminate assembly before placing the laminated plates into the wrapping operation. It is believed that the laminated plates, now the insert, will not affect the lay-up procedure or the performance of the fabricated part. Post-test analysis of the insert can be made by either X-raying in a tangential direction to the exposed fired surface or, most preferably, by removing the insert and analyzing it separately.

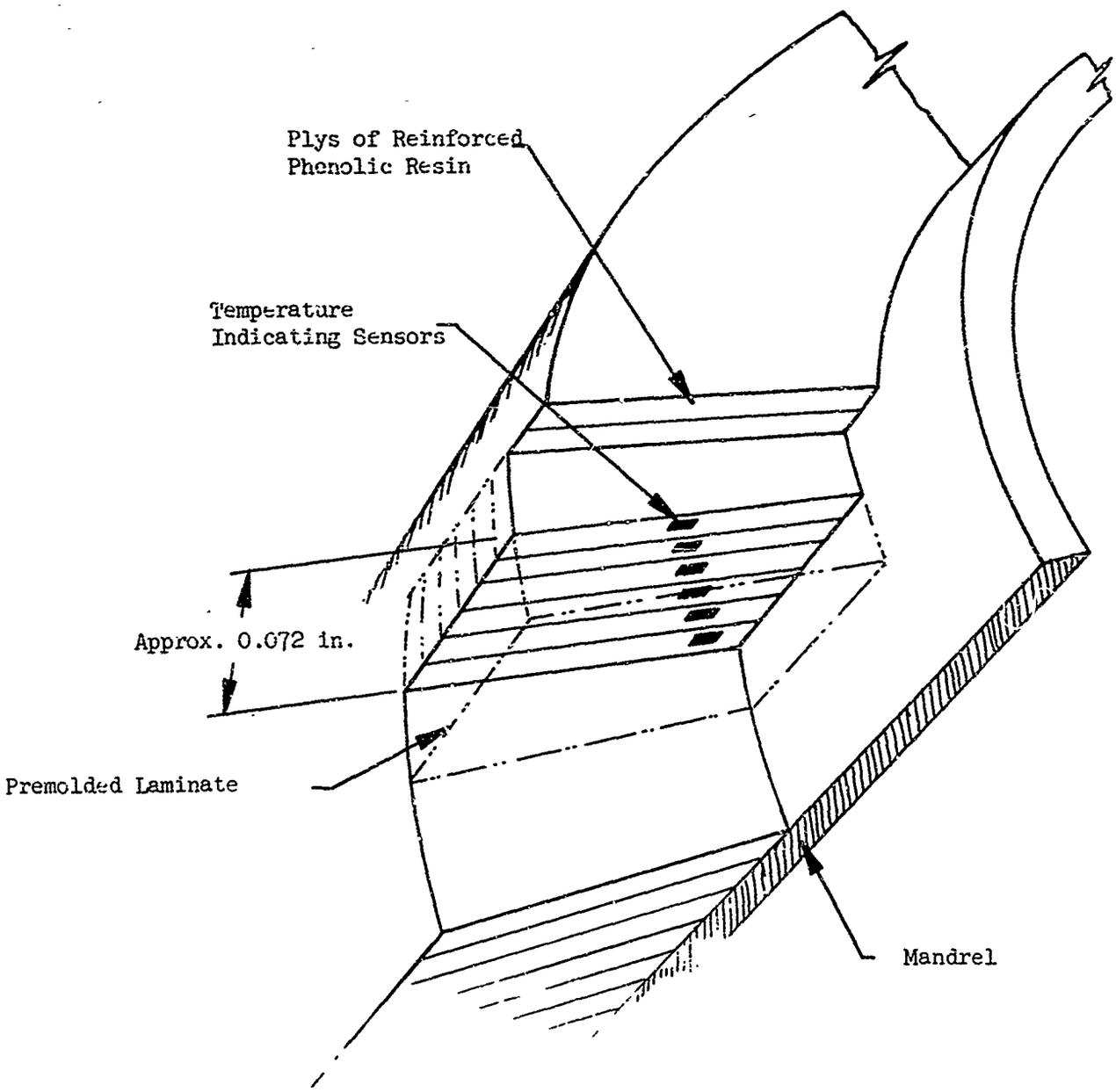

Figure 34. Molded Temperature-Sensor Laminate

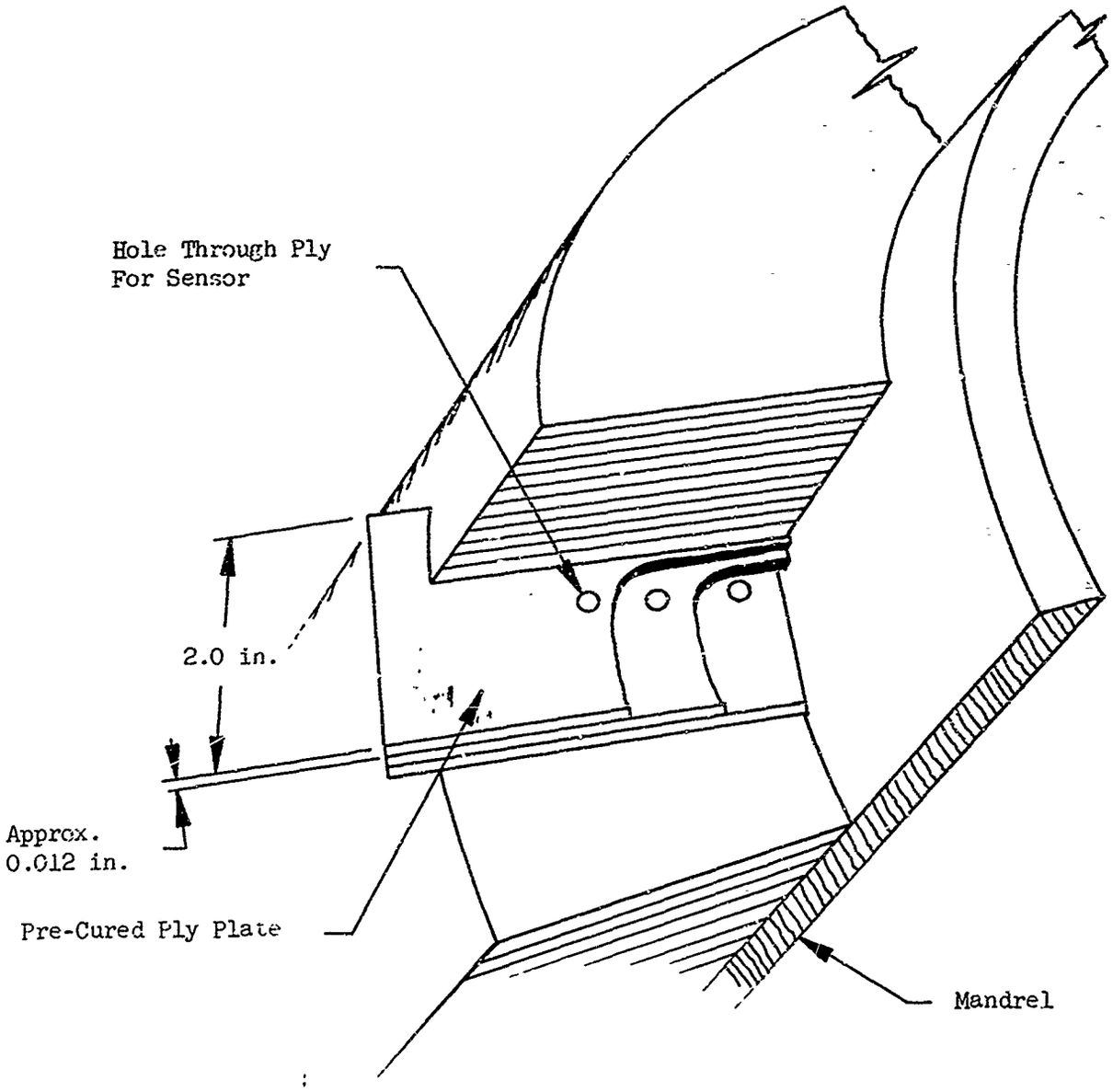

Figure 35. Precured Plies for Sensor Laminated Plate Set-Up

III, F, Alternative Method to Distribute Temperature Sensors and Thermocouples Within the Ablative Liner (cont.)

Random scattering or placing of the sensors during regular lay-up of the plies is not suggested because of the uncertainty of obtaining any ordered arrangement of the sensors during and after the debulk and cure cycles. Resin movement during the curing process of the plies would cause a very random distribution of the sensors and would prevent any control on predetermined locations for the sensors.

Instrumentation of thermocouples in an ablative material can be accomplished in a similar procedure as discussed above. In this case, thermocouples can be placed between ply plates at specific locations and then the entire assembly precured into a laminate (Figure 36). The laminated plate can be placed into position during fabrication lay-up, as indicated before, without affecting any other procedures. The laminated plate can be made to be somewhat smaller in width than the regular plies so that the lead wires can extend freely, as shown in Figure 37.

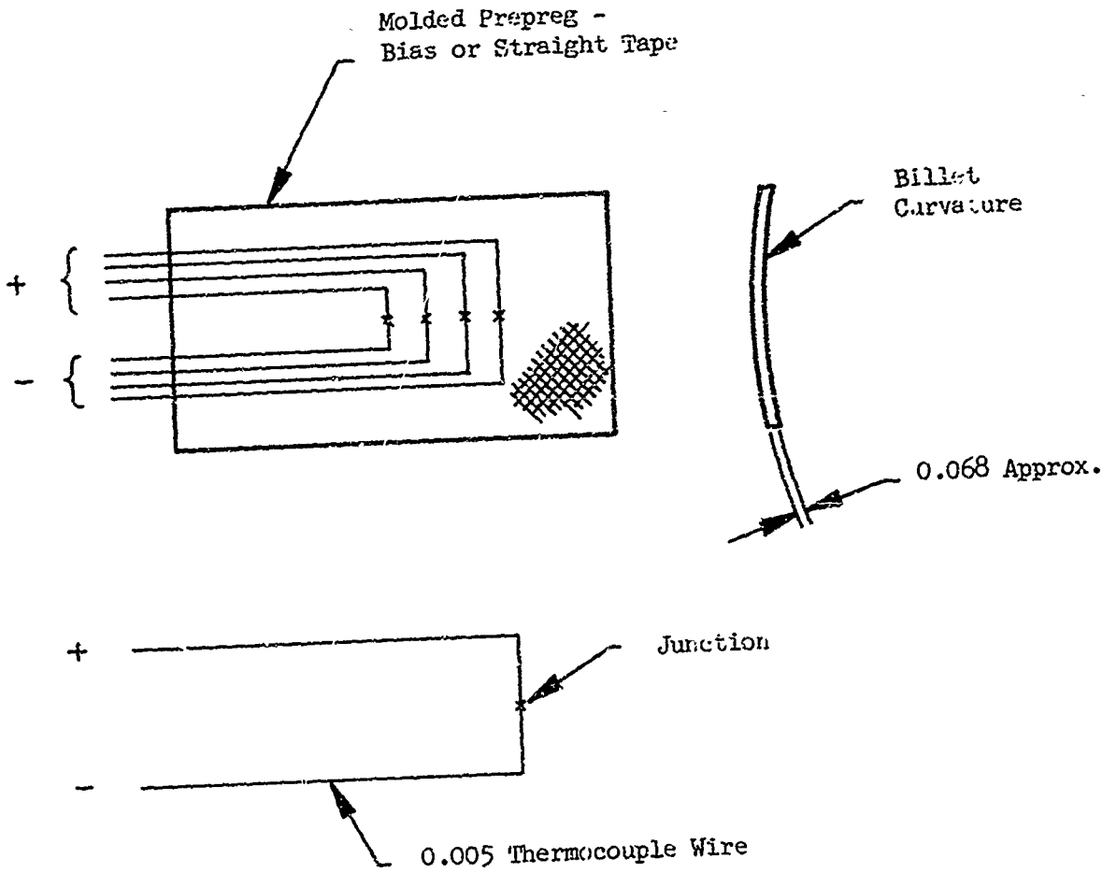

Figure 36. Molded Prepreg Thermocouple Plate

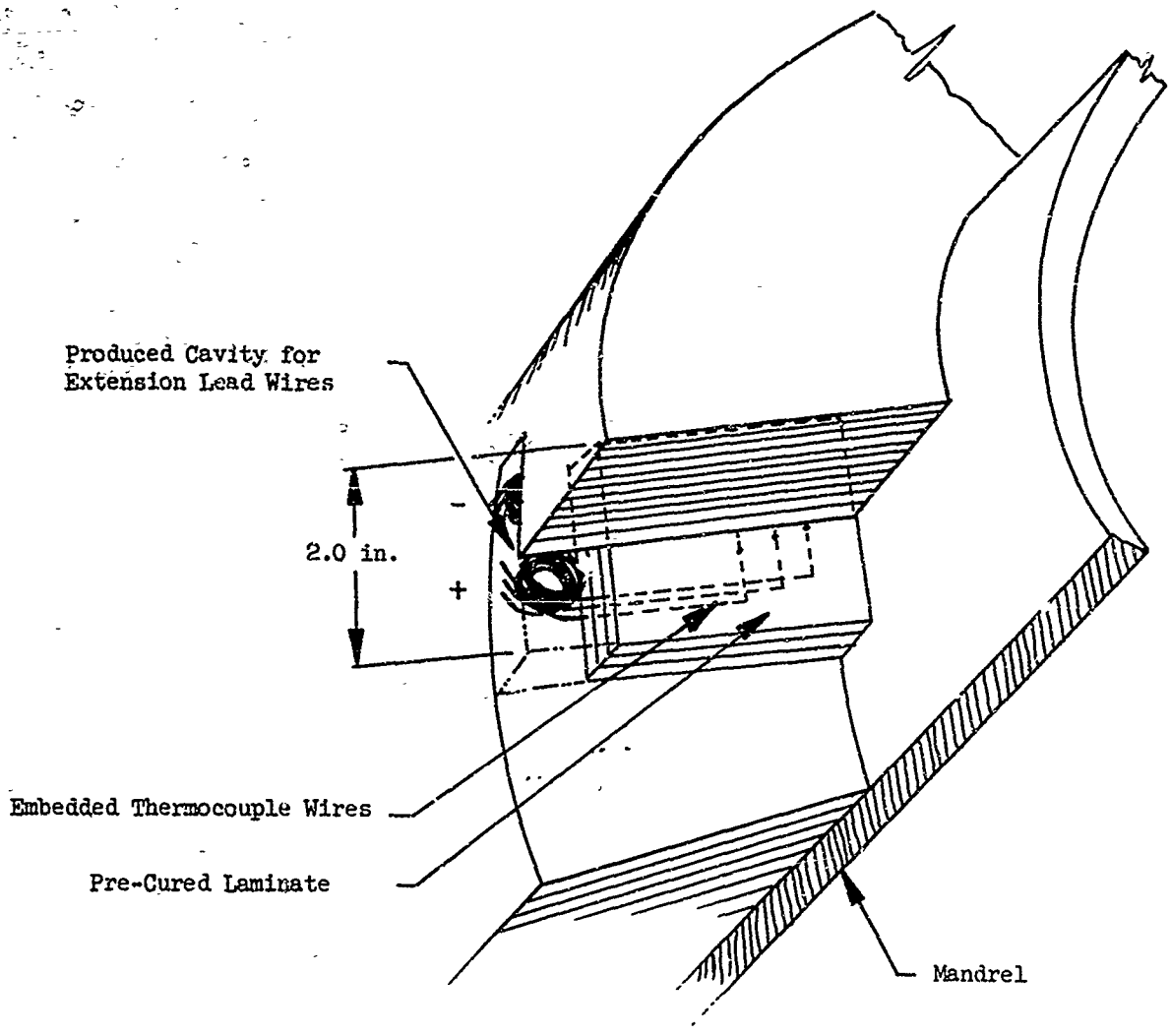

Figure 37. Laminated Plate Set-Up Showing Extended Lead Wires

SECTION IV

PROGRAM PLAN

The program is planned as a 12-month technical program and is divided into three phases, as shown in Figure 38. During the third phase, a break in the program is planned to allow for installation of the plugs supplied by Aerojet to AFRPL into ablative components, the test firing, disassembly of the components, and return to Aerojet for posttesting

A. TEST PLAN

1. Phase I. Study, Duration — Two and a Half Months

a. Task 1. State-of-the-Art Survey

A search of the literature was performed and sources of sensor fabrication which might provide an advantage over those proposed by Aerojet were sought.

b. Task 2. Analysis

A thorough study of the proposed sensor system was made with emphasis on the following factors:

(1) Fabrication cost

(2) Calibration accuracy

(3) Ease of installation and interpretation

(4) Minimization of effects of sensors on ablative performance

(5) Ease of identification of sensor types

(6) Sizes, shapes, compositions, and location of sensors

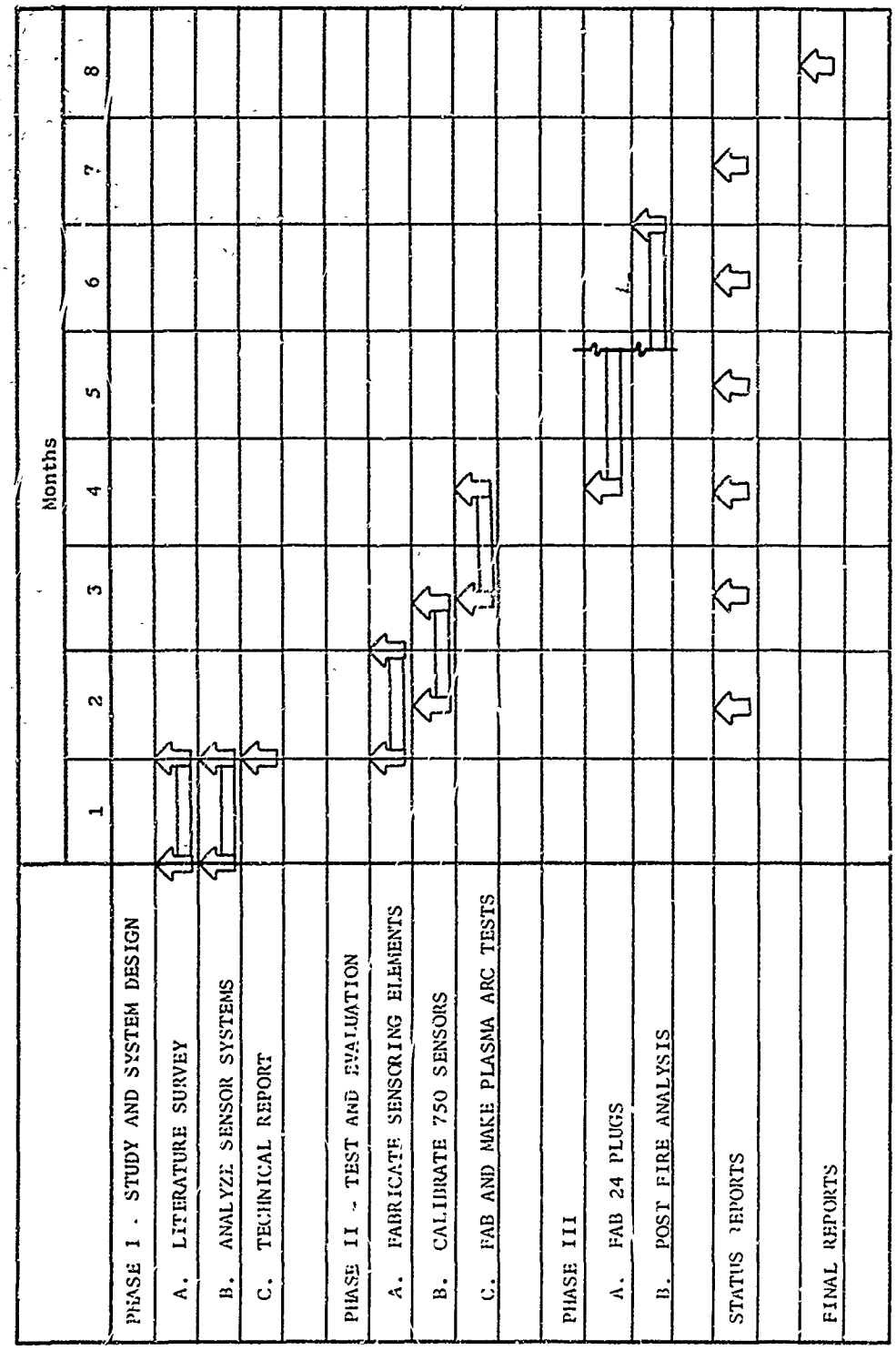

Figure 38. Program Schedule

IV, A, Test Plan (cont.)

2. Phase II. Test and Evaluation, Duration — Three Months

a. Task 1. Fabrication and Encapsulating Sensors

It is currently planned to machine the configuration shown in Figure 27 from graphite stock, insert powders of the proper composition in the cavity, and close the capsule.

b. Task 2. Calibration

Three sensor capsules of each of the 15 materials selected to cover the 3100 to 6000°F temperature range will be installed in graphite specimens prepared for the melting point furnace. The first specimen will be tested at a temperature 50°F below the melting temperature of the sensor and the other will be tested at a temperature 50°F above the melting temperature. The third specimen will be tested at a temperature to verify the initial results. The required tests are 45.

c. Task 3. Plasma-Arc Tests

Plug assemblies will be fabricated in accordance with the sketch (Figure 32) as defined in Phase I of this program to include four thermocouples (one of W-3Re/W-25Re) and 45 temperature sensors. These sensors will be three of each of 15 types designed to cover the temperature range from 3100 to 6000°F in approximately 75°F increments. Two plugs will be fabricated from each of nine ablative materials to be supplied by AFRPL.

The plug assemblies will be installed in small billets of similar material and will be tested in the plasma arc using an inert plasma gas. The temperature rise of the W-3Re/W-25Re thermocouple will be monitored during test and when it reaches 4000°F, the test will be terminated.

IV, A, Test Plan (cont.)

The tests will be conducted in two series; one of each ablative material in the first series after which a post-analysis will be performed using first radiography and second, visual examination of the sensors to determine if melting occurred. Then, modification of the system will be made and the duplicate specimen of each ablative material will be tested in the second series and evaluated.

Required are 18 plasma tests, 800 sensors.

d. Task 4. Thermophysical Property Measurements

Heat capacity, density, and thermal conductivity measurements will be made as "spot" checks on the following materials to confirm that these materials are identical to the NOMAD materials used:

(1) Carbon-reinforced phenolic

(2) Asbestos-reinforced phenolic

(3) Kraft paper-reinforced phenolic

(4) Carbon felt-reinforced phenolic

The same properties for five pyrolyzed graphite-reinforced phenolic materials will be furnished to Aerojet by AFRPL. Density determinations will be at room temperatures and heat capacity and thermal conductivity determinations will be made up to 200°C.

3. Phase III. Field Utilization, Duration — Seven Months

a. Task 1. Instrumented Plug Fabrication

At the completion of Phase II, a plug/sensor/thermocouple design will be coordinated with the AFRPL Project Engineer. Then, 12 instrumented

IV, A, Test Plan (cont.)

plugs will be fabricated using ablative materials supplied by AFRPL. Each will contain 35 sensors (covering the range established in Phase II plasma-arc tests as compatible with the upper limits of a W-3Re/W-25Re thermocouple and the surface temperature), a W-3Re/W-25Re thermocouple and three chromel/alumel thermocouples. These plugs will be provided to AFRPL for disposition to the fabricators of ablative plastic components.

b. Task 2. Analytical Predictions

A thorough study and review will be made of all data generated on the NOMAD program concerning the same phenolic-reinforced materials that will be test fired on this program, and also, of all plasma-arc data generated in Phase II involving these materials. The charring-ablation computer program will then be used to predict the regression and temperature profiles for all of the materials to be test fired at locations in the nozzle where the instrumented ablative plugs will be inserted.

c. Task 3. Post-Test Analysis

Upon return of the instrumented plugs to Aerojet, they will be oriented properly using the thermocouples as references and radiographed. After radiography, the plugs will be carefully disassembled to recover the sensor capsules which will be opened and visually examined for evidence of melting. Thermocouple measurements and temperature versus depth diagram will be constructed. Any deviations or discontinuities will be explained.

IV. Program Plan (cont.)

B. LIST OF CRITERIA TO BE FOLLOWED IN COMPLETING PHASES II AND III

1. Phase II. Test and Evaluation

In fabricating the temperature indicating system for plasma-arc testing and evaluation, the following list of specifications and procedures will be followed:

a. Approximately 10 cc of 15 different sensor materials will be made to the composition shown in Table I. These systems will be calibrated in triplicate by use of graphite melting point capsules (shown in Figure 30) and a Pirani furnace for the precision determination of melting temperatures. Each sensor material will be heated to three different temperatures: one 50°F above the melting temperature, one 50°F below the melting temperature, and the remaining one will be heated to the melting temperature. The heat-treated sensor materials will then be X-rayed and metallographically examined to determine whether or not melting has occurred.

b. The graphite microcapsules (a total of 810 for Phase II) will be made of POCO graphite to the dimensions shown in Figure 27.

c. Each graphite microcapsule will be hand packed with 325 mesh size sensor material; epoxy resin will be used to bond the capsule lid or cap to the graphite crucible.

d. The graphite capsules and ablative spacers will be bonded into place by the use of epoxy resin.

e. Duplicate ablative plugs of all phenolic materials, except one (asbestos phenolic), will be instrumented with 15 sensor materials and four backup thermocouples for plasma-arc testing and evaluation. One

IV, B, List of Criteria to be Followed in Completing Phases II and III (cont.)

ablative plug specimen of asbestos phenolic will be tested with instrumented sensor materials which will cover the temperature range of 3500 to 5000°F.

f. The packed microcapsules will be dispersed throughout the ablative plug in a manner as shown in Figure 32; three microcapsules containing identical sensor material and separated axially 0.030 in. apart will be used to ascertain a particular isotherm. The microcapsules will be dispersed radially (at least one diameter apart) as shown and will be dispersed axially to cover an axial distance of 0.200 in.

g. Four bare-wire type thermocouples will be instrumented into each ablative plug as shown in Figure 32; a tungsten-rhenium (0.003-in.-OD) thermocouple will be placed at a level corresponding to the 4000°F sensor material, and three chromel-alumel thermocouples (0.003-in.-OD) each will be placed 0.100 in. apart and below the tungsten-rhenium thermocouple. These thermocouples will be used to monitor the temperature-time history during plasma-arc testing.

h. The instrumented ablative plugs will be X-rayed before and after plasma-arc testing to precisely locate sensors and thermocouples and to determine whether or not melting occurred at specific locations within the ablative plug. Random metallography will also be conducted to confirm the X-ray photographs.

i. An instrumented and shrouded ablative plug of each phenolic material will be test-fired and analyzed before a duplicate test is made. This will allow for modification and redesign, if necessary, for any of the materials.

IV, B, List of Criteria to be Followed in Completing Phases II and III (cont.)

j. An analysis of each fired ablative plug will include the behavior of each sensor material as to whether it melted, vaporized, reacted away, etc., the apparent compatibility of each sensor with the ablative material, the spacial movement, if any, of the graphite capsules during firing, the temperature profile through the charred material, as indicated by the sensor materials, temperature-time histories as indicated by the thermocouples, and thermocouple and sensor temperature comparisons to determine thermocouple accuracies.

k. The plasma-arc tests will be conducted at a cold-wall heat flux that will simulate motor firing conditions.

l. The ablative materials that will be analyzed in Phase II are (1) MX 4926, carbon phenolic, (2) MXA 6012, asbestos phenolic, (3) FM 5272, paper phenolic, (4) MXC 113, carbon felt phenolic, and (5) five different pyrolyzed (precharred) carbon and graphite phenolics.

2. Phase III. Field Utilization of System

Based upon the results and analyses of Phase II, 12 instrumented ablative plugs will be fabricated and delivered to an AFRPL vendor according to the following procedures and specifications:

a. The graphite microcapsules (a total of 540 for Phase III) will be made as already indicated in b, c, and d of Part A, Phase II, above.

b. The sensors will be distributed radially as mentioned above in f, but will be distributed axially according to the results obtained from the NOMAD Program, to the results obtained from the plasma-arc firings of

IV, B, List of Criteria to be Followed in Completing Phases II and III (cont.)

Phase II, and to the results obtained from the Charring Ablation Computer Program.

c. The instrumented ablative plugs will be X-rayed before and after test as indicated in h. above.

d. Four sheathed-type thermocouples will be instrumented into each ablative plug; a tantalum-sheathed tungsten-rhenium probe will be placed at the 4000°F isotherm level, and three inconel-sheathed chromel-alumel thermocouples will be each placed 0.100 in. apart, one below the other.

e. The analysis of each motor-fired ablative plug will be analyzed as indicated in j. above.

f. Duplicate instrumented ablative plugs will be made for MX 4926, MXC 113, and for three pyrolyzed materials. Single ablative plugs will be made for MXA 6012 and FM 5272. The 12 ablative plugs will then be hand carried to the motor fabricator designated by AFRPL.

APPENDIX I

OPEN LITERATURE REFERENCES

Appendix I

OPEN LITERATURE REFERENCES

Asamoto, R. R. and Novak, P. E., Tungsten-Rhenium Thermocouples for use at High Temperatures, Review of Scientific Instruments, V.38, No. 8, August 1967, p. 1047 (2300 to 3000°C in Vacuum. Thoria insulation used.)

Bacon, J. F. et al., High Temperature Vacuum Furnace with Metallic Sheet Resistance Elements. Review of Scientific Instruments, V. 34, No. 11, p. 1200, Nov 1963 (to 2800°C).

Bedford, R. E., Reference Tables for Platinum 20%, Rhodium/Platinum 5% Rhodium Thermocouples, Review of Scientific Instruments, V. 35, No. 9, p. 1177, Sep 1964 (to 1750°C).

Black, F. S., High Temperature Sensors for a Re-Entry Research Vehicle, SAE Paper 750K, 1963 (A63-23891).

Blum, N. A., Recording Optical Pyrometer, Review of Scientific Instruments, V. 30, No. 4, p. 251, Apr 1959.

Camac, M. and Flinberg, R., High Speed Infrared Balometer, Review of Scientific Instruments, V. 33, No. 9, p. 964, Sep 1962, (5 to 30-micron range).

Cohen, J. and Eaton, W., High Temperature High Vacuum Resistance Furnace, Review of Scientific Instruments, V. 31, No. 5, p. 522, May 1960.

Clark,R.B.,Calibration and Stability of W/WRe Thermocouples to 2760° (5000°F), in: Instrument Society of American Annual Conf., V. 19, P. 2, (A65-11197).

Daniels,W.B.,Simple Apparatus for the Generation of Pressures Above 100,000 ATM. Simultaneously with Temperatures above 3000°C. Review of Scientific Instruments, V. 32, No. 8, p. 885, Aug 1961.

Danishevskii, S. K., et al., Thermocouples Made of Tungsten Alloys with Rhenium for Measuring Temperature up to 2500°C, in: Industrial Laboratory, V. 29, Mar 1964, p. 1242-1244 (A64-16973).

Dergunov, N. N., and Barabanov, V. N., Tekhnika Eksperimenta pir Issledovanii Uglegrafitovykh Materialou pir 20-3200°C. Trans. in Industrial Laboratory, V. 30, No. 8, 1964, p. 997-1005 (EI 1965, p. 1287).

Grey, J., et al., Temperature Measurement in a Graphite Environment from 1600°C to 2500°C, Hoskins Mfg. Co., Detroit, Mich. In-Instrument Society of America, Annual Conference, 19th, New York., Oct. 12-15, 1964 Proceedings, V. 19; Pt II, Physical and Mechanical Measurement Instrumentation, Pittsburgh, Instrument Society of America, 1964. 12p. Preprint 16.13-3-64.

OPEN LITERATURE REFERENCES (cont.)

Hall, F. B., and Spooner, N., Application and Performance Data for Tungsten-Rhenium Alloy Thermocouples, Sept 1963, SAE Paper 750C (A63-23914).

Hall, T., Some High Pressure, High Temperature Apparatus Design Considerations: Equipment for Use at 100,000 ATM and 3000°C, Review of Scientific Instruments, V. 29, No. 4, p. 267, Apr 1958.

Hall, T., Ultra-High-Pressure, High Temperature Apparatus: The "Belt". Review of Scientific Instruments, V. 31, No. 2, p. 125, Feb 1960, (2000°C).

Hicks, E.W., Investigation of Tungsten/Tungsten-26% Rhenium Thermocouples Above 3500°F in Oxidizing Environments, in: Instrument Society of America 19th Annual ISA Conference and Exhibit, New York. Oct 12 - 15, 1964. V. 19, pt. 2, preprint 16, 10-3-64 (TL Q 184 Pro 1964 pt. 2).

Hicks, E. W., The Requirements for a Direct-Reading 5000°F Thermocouple, in: Instrument Society of America 18th Annual ISA Conference and Exhibit, Chicago, Sep 9 - 12, 1963, V. 18, pt. 1, Preprint 29.2.63 (TL Q 184 Pro 1963).

Johnson, P., Ultra High Temperature Thermocouple for Aerospace Application, in: Instrument Society of America National Aerospace Instrumentation Symposium 12th, Philadelphia, May 2 - 4 1966, pp 275-277 (A67-11139.) (to 5200°F).

Jones, R. A., and Hunt, J. L., Use of Temperature Sensitive Coatings for Obtaining Quantitative Aerodynamic Heat-Transfer Data, AIAA Journal, 1964.

Kasanof, D. R., and Kimmel, E., Recent Developments in Fusible Temperature Indicators in Temperature - Its Measurement and Control in Science and Industry No. 3, Pt 2, Reinhold, 1962.

Kiyoura, R., Studies on the Tungsten Furnace and Its Temperature Measurement by W-Wre Thermocouple up to 2700°C., Tokyo Inst. of Tech., Research Lab. of Engineering Materials, Tokyo, Japan. Sata, T., Tokyo Institute of Technology, Bulletin No. 53, 1963, pp 39-49.

Kostowski, H. J., The Accuracy and Precision of Measuring Temperatures above 1000°K, in: International Symposium on High Temperature Technology, Asilomar Conference Grounds, Calif. Oct 6 - 9, 1959, McGraw Hill, c.1960 (TL QC 276 Int).

Kuhlman, W. C., Status Report of the Investigation of Thermocouple Materials for Use at Temperatures Above 4500°F, SAE Paper 7500, 1963, (A63-25879).

Lachman, J. C., New Developments in Tungsten/Tungsten-Rhenium Thermocouples, in: Instrument Society of America, 1961 Fall Instrument-Automation Conference and Exhibit, Los Angeles, Sep 11 - 15, 1961, V. 16, Pt. 2, Preprint 150-LA-61 (TL Q 184 Pro 1961).

OPEN LITERATURE REFERENCES (cont.)

Moen, W. K., Significance of Errors in High Temperature Measurement, North American Aviation, Inc., Space and Information Division, Downey, Calif. SAE, NASA Engineering and Mfg. Meeting, Los Angeles, Calif., Sept. 23-27, 1963, Paper 750F.

Moen, W. K., Spacecraft Thermocouple Installation Design, in: Instrument Society of American Annual Conf., 1964. V. 19, Pt. II, (Says thermocouples should not be used from 2000 to 5000°F), (A65-11195).

Nadler, M. R. and Kempter, C. P., Thermocouples for use in Carbon Atmospheres, Review of Scientific Instruments, V. 32, No. 1, p. 43, Jan 1961, (to 2200°C).

Nanigian, J., Ribbon Thermocouples in the 3000 to 5000°F Range, Instruments and Control Systems, V. 39, May 1966, pp 93-99, (A66-32038).

Nanigian, J., Temperature Measurements in the 3000 to 5000°F Range Using Ribbon Thermocouples, Nanmac Corp., Needham, Mass. Instrument Society of America, Annual Conference, 19th, New York, N.Y., Oct. 19, 1964, paper. 12 p.

Nilson, J. R., Elimination of Electrical Interference in High Temperature Thermocouple Installations, in: Instrument Society of America 1960 Summer Instrument-Automation Conference and Exhibit, San Francisco. May 9 - 12, 1960. Preprint 36 -SF60 (TL Q184 Pro 1960).

Nydick, S. E., Thermocouple Errors in Ablation Materials, Instrument Society of America Annual Conference and Exhibit, 21st, N.Y.. Oct 24 - 27, 1966 (A67-11104).

Olsen, L. O. (NBS), Some Recent Developments in Noble Metal Thermocouples, SAE Paper 750A, 1963, (A63-23892).

Pentecost, J. L., and Eliason, L. K., Characterizing Materials Above 1500°C, Int Symposium on Magnetohydrodynamic Electric Power Generation, U.S. - Proc. Jul 6 - 11, 1964 (EJ. 1965, p. 1282).

Pustell, R. A., 4300°F Thermocouples for Re-Entry Vehicle Applications, General Electric Co., Instrument Dept., West Lynn, Mass. SAE, NASA Engineering and Mfg. Meeting, Los Angeles, Calif., Sept. 23-27, 1963, Paper 750E. 10 p.

Samsonov, G. V., Thermocouples for Measuring High Temperatures. Akademiia Nauk Ukrainskoi SSR, Institut Problem Materialovedeniia, Kiev, Ukrainian SSR. Stadnyk, B. I., Teplofizika Vysokikh Temperatur, V. 2, July - Aug 1964, pp 634-647, High Temperature, V. 2, Jul - Aug. 1964, pp 573-583.

OPEN LITERATURE REFERENCES (Cont.)

Sanders, V. D., Review of High Temperature Immersion Thermal Sensing Devices for In-Flight Engine Control, Review of Scientific Instrument, V. 29, No. 71, p. 917, Nov 1958 (3500 to 4000°F).

Sims, C. T., Refractory-Metal Thermocouples Containing Rhenium, Review of Scientific Instruments, V. 30, No. 2, p. 112, Feb 1959, (Useful in Vacuum on Neutral or Reducing Atmosphere to 2600°C).

Smetanina, L. I., The Dynamic Method of Measuring High Temperatures, Teplofizika Vysokikh Temperatur, V. 2, Jan. - Feb. 1964, pp 94-97, High Temperature, V. 2, Jan. - Feb. 1964, pp 80-83.

Stadnyk, B. I., and Samsonov, G. V., Thermocouples for High-Temperature Measurements, Teplofizika Vysokikh Temperatur, V. 2, Jul-Aug 1964, In Russian (A64-27336).

Taylor, J. L., Apparatus for Tensile Testing to 5400°F in Vacuum, Review of Scientific Instruments, V. 34, No. 5, p. 500, May 1963.

Thomas, D. B., Studies on the Tungsten-Rhenium Thermocouple to 2000°C, in: Instrument Society of America 1963 Annual Instrument-Automation Conference and Exhibit, Chicago, Sep 9 - 12, 1963. V. 18, Pt. 2, Preprint 57.3.63 (TL Q 184 Pro 1963).

Tinkaev, V. I. and Shashkov, A. G., High-Temperature Materials of Advanced Technology and Methods for Studying their Thermophysical Properties at Temperatures up to 3500°C, Inzhenero-Fizicheskii Zhurnal, V. 12, Feb 1967, pp 263-277 (A67-25321).

Walker, B. E., et. al., Instability of Refractory Metal Thermocouples, Review of Scientific Instruments, V. 36, No. 6, p. 816, Jun 1965 (1000 to 2000°C Under Vacuum).

Walker, B. E., et. al., Thermoelectric Instability of Some Noble Metal Thermocouples at High Temperatures, Review of Scientific Instruments, V. 33, No. 10, p. 1029, Oct 1962. Erratum V. 34, No. 12, p. 1456 (Platinum, Rhodium, Irridium Metals in Temperature Range 1000 to 1700°C).

Wilson, W. B., Device for Ultra High Pressure High Temperature Research, Review of Scientific Instruments, V. 31, No. 3, p. 331, Mar 1960.

Witteman, W. J., and Workman, H., Cylindrical High Temperature, High Pressure Apparatus, Review of Scientific Instruments, V. 35, No. 4, p. 461, Apr 1964.

Yanowitz, H., A New Heat Flux Gage for Use on Recessive Surfaces, Instrument Society of America Annual Conf. and Exhibit, 21st, N.Y. Oct 24 - 27. p.66 (A67-11106).

TECHNICAL REPORTS

Aerojet-General Corporation

Carbon Resistant Coating for Tungsten-Rhenium Thermocouples. R. G. Hoff. 23 May 1966 (AGC RN-TM-0325) (TL No. 6U3742).

Deflection Transmission Cable Link for Use in Thermal Environments in Excess of 3500°F, Proposal to Aeronautical Systems Division, Proposal No. SRR-63013. Feb 1963 (AGC SRR-63013 REF, TL No. 5U3808).

Design, Development, and Fabrication of Twelve Prototype Thermocouples, V. 1: Technical; A proposal. Mar 1964 (LR 640174, TL No. 4U3705).

Exploratory Development of Thermionic Emission Techniques for Transduction of Elevated Temperature, V. 1. A proposal (LR 640737. TL No. 4U8524).

Feasibility Report for a Method of Piezoelectric Accelarometer Temperature Compensation; REON Technical Memorandum, D. G. Kneeland, 26 Jan 1966 (AGC RN-TM-0300, TL No. 6U1374).

Nerva Instrumentation Quarterly Review Minutes, Apr 1964, (RN-S-0096). (TL No. 4U5468).

Thrust Chamber Temperature Profile Probe, Nerva Program, Summary Report, Jun 1966, Contract SNP-1 (AGC RN-S-0297, TL No. 6U6670).

Transient Temperatures and Associated Deflections in Model Rocket Nozzle Inserts, S. K. Ferriera, Apr 1964 (TM-248, TL No. 4U4998).

Tungsten-Rhenium Thermocouples, May 1965, Report RN-S-022 (TL RC 0028).

Accuracy of Temperature Measurements. T. M. Anderson, 8 Dec 1964 (TM 4873:64-2-256, CTIC Abst. 10455).

Aerojet Model J153 Optical-Electronic Extensometer, Special Report, Oct 1961 (R-2103, CTIC Abst. 6373).

Equipment and Facilities for Determination of the Mechanical Properties of Refractory Materials at Elevated Temperatures, C. E. Waller and M. L. Stebsel. Special Report, Jul 1959 (CTIC Abst. 695)

Aeronautical Research Laboratory

Experimental Evaluation of a Dual-Element Transducer for High Temperature Gas Measurements, Chambers, J. T., et al., Mar 1963 (ARL-63-58, TL No. 4U0564).

Aeronautical Systems Division

Development of an Ultra-High Temperature Pyrolytic Graphite Thermocouple, Kline, C. A., Jan 1964 (TDR-63-844, TL No. 4U5853).

Research and Evaluation of Materials for Thermocouple Application Suitable for Temperature Measurements up to 4500°F on the Surface of Glide Re-Entry Vehicles (TDR-63-233, TL No. 3U4973).

Thermal Properties of Twenty-six Solid Materials to 5000°F or Their Destruction Temperatures, Aug 1962 (TDR-62-765, TL No. 3U4197).

Aerospace Corporation

Temperature Measurement, Slaughter, J. I., Oct 1962 (TDR-169(3240-20) T, SSD-TDR-62-140, TL No. 3U5615).

Aerospace Research Laboratories

Temperature Determination in Moderately Dense, High-Temperature Gases by Transient Thermocouple Probes, Interim Technical Report, P.S. Tschang (Columbia Univ.). May 1964. Contract AF 49(638)-1395, (ARL 65-95, AD 617 702. TL No. 6U0439).

AF Cambridge Research Laboratories, Bedford, Massachusetts

Study of High Temperature Thermocouples, Final Report, 1 Jun 1963 - 15 Dec 1964, Hall, B. F., Jr., and Spooner, N. F., (Hoskins Mfg. Co.). 23 Mar 1965, Contract AF 19(628)-2957 (AFCRL 65-251, AD 619 038, TL No. 5U7365).

American Standards Association, New York, N.Y.

Temperature Measurement Thermocouples, American Standard (Instrument Society of America), 9 Jun 1964 (ASA C96-1-1964, TL No. 6U2051).

Armour Research Foundation

Development of High Temperature Thermocouples, Sep 1948 (TL No. 3U4071).

Atomic Energy Commission

High-Temperature Sensors for Borax-V Boiling Fuel Rods, E. J. Brooks, Oct 1962, Contract W-31-109-Eng-28 (AEC ANL-6636, TL No. 5U2450).

High Temperature Thermometry Seminar, Oak Ridge National Laboratory, Oct 1 - 2, 1959 (TID-7586 (PT. 1), TL No. 4U5365).

High-Temperature High-Vacuum Thermocouple Drift Tests, Hendricks, J. W., McLeroy, D. L., In Its High Temperature Thermometry, Mar 1966, 26 p, see N67-19621 09-22 CFSTI.

In-Pile Performance of High-Temperature Thermocouples, Carroll, R. W., Reagan, P. E., In Its High Temperature Thermometry, Mar 1966, 9 p, see N67-1962109-22 CFSTI.

Summary of Experience with High-Temperature Thermocouples Used in the ORNL-GCR Program Fuel Irradiation Experiments, Briggs, N. H., Long, E. L., Jr., McQuilkin, F. R., In Its High Temperature Thermometry, Mar 1966, 22 p, N67-19621-09-22 CFSTI.

Thermal EMF Drift of Refractory Metal Thermocouples in Pure and Slightly Contaminated Helium Atmospheres, Bennett, R. L., Hemphill, H. L., Rainey, W. T., Jr., In Its High Temperature Thermometry, Mar 1966, 2 p, see N67-19621 09-22 CFSTI.

Thermal EMF Drift of High-Temperature Thermocouples in Helium and Argon, Briggs, N. H., Johnston, W. W., Jr., In Its High Temperature Thermometry, Mar 1966, 3 p, see N67-1962109-22 CFSTI.

Argonne National Laboratory

High-Temperature Sensors for Borax-V Boiling Fuel Rods, Brooks, E. J., Kramer, W. C., and McGowan, R. D., Oct 1962, 41 p, Contract W-31-109-Eng-38, ANL-6636.

Refractory Oxide Insulated Thermocouple Analysis and Design, Popper, G. F., Zeren, T. Z., In AEC High Temperature Thermometry, Mar 1966, 26 p, see N67-19621 09-22 CFSTI.

Arnold Engineering Development

Equations and Tables for Thermocouples 32°F Reference Junction, Spengler, W. E., and others, Mar 1964, AEDC TR-64-55, AD 432 828 (N64-17456).

Auto-Control Laboratories, Inc.

High Temperature Thermocouple Research and Development Program Monthly Progress Report, No. 11, 1 Apr - 1 May 1964, Smith, R. R., Jr., 10 May 1964, 19 p, NAS 8-5438, NASA-CR-58569, T-1097-11 OTS.

High Temperature Thermocouple Research and Development Program, Appendix 3, Miscellaneous Technical Data Summary Report, Smith, R. R., Jr., 18 June 1965, 79 p, NAS8-5438, NASA-CR-67347 T-1097, Appendix 3.

High Temperature Thermocouple Research and Development Program, Summary Report, Smith, R. R., Jr., 18 June 1965, 34 p, NAS8-5438, NASA-CR-67348 T-1097.

High Temperature Thermocouple Research and Development Program, Appendix 2, Calibrations, Smith, R. R., Jr., 18 June 1965, 99 p, NAS8-5438, NASA-CR-67197 T-1097, Appendix 2.

Barnes Engineering Company

Study of a Temperature Measuring System for the 1000° to 2500°C Range, Guy Moffitt, Wright-Patterson AFB, Ohio, Flight Control Lab., Feb 1962, 106 p, Contract AF 33(616)-7479, ASD-TR-61-847, AD-274794.

Study of a Temperature Measuring System for the 1000 to 2500°C Range, Final Report, July 1, 1960 - Aug 31, 1961, Guy Moffitt, Wright-Patterson AFB, Ohio, Flight Control Lab., Oct 1961, 108 p, Contract AF 33(616)-7479, ASD-TR-61-487, BEC-4247.

Battelle Memorial Institute

Continuation of the Small-Scale Operation of a Transducer Information Center, Chapin, W. E., et al. Oct 1956 (AFFDL-TR-66-66, TL No. 7U5933).

Defense Documentation Center, Alexandria, Virginia

High Temperature Instrumentation, A Report Bibliography, Covering Period 1961 - Jul 1962 (DDC ARB-11040, AD 446 929, TL No. 5U0884).

Diamond Ordnance Fuze Laboratory

Measurement of Temperature, Advanced State-of-the-Art Bibliography, Joseph Pearlstein, Aug 1961 (TR-969, TL No. 2-1729).

Fairchild Engine and Airplane Company

The Development of Thermocouples, Feb 1948 (NEPA-ARM-3. TL No. 3U4415).

Foreign Technology Division

Boride Zirconium Tips for Immersion Thermocouples, Samsonov, G. V., et al, Jul 1962 (TT-62-732/ 1 + 2, TL No. 3U4203).

Flight Dynamics Laboratory

A Probe for the Instantaneous Measurement of Surface Temperature, Jan 1964 (RTD-TDR-63-4015, TL No. 4U6548).

General Electric Company

ARP Materials, Final Report, 20 Sep 1965 - 31 Oct 1966, 15 Nov 1966. Contract AF 04(694)-667 (GE D-66SD 9207 Secret-RD, SA-67-00133(0002)-67, AD 376 968, TL No. 7S1657).

Survey for a High Temperature Sensor for Southwest Atomic Energy Associates, Asamoto, R. R., and Novak, P. E., Jul 1965 (GEAP-4903).

Research and Evaluation of Materials for Thermocouple Application Suitable for Temperature Measurements up to 4500°F on the Surface of Glide Re-Entry Vehicles, Kuhlman, W. C., May 1963, Contract AF 33(647)-8472, (8472 63-5, CTIC Abst. 4770).

Research and Evaluation of Materials for Thermocouple Application Suitable for Temperature Measurements up to 4500°F on the Surface of Guide Re-Entry Vehicles, Final Report, Mar 15, 1962 - Mar 15, 1963, Kuhlman, W. C., Wright-Patterson AFB, Ohio, Directorate of Materials and Processes, May 1963 83 p, Contract AF 33(657)-8472, ASD-TDR-63-233.

Hoskins Manufacturing Company

Study of High Temperature Thermocouples, Final Report, June 1, 1963 - December 15, 1964, Hall, B. F., Jr., Spooner, N. F., 23 March 1965, 89 p, AF 19(628)-2957, AFCRL-65-251, AD-619038.

Instrument Society of America, Pittsburgh, Pa.

Temperature Measurements in a Graphite Environment from 1600 to 2500°C. Hall, B. F., Jr., and Spooner, N. F., (Hoskins Mfg. Co.). Paper to be presented at the 19th Annual ISA Conference and Exhibit, N.Y., 12 - 15 October 1964 (ISA PP-16.13-3-64, TL No. 5U7986).

Johns Hopkins University

Instruments for the Measurement of Local Flame Temperature in High-Velocity Streams, Conrad Grumfelder, January 1953 (CM-768- TL No. 3U4398).

National Aeronautics & Space Administration, Washington, D.C.

Comparison of Measurements of Internal Temperatures in Ablation Material by Various Thermocouple Configurations, M. B. Dow, November 1964 (NASA TN D-2165, TL No. 5U0245).

Development of a Vapor-Pressure-Operated High-Temperature Sensor Device, Final Report, J. R. Van Orsdel and others (Battelle Memorial Inst.), 11 March 1965, Contract NAS 3-5202 (NASA CR-54369, TL No. 6U3329).

Effect of Thermocouple Wire Size and Configuration of Internal Temperature Measurements in a Charring Ablator, Technical Note, W. D. Brewer, March 1967, (NASA TN D-3812, TL No. 7U1990).

Small Plasma Probes with Guard Rings and Thermocouples, J. F. Morris, October 1966 (NASA TM X-1294, TL No. 6U7024).

Forebody Temperatures and Calorimetric Heating Rates Measured During Project Fire II Re-Entry at 11.35 Kilometers per Second, by Elden S. Carnette, November 1966, NASA TM X-1305, (TL 6C 7420).

National Bureau of Standards

Bibliography of Temperature Measurement, January 1953 - June 1960, April 1961, Monograph - 27 (TL 1-6433).

Naval Ordnance Test Station

Design and Use of Fine Wire Thermocouples for Research, M. H. Hunt, September 1959 (NAVORD 5828, TL 3U4207).

Naval Research Laboratory

Thermoelectric Instability of Some Noble Metal Thermocouples at High Temperatures, B. E. Walker, et al, June 1962 (NRL Rept 5792, TL No. 3U4205).

Oak Ridge National Laboratory

Smoothed Thermocouple Tables of Extended Significance (°C), March 1965, various sections, ORNL 3649, v. 1,2 (N65-20151 - 20159 N65 20680 - 20684).

Pratt & Whitney

High Temperature Thermometry at Canel, P. Bliss, February 1965, presented at AEC Tech. Meeting on High Temperature Thermometry, Washington, D.C., 24-26 February 1965, AEC Conf. 650204-8, TIM-888 (Thermocouple Film Diagram for High Temperature Applications) (N66-20304, p. 1659).

Thermocouple Development - Lithium Cooled Reactor Experiment, S. Faniciullo, March 1964, (PWAC-422 (N64-16000 - 07-15).

Sandia Corporation

Measurements of High Temperatures, Barber, J. A., in AEC High Temperature Thermometry, March 1966, 30 p, see N67-19621 09-22 CFSTI.

Society of Automotive Engineers

Pulse Technique Extends Range of Chromel-Alumel to 7000°F, Wormser, A. F., and Pfuntner, R. A., April 1962, Pap. 524A (TL 3U1632).

Tungsten/Tungsten-Rhenium Thermocouple Research and Development, McGruty, J. A., and Kuhlman, W. C., April 1962, Pap. 524C (TL No. 4U2469).

Southern Research Institute

Evaluation of the Performance of Tungsten - Tungsten 26 Rhenium Thermocouples to About 5000°F, Allen J. G., and Pears, C. D., July 1963 (N64-17269).

The Thermal Properties of 13 Solid Materials to 5000° for Their Destruction Temperatures, Neel, D. S., et al, Tech. Doc. Rpt., February 1962, Contract AF 33(616)-6312, (S14 6312 62-2, CTIC Abst. 5620).

Stanford Research Institute

High Temperature - A Tool for the Future, Proceedings of the Symposium Held at Berkeley, Calif., June 25 - 27, 1956, Menlo Park (SRI, c1956, 218 p. TL No. QC 277 Sta).

St. Louis University

Temperature Measurements in Oxy-Hydrogen Flames Using Scattered Neutrons, Delaney, R. M., and Weber, A. H., (AROD 2504:2, TL No. 3U4400).

Thompson Ramo Woolridge

Development of Advanced Nozzle Designs for Large Solid Propellant Motors, FR 4900 13 (TL 3C 5096).

Report AFRPL-TR-67-284

APPENDIX II

TERNARY PHASE EQUILIBRIA IN TRANSITION METAL-CARBON-SILICON SYSTEMS

Contract AF 33(615)-1249

Report AFRPL-TR-67-284
Appendix II

TERNARY PHASE EQUILIBRIA IN TRANSITION METAL-CARBON-SILICON SYSTEMS

Contract AF 33(615)-1249

In this project, experimental and theoretical investigations of refractory metal carbide and boride phase relationships have been performed. As a result of this work, the melting temperatures of these refractory materials and the intermediate phases that form have been accurately established. The following reports have been issued in this program.

Part I--Related Binary System

Volume I	Mo-C System
Volume II	Ti-C and Zr-C Systems
Volume III	Mo-B and W-B Systems
Volume IV	Hf-C System
Volume V	Ta-C System
Volume VI	W-C System, Supplemental Information on the Mo-C System
Volume VII	Ti-B System
Volume VIII	Zr-B System
Volume IX	Hf-B System
Volume X	V-B, Nb-B, and Ta-B Systems

Part II-Ternary Systems

Volume I	Ta-Hf-C System
Volume II	Ti-Ta-C System
Volume III	Zr-Ta-C System
Volume IV	Zr-Hf-C, Ti-Hf-C, and Ti-Zr-C Systems
Volume V	Ti-Hf-B System
Volume VI	Zr-Hf-B System
Volume VII	Ti-Si-C, Nb-Si-C, and W-Si-C Systems
Volume VIII	Ta-W-C System
Volume IX	Zr-W-B System. Pseudobinary Systems TaB_2-HfB_2

Volume X	The Systems Zr-Si-C, Hf-Si-C, Zr-Si-B, and Hf-Si-B
Volume XI	Hf-Mo-B and Hf-W-B Systems
Volume XII	Ti-Zr-B System, Pseudobinary Systems ZrB_2-NbB_2, ZrB_2-TaB_2, and HfB_2-NbB_2
Volume XIII	Phase Diagrams of the Systems Ti-B-C, Zr-B-C, and Hf-B-C

Part XII--Special Experimental Techniques

Volume I	High Temperature Differential Thermal Analysis
Volume II	A Pirani-Furnace for the Precision Determination of the Melting Temperatures of Refractory Metallic Substances

UNCLASSIFIED

Security Classification

DOCUMENT CONTROL DATA - R&D

(Security classification of title, body of abstract and indexing annotation must be entered when the overall report is classified)

1. ORIGINATING ACTIVITY (Corporate author) AEROJET-GENERAL CORPORATION Sacramento, California 95809	2a. REPORT SECURITY CLASSIFICATION Unclassified 2b. GROUP

3. REPORT TITLE

DEVELOPMENT OF A TEMPERATURE-INDICATING SENSOR FOR USE IN ABLATIVE ROCKET NOZZLES

4. DESCRIPTIVE NOTES (Type of report and inclusive dates)

Phase I Report , 1 August 1967 through 6 October 1967

5. AUTHOR(S) (Last name, first name, initial)

DeAcetis, J., and Rousar, D. C.

6. REPORT DATE	7a. TOTAL NO. OF PAGES	7b. NO. OF REFS
January 1968	100	1

8a. CONTRACT OR GRANT NO.	9a. ORIGINATOR'S REPORT NUMBER(S)
F04611-67-C-0118	AFRPL-TR-67-284
b. PROJECT NO.	
c. N/A	9b. OTHER REPORT NO(S) (Any other numbers that may be assigned this report)
d.	

10. AVAILABILITY/LIMITATION NOTICES

Foreign announcement and dissemination of the report by DDC is not authorized.

11. SUPPLEMENTARY NOTES	12. SPONSORING MILITARY ACTIVITY
None	Air Force Rocket Propulsion Laboratory Research and Technology Division Air Systems Command, Edwards, Calif. 93523

13. ABSTRACT

The primary purpose of this program is to develop a high temperature (3500-6000°F) indicating system in order to obtain internal temperature measurements in ablative type materials during rocket motor firings.

During the first phase of work, a state-of-the-art survey was conducted to determine those necessary factors which would permit the accurate measurement of in depth temperatures. A high-temperature indicating system was designed based upon the phase equilibrium of refractory materials in the 3500-6000°F range.

DD FORM 1 JAN 64 1473

UNCLASSIFIED

Security Classification

UNCLASSIFIED

Security Classification

14. KEY WORDS	LINK A		LINK B		LINK C	
	ROLE	WT	ROLE	WT	ROLE	WT
High Temperature Sensing Elements Sensors High Temperature Measurements Techniques to Obtain High Temperatures						

INSTRUCTIONS

1. ORIGINATING ACTIVITY: Enter the name and address of the contractor, subcontractor, grantee, Department of Defense activity or other organization *(corporate author)* issuing the report.

2a. REPORT SECURITY CLASSIFICATION: Enter the overall security classification of the report. Indicate whether "Restricted Data" is included. Marking is to be in accordance with appropriate security regulations.

2b. GROUP: Automatic downgrading is specified in DoD Directive 5200.10 and Armed Forces Industrial Manual. Enter the group number. Also, when applicable, show that optional markings have been used for Group 3 and Group 4 as authorized.

3. REPORT TITLE: Enter the complete report title in all capital letters. Titles in all cases should be unclassified. If a meaningful title cannot be selected without classification, show title classification in all capitals in parenthesis immediately following the title.

4. DESCRIPTIVE NOTES: If appropriate, enter the type of report, e.g., interim, progress, summary, annual, or final. Give the inclusive dates when a specific reporting period is covered.

5. AUTHOR(S): Enter the name(s) of author(s) as shown on or in the report. Enter last name, first name, middle initial. If military, show rank and branch of service. The name of the principal author is an absolute minimum requirement.

6. REPORT DATE: Enter the date of the report as day, month, year; or month, year. If more than one date appears on the report, use date of publication.

7a. TOTAL NUMBER OF PAGES: The total page count should follow normal pagination procedures, i.e., enter the number of pages containing information.

7b. NUMBER OF REFERENCES: Enter the total number of references cited in the report.

8a. CONTRACT OR GRANT NUMBER: If appropriate, enter the applicable number of the contract or grant under which the report was written.

8b, 8c, & 8d. PROJECT NUMBER: Enter the appropriate military department identification, such as project number, subproject number, system numbers, task number, etc.

9a. ORIGINATOR'S REPORT NUMBER(S): Enter the official report number by which the document will be identified and controlled by the originating activity. This number must be unique to this report.

9b. OTHER REPORT NUMBER(S): If the report has been assigned any other report numbers *(either by the originator or by the sponsor)*, also enter this number(s).

10. AVAILABILITY/LIMITATION NOTICES: Enter any limitations on further dissemination of the report, other than those imposed by security classification, using standard statements such as:

(1) "Qualified requesters may obtain copies of this report from DDC."

(2) "Foreign announcement and dissemination of this report by DDC is not authorized."

(3) "U. S. Government agencies may obtain copies of this report directly from DDC. Other qualified DDC users shall request through

_____."

(4) "U. S. military agencies may obtain copies of this report directly from DDC. Other qualified users shall request through

_____."

(5) "All distribution of this report is controlled. Qualified DDC users shall request through

_____."

If the report has been furnished to the Office of Technical Services, Department of Commerce, for sale to the public, indicate this fact and enter the price, if known.

12. SUPPLEMENTARY NOTES: Use for additional explanatory notes.

12. SPONSORING MILITARY ACTIVITY: Enter the name of the departmental project office or laboratory sponsoring *(paying for)* the research and development. Include address.

13. ABSTRACT: Enter an abstract giving a brief and factual summary of the document indicative of the report, even though it may also appear elsewhere in the body of the technical report. If additional space is required, a continuation sheet shall be attached.

It is highly desirable that the abstract of classified reports be unclassified. Each paragraph of the abstract shall end with an indication of the military security classification of the information in the paragraph, represented as *(TS), (S), (C), or (U)*.

There is no limitation on the length of the abstract. However, the suggested length is from 150 to 225 words.

14 KEY WORDS: Key words are technically meaningful terms or short phrases that characterize a report and may be used as index entries for cataloging the report. Key words must be selected so that no security classification is required. Identifiers, such as equipment model designation, trade name, military project code name, geographic location, may be used as key words but will be followed by an indication of technical context. The assignment of links, rules, and weights is optional.

UNCLASSIFIED

Security Classification